VIBRATIONAL SPECTRA OF SOME HEXAFLUOROMETALLATES(IV)

THESIS

submitted for the Degree

of

Master of Science in Chemistry

at

THE UNIVERSITY OF GLASGOW

by

A. BUTUCELEA

1971

Supervisor:

Prof. D.W.A. SHARP

Ramsay Professor of Chemistry

The author thankfully aknowledges a research fellowship and full support from the University of Glasgow granted during accomplishment of this work, in 1969, as well as for permission to submit the results for the degree of Master of Science in chemistry. He is warmly grateful to Professor D.W.A. Sharp for his careful supervising and for his friendly consideration of the author's personal problems during his stay in Scotland. He warmly thanks Dr. A.P. Lane and Dr. Ann Chadwick for many valuable discussions on the vibrational spectroscopy of solids, and is indebted to the whole staff of the Chemistry Department of the University of Glasgow for the friendship they surrounded him all along.

The author would like also to express his gratitude to Professor V.E. Sahini, from the University of Bucharest, and to the Institute of Physical Chemistry of Bucharest, for permission to leave the Institute for one year and carry out this work.

CONTENTS

SUMMARY

Vibrational spectra of some hexafluorosilicates, -germanates, and -manganates(IV), with general formula A_2MF_6, were recorded in solid state, with emphasis on the far-infrared region of wavelengths. The spectra were obtained with a Fourier Transform Interferometer and a Cary 81 Raman Spectrometer having an He-Ne laser as exciting source. Many of these spectra are reported for the first time. They are discussed in terms of factor group analysis, of which an up-to-date survey is made in Chapter 1. Factor group analyses are carried out for 4 of the most frequently encountered crystalline structures of A_2MF_6 compounds, i.e. O_h^5, D_{3d}^3, C_{6v}^4, and D_3^2 space group (Chapter 3) and the results are compared with the experimental spectra (Chapter 5). Lattice modes and the behaviour of all vibrational modes under the particular symmetries of the molecular species in the crystal are largely discussed. Force constants are calculated by a least square procedure according to a computer program written by the author (Chapter 6). The calculated force constants are used to explain the experimental vibrational spectra of the A_2MF_6 compounds investigated, especially in the lattice frequency region, and to draw some conclusions about the nature of the bonding in these compounds (Chapter 7).

INTRODUCTION

The vibrational spectroscopy of inorganic compounds, which has been for a long time a most fruitful means of elucidating their structure, has found a renewed interest in recent years with the advent and rapid growth of two powerful tools - far-infrared absorption and reflection spectroscopy by interferometric methods, and Raman scattering spectroscopy with laser excitation.

These techniques have allowed investigation of two problems which had not been approachable by the older methods of the conventional spectroscopy: (i) the wavelength range may be now extended down to very low values (10-20 cm^{-1}), both in infrared and Raman spectra, and (ii) the laser enables one to obtain Raman spectra from solid and/or coloured samples. On the other hand, the last decade brought about significant progresses in the conventional instrumentation itself, by improving the accuracy in band location (± 0.2 cm^{-1}), intensity and polarisation measurements, and by increasing the spectral resolution of fine structured bands (down to 0.25 cm^{-1} for infrared and 1 cm^{-1} for Raman spectra, see Chapter 2), due to the use of the grating or of more sensitive receptors.

Under these circumstances, a reconsideration of older studies on these compounds seems necessary - especially for finding, exactly locating and assigning the absorption or scattering bands in the range below 400 cm^{-1} (far-infrared), which had not

been within easy reach of conventional spectroscopy, and to get good spectra in the solid phase both in absorption spectroscopy and Raman scattering. Many of the older data are not very accurate with respect to the phases investigated - some compounds were studied in mixed or non-defined phases and, moreover, some others in solution; force constant calculations based on such data, or attempts at interpretation of the bonding must therefore be considered as partly suspect. Furthermore, the problem of the low energy lattice vibrations, generally below 200 cm^{-1}, could not be solved with conventional instrumentation and for many years the theoretical results of factor group (see Chapter 1) and other methods of vibrational analysis have lacked complete experimental support.

In the last few years, quite a lot of work has been carried out upon inorganic compounds, paying proper attention to the phase present and to the correct assignment of the bands, based on accurate polarisation determinations in the infrared spectra and depolarisation studies of the Raman bands. The data obtained and the increasing computing facilities have encouraged force constant calculations upon many classes of compounds. The information thus obtained has proved to be of great interest for chemical bond theory.

It is not necessary to emphasize the importance of a complete and detailed study of <u>all</u> the vibrations of a crystal. Knowledge of the symmetry species of normal modes enables conclusions to be drawn about the crystalline environment of a certain molecular unit, the structure of the crystal and the relative strength and type of

inter- and intramolecular bonds. More force constants may be calculated, and with greater accuracy, when more bands are correctly and precisely assigned; the potential force field may thus be known with less uncertainty. This fact has important consequences upon other physical studies, e.g. electrical, mechanical and thermal properties of crystals (see Chapter 1).

We have undertaken the study of crystalline and molecular optical vibrations for the class of ternary fluorides of general formula A_2MF_6, where M is Si, Ge, and Mn, and A - an alkali metal. The main reason for choosing Si, Ge and Mn as central atoms was that the three respective potassium salts, K_2MF_6, are usually taken as representative of the three structures in which most of the remaining A_2MF_6 compounds crystallize, having the O_h^5, D_{3d}^3, and C_{6v}^4 space groups (see Table 9, Chapter 4). Thus, the study could complete in the lattice vibrations range of the spectrum the existing data[1,2] on spectra-to-structure correlations for these typical compounds. Furthermore, some hexafluorosilicates, hexafluorogermanates and hexafluoromanganates(IV) crystallize in the cubic O_h^5 space group, for which the force constants may be easily evaluated (see Chapter 6). This permits some conclusions to be drawn on the nature of the bonds in all the remaining compounds of silicon, germanium and manganese (Chapter 7). The influence of the alkali metal ion A^+ upon the frequencies of the lattice vibrations of the three mentioned regular structures and upon some of the force constants may be also investigated. Finally, knowledge of the vibrational spectra in the solid state, over the entire frequency range (4000-40 cm^{-1}), together with the

unambiguous assignment of the bands, offers, by comparison with theoretical predictions, a test of the method of factor group analysis itself.

Some other related work has been published. Poulet and Debeau[3] have given a complete vibrational analysis, including force constant calculations, for a large number of cubic (O_h^5) A_2MX_6 compounds (X - halogen); a similar analysis has been carried out for some trigonal A_2MF_6 compounds by Sharp and Lane[4]; a detailed treatment of K_2NiF_6 has been made by Reisfeld[5]. All these papers, though dealing with particular A_2MX_6 structures, contain consistent solid state spectral data, which can be used for further work. The previously quoted papers[1,2] were dedicated to all three structures of A_2MF_6 compounds, but only spectra above 400 cm^{-1} were reported.

The present work reports the spectra of the representative compounds K_2SiF_6, K_2GeF_6 and K_2MnF_6 over the frequency range 2000-40 cm^{-1}, in solid state, and also the spectra of the similar compounds in which the K^+ cation is replaced by Rb^+ and Cs^+; the spectra of sodium salts, which occur with a lattice with lower (D_3^2) symmetry (see Table 9) due to the smaller size of Na^+ cation, are also reported. The low frequency spectra corresponding to the lattice vibrations are reported for the first time for most of these compounds. Factor group analyses are carried out for the typical K_2SiF_6, K_2GeF_6, K_2MnF_6, and Na_2MF_6 structures (Chapter 2) and correlation with experimental results is established whenever possible. Force constant calculations are carried out for 6 cubic A_2MF_6 structures out of the above mentioned compounds, and for K_2NiF_6, based on data of ref.[5]

Chapter 1 VIBRATIONAL SPECTRA OF CRYSTALS

The crystal is essentially an ordered, periodical arrangement of atoms. The main feature of a crystal is the existence of the unit cells - elementary volumes having identical sizes, shapes, orientation and composition, and which, taken together, fill the entire space of the crystal. The number of molecules in a unit cell is an integer. Starting from any one of the unit cells, the crystal may be reproduced by primitive translations of that cell along three independent directions. If $\vec{t}_1$, $\vec{t}_2$ and $\vec{t}_3$ are 3 primitive vectors of the smallest unit cell, then[6]

$$\vec{R}_n = n_1\vec{t}_1 + n_2\vec{t}_2 + n_3\vec{t}_3, \qquad (1)$$

where n_1, n_2 and n_3 are integers, represents the translation vectors to all the unit cells of an infinite crystal.

The unit cell itself has certain symmetry properties, which are best described in terms of rotation, reflection and non-primitive translations; a certain combination of these operations transforms the unit cell into itself.

The totality of operations, including primitive translations, which, when applied to a primitive unit cell leave the crystal invariant, form a group which is called the space group of the crystal. Since there are certain restrictions with respect to the permissible combinations between the point groups and the primitive and non-primitive translations, the number of space groups is limited. In three-dimensional space there exist 230 space groups and any crys-

tal must fall into one of these space groups. They may be generated by combining 14 different sets of vectors $\vec{t}_1$, $\vec{t}_2$, $\vec{t}_3$ (each describing a Bravais lattice) with 32 possible crystallographic point groups (each forming a crystal class). The 230 space groups may be classified according either to Schoenflies[7], or to the International Tables for X-Ray Crystallography (1952). Both these notations are useful in the study of vibrational and electronic spectroscopic properties of the crystals.

The 14 Bravais lattices are usually classified in 7 crystallographic systems: triclinic, monoclinic, orthorhombic, tetragonal, trigonal, hexagonal, and cubic, according to the various possible magnitudes and orientations of the vectors $\vec{t}_1$, $\vec{t}_2$ and $\vec{t}_3$. Sometimes, the trigonal system is included in the hexagonal system. For each Bravais lattice, a primitive unit cell may be chosen, the choice being not unique. For vibrational analysis, the unit cell to be chosen is the smallest possible (see later).

The space group S is an infinite group. However, the translations which carry a point of a unit cell into the equivalent point of another unit cell may be considered as identity operations. The remaining operations, relating to the symmetry properties of the unit cell itself, form by themselves a group, called the factor group F. We can write symbolically:

$$S = F \times T,$$

where T is the infinite group of the primitive translations. The factor group is always isomorphous with one of the crystallographic point groups. This does not mean that all the operations in a fac-

tor group and its isomorphous point group are identical: the factor group may contain non-point operations, such as screw rotations and/or glide reflections. This circumstance may lead to some difficulties in carrying out the factor group analysis (FGA, see later).

Any point in a crystal has a 'local' symmetry, i.e. the point is left invariant by some operations of the factor group. For most points, only the identity operation E leaves the point invariant. Some particular points are, however, situated at the intersection of two or more symmetry elements, and these are left invariant by the corresponding operations. All the symmetry operations which leave a certain point invariant form a group, called the site group of that point. This group describes the symmetry of the crystal as 'viewed' from the considered point, or the local symmetry around the point. The site group is isomorphous with a subgroup of the factor group and includes only point symmetry operations. Obviously, the site group must be also a subgroup of the molecular group to which the molecule or ion under study belongs.

The first step towards the understanding of the influence of the lattice environment upon the vibrational modes (or other physical properties) of the molecule consists in finding the type of the site occupied by the molecule or ion in the crystal. Sometimes, the site group analysis (SGA) alone is sufficient to provide the selection rules and to explain some features of the spectra in solid phase[8]. This is nevertheless only a preliminary approach, in which the motions of the molecule are supposed to have no relation at all with the motions of the rest of the crystal. This approach,

therefore, will not result in the knowledge of the lattice modes. Consideration of the interactions between the constituents of a crystal, which cannot be always neglected, the factor group analysis, permits knowledge of all vibration modes of the crystal.

Vibrations of Molecular Crystals

Vibrational spectroscopy of solids is a helpful instrument for studying the molecular structure, the molecular and atomic motions, and the intermolecular forces in crystals. The greatest advantage is taken from it when the spectra are obtained from single crystal samples. Nevertheless, the spectra still remain useful when polycrystalline samples only are available; in fact, this is for the present the most common situation, since most compounds cannot be grown into single crystals of suitable size and/or cut along any desired plane for subsequent spectroscopic examination.

In what follows, a short discussion will be given on some particular aspects of the vibrational spectroscopy of crystals, especially those related to the problems of structure elucidation. The discussion will be limited to the families of molecular and ionic crystals only, i.e. the crystals in which individual molecular units, or polyatomic ions, can still be identified, and in which the forces between these units are weak compared to the intramolecular forces.

For a non-linear free molecule containing r atoms, there are $3r - 6$ normal modes of vibration[9], which can be classified among various symmetry species - the irreducible representations of the molecular group to which the molecule belongs. When such molecules

are brought together to form a crystal, the study of the vibrations of its constituents may be reduced to the study of a single unit cell, owing to the translational periodicity of the lattice[10]. If n is the number of molecules (or ions) per unit cell, the total number of modes of vibration of the unit cell will be $3rn$. Of these, $(3r - 6)n$ belong to the molecules, which do not lose their individuality in the crystal, and are therefore termed 'molecular' or 'internal' modes. The remaining $6n$ modes are characteristic for the motions of the molecules one against another and are called 'lattice' or 'external' modes of vibration.

The distinction of the vibration modes into 'molecular' and 'lattice' modes is very useful in the vibrational analysis, but it has no sound physical justification. The energy levels of a solid constitute an intrinsic property of the solid as a whole. Since the forces between atoms are usually larger within the molecular groups constituting the crystal than the intermolecular forces, the lattice vibrations will have generally lower frequencies than the molecular vibrations, but not all bands appearing in the far infrared should be automatically assigned to the lattice modes.

The lattice modes can be further classified according to the type of intermolecular motion, into 'rotatory' (or 'librational') ($3n$ of them) and 'translatory' $[3(n - 1)]$. The remaining 3 modes represent the motions (translations) of the unit cell as a whole and are called 'acoustic' (for reasons which will be discussed later in this chapter). The $3rn - 3$ modes which remain after subtraction of the acoustic modes from the total number of modes are cal-

led 'optical'.

The study of the interactions governing the behaviour of solids by means of infrared and Raman spectroscopy involves measurement of both optically active lattice and molecular modes. By 'measurement' one usually means location of the infrared absorption bands and Raman scattering bands, and sometimes determination of intensities and polarisation. Much information is also available from band shapes and fine structure.

All these factors may be influenced by the conditions in which the molecule exists in the crystal. The potential energy function of the free molecule (or ion) is usually significantly perturbed by the field of the surrounding lattice. Moreover, interactions occur in the crystal between the internal modes of the molecule, or between the internal and the lattice modes, which meet the necessary symmetry requirements. These interactions may lead to appreciable changes in the spectra as compared with those of the free molecule, and the correct interpretation of these modifications may result in useful conclusions about the structure and dynamics of the crystal.

Usually, two kinds of approximations are used in the study of the crystal vibrations:

(i) Born-Oppenheimer approximation. Generally, the Hamiltonian of a crystalline system is a function of the coordinates and momenta of all nuclei and electrons. However, the large difference in the masses and, hence, in the velocities of these particles makes plausible the assumption that the electrons follow the nuclear

motions adiabatically, moving as if the nuclei were fixed. This assumption leads to a separation between electronic and nuclear motions. To explain an important class of phenomena, including electronic conduction or electric resistivity in crystals, this approximation is no longer considered suitable and electron-phonon interactions have to be taken into account. On the other hand, coupling of the electronic and vibrational excitations (exciton-phonon interaction) might influence[11] the line shape and line temperature dependence in the electronic spectra, or the processes of energy transfer and excitation trapping[12].

(ii) Harmonic approximation. After the adiabatic separation of the electronic motions, the Hamiltonian of the nuclei will consist of the kinetic energy of these nuclei, plus the potential energy, which is a function of the nuclear coordinates and has the periodicity of the lattice. This potential function, which has a minimum value for the equilibrium configuration, may be expanded in powers of the nuclear displacements u_k from the equilibrium positions:

$$V = \sum \phi_k u_k + \tfrac{1}{2} \sum \phi_{kl} u_k u_l + (1/6) \sum \phi_{klm} u_k u_l u_m + \ldots$$

Usually this expansion is terminated after the 2nd power:

$$V = \tfrac{1}{2} \sum \phi_{kl} u_k u_l \qquad (2)$$

(the first term vanishes because V must have a minimum in the equilibrium configuration and thus its first derivatives must vanish). ϕ_{kl} is the real symmetric matrix of the force constants. This approximation is called harmonic and is most often sufficient

for spectroscopic calculations. However, phenomena such as thermal expansion, heat conduction, elastic behaviour etc., can only be explained by taking into account the phonon-phonon interaction, i.e. higher (anharmonic) terms in the expansion of V.

The dynamics of a crystalline lattice may be best understood by considering the crystal as a system of coupled oscillators[13], sometimes with the simplifying assumption that the coupling is effective between nearest neighbouring atoms only. The deviations of the atoms from their equilibrium positions are supposed to be small enough not to destroy the structure of the lattice. The restoring forces are, in the harmonic approximation, proportional to these deviations. The potential energy function V, defined by

$$\vec{F} = -\nabla V \tag{3}$$

is subject, owing to the translational periodicity of the lattice, to the condition

$$V(\vec{r} + \vec{R}_n) = V(\vec{r}) \tag{4}$$

where $\vec{R}_n$ is the translation vector defined by (1), and $\vec{r}$ is the position vector of a point in the unit cell.

We will treat first the unidimensional case of a chain of N identical atoms (Figure 1), 1 and N being the terminal atoms. If u_n is the displacement of the nth atom and Φ is the respective force constant, the potential function is

$$V(x) = \tfrac{1}{2}\Phi\left[\sum_{1}^{N-1}(u_{n+1} - u_n)^2\right] + V'(x) \tag{5}$$

when the assumption is made that the coupling exists between nearest

neighbours only. For the terminal atoms a supplementary condition must be given, in order to specify the form of V'; when these are to be treated in the same manner as the other (middle) atoms, use is made[14] of the Born-von Karmann cyclic boundary condition:

$$u_{n+N} = u_n. \tag{6}$$

This condition means that the atoms 1 and N are bonded together by similar forces to those acting between internal atoms. For

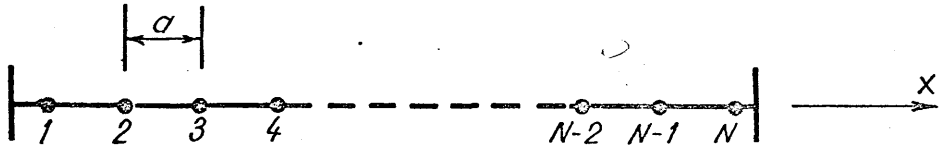

Figure 1

such a cyclic chain, the potential (5) for the longitudinal vibrations becomes

$$V(x) = \tfrac{1}{2}\Phi\left[\sum_{1}^{N-1}(u_{n+1} - u_n)^2 + (u_N - u_1)^2\right].$$

The Hamiltonian of the system is

$$H = \sum_{1}^{N}\frac{p_n^2}{2m} + \tfrac{1}{2}\Phi\left[\sum_{1}^{N-1}(u_{n+1} - u_n)^2 + (u_N - u_1)^2\right], \tag{7}$$

where p_n is the momentum of the nth atom and m its mass. Resolution of the Schroedinger equation

$$HB_n^k = \omega_k^2 B_n^k, \tag{8}$$

where B_n^k are N independent orthonormal eigenvectors, leads to the following values for the eigenvalues and eigenvectors[15]:

$$\omega_k = 2\omega_o\left|\sin\frac{ka}{2}\right| \tag{9}$$

$$B_n^k = \frac{1}{\sqrt{N}}\exp(ikna) \tag{10}$$

where $\omega_o = \sqrt{\Phi/m}$. Owing to the cyclic condition (6), $\exp(ikNa) = 1$ and therefore $\underline{k}$ is restricted to certain permissible values given by[16]

$$|k| = \frac{2\pi}{Na} \cdot p \quad (p = 1,2,\ldots,N). \tag{11}$$

Since $\underline{k}$ occurs only in $\exp(ikna)$, adding to $\underline{k}$ multiples of $2\pi/a$ changes nothing and we can further restrict $\underline{k}$ to the interval

$$-\pi/a \leqslant k \leqslant +\pi/a \tag{12}$$

Let us consider now a linear cyclic chain which consists of N cells of length $\underline{a}$, each cell containing $\underline{m}$ atoms (linear chain with a 'basis'). The eigenvectors may be chosen in the form[15]

$$B_n^k = \frac{1}{\sqrt{N}} f_v^k \exp(ikx) \tag{13}$$

where $x = na + v$ represents the equilibrium position of the atoms and $\underline{v}$ is the distance from the origin of the unit cell to the equilibrium position of the atom. These functions are plane waves, modulated by means of a function f_v^k which has the periodicity of the lattice. The eigenvalues are obtained by solving the equations

$$\sum_{v'} C_{vv'}(k) f_{v'}^k = \omega_k^2 f_v^k \tag{14}$$

which result from the general equations (8) by using the modulated expression (13) for B_n^k and where $C_{vv'}$ is a Hermitean matrix with $\underline{m}$ rows and $\underline{m}$ columns. For each value of $\underline{k}$ in the interval $(-\pi/a, +\pi/a)$, these equations give $\underline{m}$ frequencies and $\underline{m}$ vectors f_v^k. Therefore, there will be $\underline{m}$ branches of the frequency as a function of $\underline{k}$. One branch represents the sound waves when $\underline{k}$ is small, and is therefore called <u>acoustic</u>. The acoustic modes are excited when all atoms

in the unit cell move together (in phase) and for $k = 0$ the frequency of this vibration is zero (there is no displacement of charge). The other branches have high frequency values even for $k \longrightarrow 0$. Since this type of vibration produces a displacement of the charges of the atoms they appear in the infrared spectra and are called optical. In the optical modes, the atoms in the cell vibrate one against other (out of phase, Figure 2a). For $k = 0$, all the atoms which occupy identical positions in different unit cells move in phase irrespective of the kind of branch.

For a three-dimensional crystal (with 'basis', i.e. a 'complex' unit cell) containing N unit cells and m atoms per unit cell (the atoms being different either by their kind or by the site they occupy in the cell), following the same argument, the eigenvectors can be chosen so that they are multiplied by a phase factor $\exp(i\vec{k}\cdot\vec{R})$ under a translation $\vec{R}$ which carries a cell to another identical cell;

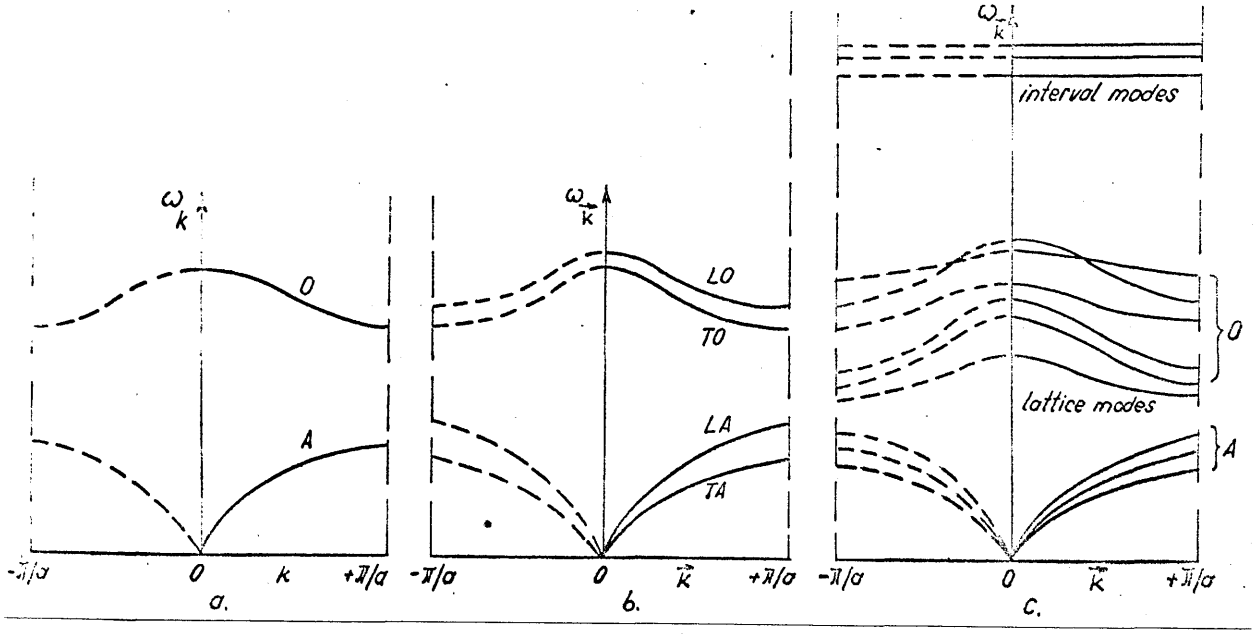

Figure 2

the modulating factor $\underline{f}$ is a $\underline{m}$-component vector which has the periodicity of the lattice. For each $\vec{k}$ there are $3\underline{m}$ independent eigenvalues which can be determined from spatial equations similar to (14). There are now $3\underline{m}$ branches of frequency as functions of the wave vector $\vec{k}$, three out of which are acoustic and the remaining ones optical. In Figure 2b these branches, known as dispersion curves, are shown for the NaCl crystal ($m = 2$, 6 branches). Longitudinal and transverse modes are indicated by L and T, respectively, The TA and TO modes are doubly degenerate for NaCl (and other cubic crystals). For crystals such as diamond, with two identical atoms per unit cell, LO and TO are degenerate for $\vec{k} = 0$. The shape of various dispersion curves of a crystal may be found from elastic constants, specific heat, neutron scattering and other studies.

The group velocity of a wave which propagates through a solid is given by the slope of the corresponding dispersion curve,

$$v_g = 2\pi \frac{\partial \omega_k}{\partial k} . \qquad (15)$$

For $|\vec{k}| = 0$, this velocity is different from zero for the acoustic modes only; the optical modes, for which $v_g = 0$ at $|\vec{k}| = 0$ and $\pm\pi/a$, are standing waves. In the general case, for every branch and every value of $\vec{k}$ there would be a different velocity of propagation of the corresponding wave through the crystal. In particular, T and L modes would propagate with different velocities, unless they are degenerate. As a rule, the velocity of any T mode is not larger that of the corresponding L mode.

It should be mentioned that this concept of T and L modes follows

the terminology used in the study of sound propagation in elastic solids and it is not strictly correct when other than acoustic modes are concerned. Moreover, this terminology is improper, even for the acoustic modes, for an anisotropic crystal.

Quantum-mechanically, and by analogy with the treatment of the electromagnetic radiation, the propagation of an elastic wave through a crystal may be interpreted as the propagation of a particle, the phonon. The wavelength λ of the wave associated to this phonon is given by

$$|\vec{k}| = 2\pi/\lambda . \tag{16}$$

The approximation $|\vec{k}| = 0$ works at long wavelengths, i.e. at wavelengths much larger than the lattice constant:

$$\lambda \gg a. \tag{17}$$

For the optical lattice vibrations, which generally appear below 200 cm^{-1}, $\lambda \gtrsim 500$ Å and this condition is fulfilled, since for most lattices a does not exceed ca. 10-20 Å.

A very convenient way of visualising the effect of the wave vector $\vec{k}$ on the behaviour of various modes is to introduce the reciprocal lattice. Three new lattice vectors are defined by

$$\vec{t}_1^{\,*} = 2\pi \frac{\vec{t}_2 \times \vec{t}_3}{\vec{t}_1 \cdot (\vec{t}_2 \times \vec{t}_3)}, \quad \vec{t}_2^{\,*} = 2\pi \frac{\vec{t}_3 \times \vec{t}_1}{\vec{t}_1 \cdot (\vec{t}_2 \times \vec{t}_3)}, \quad \vec{t}_3^{\,*} = 2\pi \frac{\vec{t}_1 \times \vec{t}_2}{\vec{t}_1 \cdot (\vec{t}_2 \times \vec{t}_3)} .$$

The advantage of working in reciprocal space is that the wave vector $\vec{k}$ may be expressed very simply in terms of a translation vector[17], i.e.

$$\vec{k} = n_1^* \vec{t}_1^{\,*} + n_2^* \vec{t}_2^{\,*} + n_3^* \vec{t}_3^{\,*}, \tag{18}$$

where n_1^*, n_2^*, n_3^* are integers. For this reason the reciprocal lattice is often called the $\vec{k}$- or wave vector-space. The condition (12) previously stated for $\vec{k}$ defines in the $\vec{k}$-space a zone which is called the <u>first (basic) Brillouin zone</u>. The distribution of mode frequencies in $\vec{k}$-space is uniform, filling the first Brillouin zone. For an infinite crystal ($N \to \infty$), the states density becomes very large and the frequency spectrum is almost continous. For spectroscopic purposes only the frquencies at the middle of this zone ($|\vec{k}| \approx 0$) are of interest (because they represent stationary waves created by atoms in the cell moving with a maximum phase difference). At this particular point of the 1st Brillouin zone the frequencies of all acoustic modes are zero; in the general case of a unit cell containing more kinds of atoms, or identical atoms situated at different sites, the frequencies of all transverse or longitudinal optical modes are different, although very often some of these modes may be degenerate. For higher $|\vec{k}|$ in the zone, the frequencies of the optical modes are in general lower than for $|\vec{k}| = 0$ and at certain points they become degenerate. Moreover, the group velocities of the corresponding waves become different from zero, i.e. the waves begin to travel through the crystal and the modes can no longer be infrared or Raman active as fundamentals. Therefore, the $|\vec{k}| \approx 0$ approximation may be considered as a (translation group) <u>selection rule</u> for the infrared and Raman spectra of the lattice vibrations. As for the frequencies of the internal modes of the molecule (or ion), they remain practically unchanged when $|\vec{k}|$ varies from $-\pi/a$ to $+\pi/a$ (Fig. 2c), so that their measurement is immaterial of the choice of a particular point in the

zone (they are standing waves throughout the whole zone).

The dispersion curves ω vs. $\vec{k}$ are significantly modified in the presence of an electromagnetic field; the selection rule in the case when the photon produces a single phonon is

$$\vec{K} - \vec{k} = 0, \tag{19}$$

where $\vec{K}$ is the wave vector of the photon (for one-photon processes). This influence is particularly important for $|\vec{k}| = 0$, and for frequencies of the electromagnetic radiation which are more or less close to some excitation frequency of the crystal itself. This photon-phonon interaction, which appears particularly at the middle of the Brillouin zone, is not at present well understood and the interpretation of the infrared and Raman spectra is therefoer sometimes difficult.

Although the points of the first Brillouin zone other than the middle one are irrelevant for the infrared and/or Raman activity of the fundamental modes, they may play a very important part in the activity of combination modes[18]. For these latter bands the $\vec{k} = 0$ selection rule is no longer strictly valid and it is not justified to assign combinations of internal and lattice modes as resulting from $\vec{k} \approx 0$ motions. The selection rule for this case is

$$\vec{K} - \sum \vec{k}_i = 0, \tag{20}$$

where $\vec{k}_i$ is the wave vector of the ith mode and summation is carried over all participating modes (multi-phonon processes). The multi-phonon processes are generally weak, but still possible. The $\vec{k} = 0$ selection rule being no longer obeyed in these cases, an almost infinite number of frequencies would be possible in a

crystal - these frequencies arising from normal mode vibrations which are out-of-phase by varying amounts in successive unit cells. This means that a continous rather than a band-like absorption should be expected. Sometimes, however, infrared or Raman bands which occur in the spectra can be interpreted as a simple algebraic sum of various internal and lattice frequencies observed as fundamentals (according to the specific provisos of the group theory); this is merely due to accidental singularities in the phonon frequency distribution[18]. These singularities may be found from the shape of the dispersion curves, but such curves are only known for a limited number of cases, and then only approximately. Actually, there is evidence[19] that $\vec{k} \neq 0$ lattice modes may appear in combination with internal modes in the infrared and Raman spectra of some crystals. At present, no definite assignment of the combination bands - especially of their half-band width - could provide essential information concerning the phonons taking part in the absorption or scattering processes, and thus on the phonon-phonon interactions.

Factor Group Analysis

The motions of the nuclei can be classified according to several procedures, all of them based on group theory.

The first logical approach would be, as mentioned, to consider just the local environment of the molecule or ion. The molecule is supposed to move in a potential field which reflects the symmetry of the surrounding crystal; this is precisely the symmetry of the site group of the molecule[8,20]. Thus the analysis reduces to identifying the site group and working out the selection rules for its

irreducible representations on well-known lines[21]. The procedure accounts for a certain number of frequencies - those derived from the internal motions of the free molecule. No information concerning the intermolecular motions can be obtained. The site group analysis (SGA) is very often useful when only an analysis of the splitting of the internal modes is sought. These splittings can be easily found by simply using the correlation tables for the molecular group and certain of its subgroups - the site groups of the molecule in the crystal. In a paper of Winston and Halford[20], a thorough critical analysis of the method is carried out, with particular attention to the relation among various crystal groups. One of the main interests of the site group approach consists, according to the above quoted reference[20], in the fact that it may serve as a preliminary analysis, very easy to deal with, of the nuclear motions in a crystal. We will use it in Chapter 3 as a means to find the smallest Bravais unit cell necessary to carry out the factor group analysis.

A more elaborate approach would consist in considering the unit cell as an assembly of atoms which vibrate. The free molecule is replaced by this assembly of atoms, and the well established methods of analysis of the atomic vibrations in a free molecule can be applied with no change except for the new symmetry of the assembly. Since the operations which leave the unit cell invariant form a group, the factor group, this method is called <u>factor group analysis</u> (FGA)[10,22].

In their paper[20], Winston and Halford observed that site group

and factor group analyses must give identical results, since all the operations of the factor group can be obtained by taking all possible products of the operations contained in the site groups.

As mentioned earlier, the factor group may contain non-point operations (screw rotations or glide reflections), so that, unlike the case of molecular point groups, certain of these factor group operations can carry an atom of a unit cell into an atom of <u>another</u> unit cell. In FGA, an atom in a unit cell is considered invariant under a symmetry operation either when it is left unchanged, or when is carried into an equivalent position in another unit cell. By equivalent positions one means those positions which can be reached by primitive translations. The main problem after determining the symmetry group is to reduce the representation Γ of the motions of all atoms in the unit cell among the irreducible representations Γ_i of the factor group in question.

Let N_i be the number of times an irreducible representation Γ_i is contained in the reducible representation Γ. This number can be found[21] from the equation

$$N_i = \frac{1}{N} \sum_j h_j \chi_i(R) \chi'_j(R), \qquad (21)$$

where N is the order of the group, h_j is the number of operations in the <u>j</u>th class of the group, and $\chi_i(R)$ and $\chi'_j(R)$ are the characters of the group operation R in the representations Γ_i and Γ, respectively. The normal modes can be classified using a suitable choice of the reducible representation Γ. If Γ is defined, as in the case of the free molecule[21], by all 3<u>rn</u> Cartesian coordi-

nates (r and n being, as before, the number of atoms in the molecule and the number of molecules per unit cell, respectively), the distribution of the normal modes among the symmetry species of the factor group can be found by using the following expressions[22] for χ'_j:

- for the total number of modes n_i:

$$\chi'_j(n_i) = \omega_R(\pm 1 + 2\cos\varphi_R) \qquad (22)$$

where ω_R is the number of atoms which remain invariant (in the above defined sense) under operation R, and φ_R is the angle of rotation; the upper and lower signs referring to proper and improper rotations, respectively[21]. It should be remembered that the identity operation and the rotations around C_n axes are 'proper' rotations, while the inversion i, plane reflections σ and the rotations around S_n axes are 'improper' rotations.

- for the number of acoustic modes T:

$$\chi'_j(T) = \pm 1 + 2\cos\varphi_R \qquad (23)$$

- for the number of translatory lattice modes T':

$$\chi'_j(T') = \left[\omega_R(s) - 1\right](\pm 1 + 2\cos\varphi_R) \qquad (24)$$

where $\omega_R(s)$ is the number of structural groups which remain invariant under operation R.

- for the number of rotatory (librational) lattice modes R':

$$\chi'_j(R') = \omega_R(s\text{-}p)(1 \pm 2\cos\varphi_R) \qquad (25)$$

where $\omega_R(s\text{-}p)$ is the number of polyatomic groups (molecules or polyatomic ions) invariant under operation R. For the rotatory

lattice modes, the monoatomic groups need not be taken into account since they do not have rotational degrees of freedom. For linear polyatomic groups (oriented along a c-axis), the relation (25) is replaced by[22]

$$\chi_j'(R') = \omega_R(s-p)(\pm 2\cos\varphi_R) \text{ for all operations C and S}$$
$$\chi_j'(R') = 0 \text{ for } C_2 \text{ and } \sigma_v. \qquad (25')$$

- for the number of internal (molecular) modes n_i' may be found from the relation

$$n_i' = n_i - (T + T' + R') \qquad (26)$$

when there is a single structural group in the unit cell. For two or more structural groups, the number of internal modes of each one group is found by ignoring in turn all other groups. For n identical molecules per unit cell, the total number of internal modes must be finally $(3r - 6)n$.

Expressions (22) to (25) are substituted in (21) in order to find the distribution of the various kinds of normal modes among the symmetry species of the factor group.

In vibrational spectroscopy, the selection rules may be found by taking into account the laws of conservation (for energy and momentum). According to the first of these laws, the energy of the photon must equal the energy of the phonon which is created in the crystal. As already mentioned, the wavelength of the electromagnetic radiation used in infrared and Raman spectroscopy is much larger than the lattice constants, so that we may take $\vec{K} \approx 0$ in eq. (19). This means that in vibrational spectroscopy,

due to the conservation of momentum, only long-wavelength ($\vec{k} \approx 0$) vibrations are excited. For multiple-phonon processes, the corresponding restriction is, according to eq. (20), $\sum \vec{k}_i \approx 0$. These relations may be regarded as translation group selection rules. Once these rules are satisfied, the problem of finding which of the previously calculated normal vibration modes are infrared- and/or Raman-active may be solved in the usual way[21], i.e. by finding whether various integrals giving the intensity of infrared absorption and of Raman scattering lines, respectively,

$$\vec{M}_{if} = \int \psi_i^* \vec{M} \psi_f d\tau \tag{27}$$

$$\alpha_{if} = \int \psi_i^* \alpha \psi_f d\tau \tag{28}$$

are different from zero. Here $\vec{M}$ and α are the electrical momentum vector and the electrical polarization symmetric tensor, respectively, and ψ_i and ψ_f are the initial and final quantum states of the system. To be different from zero, the integrands in eqs. (27) and (28) (or certain of their components only) must contain the totally-symmetric representation of the factor group. The problem reduces therefore to finding the products $\psi_i^* \psi_f$ which contain one of the representations of the vector $\vec{M}$ or of the tensor α. These representations of $\vec{M}$ and α are given by[20]

$$\chi_j'(\vec{M}) = \pm 1 + 2\cos\varphi_R \tag{29}$$

$$\chi_j'(\alpha) = 2(1 \pm \cos\varphi_R + \cos 2\varphi_R) \tag{30}$$

where again the upper sign is taken for proper rotations and the lower for improper rotations. Equation (29) is identical to (23),

which gives the representations of the acoustic modes, since the electrical momentum vector $\vec{M}$ is essentially a translation vector.

As mentioned, the space group is the product of the translation and factor groups. The $\vec{k} = 0$ selection rule means that the translation group has just one irreducible representation, the totally-symmetric. The vectors and symmetric tensors are invariant under translation, so that they belong to this totally-symmetric representation. They must therefore belong to various factor group representations in the space group. This reasoning justifies the name of <u>factor group selection rules</u> given to the above procedure for finding active and inactive fundamental modes.

As an example of the use of FGA we will treat the case of GeO_2 (TiO_2 rutile structure)[23].

The rutile crystal belongs to the D_{4h}^{14} ($P4_2/m2_1/n2/m$) space group, with 2 'molecules' per unit cell. The unit cell, together with its symmetry elements are illustrated in figure 3. Since

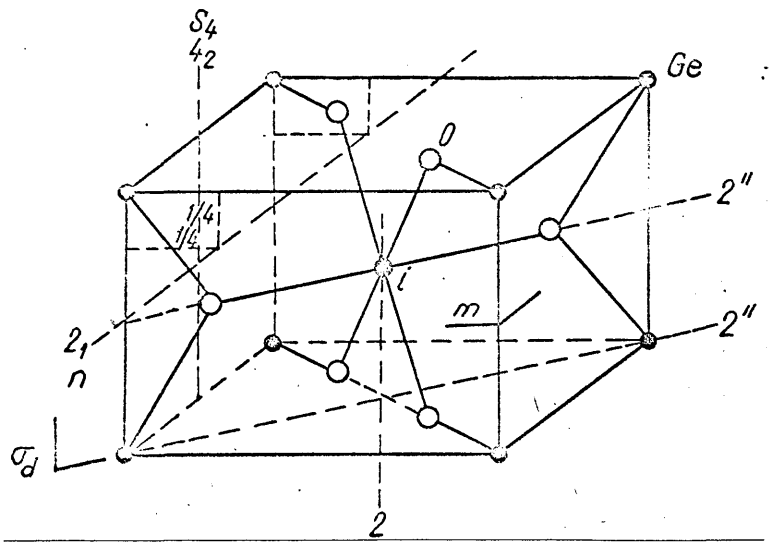

Figure 3

there are 6 atoms in the unit cell, there will be 18 degrees of freedom (modes of vibration), 3 out of which are acoustic and 15 optical. The symmetry operations of the cell (noted on Fig. 3 with the International Tables symbols) can be related to the (point) factor group D_{4h} operations in the following way:

$$E \longrightarrow E,\ 4_2 \longrightarrow C_4,\ 2_1 \longrightarrow C_2',\ 2 \longrightarrow C_2,\ 2'' \longrightarrow C_2'',\ i \longrightarrow i$$

$$S_4 \longrightarrow S_4,\ m \longrightarrow \sigma_h,\ n \longrightarrow \sigma_v,\ m' \longrightarrow \sigma_d.$$

The number of invariant atoms (ω_R), structural groups ($\omega_R(s)$) and polyatomic groups ($\omega_R(s\text{-}p)$), together with the calculated χ_j' and number of modes of each kind, are given in Table 1. It was assumed that GeO_2 is not a molecular polyatomic group. Indeed, in the crystalline state, each Ge atom is surrounded by 6 O atoms at equal distances (within 2% - this figure being not valid for other rutile structures). All the resulting modes are lattice modes. Owing to the absence of polyatomic groups, there are no rotational degrees of freedom and all modes are translatory. The infrared spectrum of GeO_2 should consist of 4 bands:

$$A_{2u} + 3E_u.$$

In the Raman spectrum there should be also 4 bands:

$$A_{1g} + B_{1g} + B_{2g} + E_g.$$

The modes A_{2g}, $2B_{1u}$ are optically inactive.

The observed infrared and Raman spectra of GeO_2 are shown in Chapter 2 (Figures 6 and 8).

Table 1

Factor group analysis for GeO_2 (rutile structure) (reference 23)

D_{4h}^{14}	E	$2C_4$ (4_2)	C_2 ($\equiv C_4^2$)	$2C_2'$ (2_1)	$2C_2''$	i	$2S_4$	σ_h (m)	$2\sigma_v$ (n)	$2\sigma_d$ (m)	Infrared	Raman	n_i	T	T'	R'	α	n_i'
A_{1g}	1	1	1	1	1	1	1	1	1	1		$\alpha_{xx}+\alpha_{yy}$, α_{zz}	1	0	1	0	2	0
A_{2g}	1	1	1	-1	-1	1	1	1	-1	-1	R_z		1	0	1	0	0	0
B_{1g}	1	-1	1	1	-1	1	-1	1	1	-1		$\alpha_{xx}-\alpha_{yy}$	1	0	1	0	1	0
B_{2g}	1	-1	1	-1	1	1	-1	1	-1	1		α_{xy}	1	0	1	0	1	0
E_g	2	0	-2	0	0	2	0	-2	0	0	(R_x, R_y)	$(\alpha_{yz}, \alpha_{zx})$	1	0	1	0	1	0
A_{1u}	1	1	1	1	1	-1	-1	-1	-1	-1			0	0	0	0	0	0
A_{2u}	1	1	1	-1	-1	-1	-1	-1	1	1	T_z		2	1	1	0	0	0
B_{1u}	1	-1	1	1	-1	-1	1	-1	-1	1			2	0	2	0	0	0
B_{2u}	1	-1	1	-1	1	-1	1	-1	1	-1			0	0	0	0	0	0
E_u	2	0	-2	0	0	-2	0	2	0	0	(T_x, T_y)		4	1	3	0	0	0
φ_R	0	90	180	180	180	180*	90*	0*	0*	0*	Number of degrees of freedom		18	3	15	0	//	0
ω_R	6	0	2	0	4	2	0	6	0	4								
$\chi_j'(n_i)$	18	0	-2	0	-4	-6	0	6	0	4								
$\omega_R(s)$	6	0	2	0	4	2	0	6	0	4								
$\chi_j'(T')$	15	-1	-1	1	-3	-3	1	5	-1	3								
$\omega_R(s\text{-}p)$	0	0	0	0	0	0	0	0	0	0								
$\chi_j'(R')$	0	0	0	0	0	0	0	0	0	0								
$\chi_j'(T)=\pm 1 + 2\cos\varphi_R$	3	1	-1	-1	-1	-3	-1	1	1	1								
$\chi_j'(\alpha)=2(1\pm\cos\varphi_R+\cos 2\varphi_R)$	6	0	2	2	2	6	0	2	2	2								

* Improper rotations

Chapter 2 PRINCIPLES OF FAR INFRARED INSTRUMENTATION

The vibrational spectroscopic studies of metal complexes had been limited until recently to the location and measurement of optically active modes whose frequencies are situated above 300-400 cm^{-1}. This region is characteristic for the various modes of the metal-ligand bond. The existing conventional instrumentation did not allow the study neither of skeletal modes of the complexes, whose frequencies are located far below the limit of these spectrometers, nor of lattice modes, which arise from the lattice specific effects.

We will sketch the improvements in the instrumentation which have brought about the extension of the band measurements below the mentioned threshold. We will divide the discussion into two sections:

(i) Absorption and Reflectance Far Infrared Spectrometry; and

(ii) Laser Raman Spectroscopy.

(i) The success and spread of the infrared spectrometry has been mostly based on the use of the principle of dispersion. Prisms and/or gratings have been used to disperse, in terms of frequency, a mixture of radiations of various wavelengths coming from an appropriate infrared source. The almost monochromatic radiation thus obtained is passed through the sample (in the absorption procedure) and the transmitted radiation is compared (by intensity) with the incident radiation. When a range of wavelengths

is passed through the sample an energy spectrum is obtained which shows certain features characteristic to the sample. If the wavelength range scanned does not contain frequencies characteristic to the molecular species present in the sample, the spectrum will consist of a continuous line corresponding to 100 % transmittance. If in the range there exist such frequencies, a corresponding number of 'absorption' bands will appear, arising from allowed transitions between various energy levels of the molecule. The dispersion procedure allows cover of a wide range of energies, from around 200-300 to above 4000-5000 cm^{-1}. The resolution power may vary very much within this range depending on the kind of dispersing unit used, but generally it is larger and more uniform when using gratings instead of prisms. Some of the spectrometers working on the grating principle have been fitted for the low frequency region (e.g. Beckman IR 11), although the weakness of the sources in this region requires large slit-widths and, consequently, have reduced resolution (0.5-1 cm^{-1}).

Alternatively, some non-dispersive methods have been developed, mostly based on filters or interferometers, but they have not had widespread use because of technical difficulties. However, in the last decade, improvements in electronic techniques, the intensity of light sources, and the sensitivity of detectors have allowed a revival of these methods, which show very good efficiency especially in the low energy region. Since it does not make use of dispersing units and narrow slits and since it enables good resolution to be reached, the interference method can give excellent

spectra even with medium light sources and light detectors.

In what follows, a description of the principle of the interferometric method will be given, since it constitutes today a highly efficient tool in the study of low energy vibrations in crystals.

Interferometry originates[24] in the works of J.B.J. Fourier (1823), who demonstrated that any complex periodical curve may be transformed into a superposition of sine and/or cosine curves. The next step was made by A.A. Michelson (1890), who built an interferometer for measuring the velocity of light; he also discovered that an interferogram may be transformed into a spectrum (energy vs. frequency) after being decoded by Fourier analysis; this spectrum contains the usual information about the characteristic absorption of the sample.

A schematic representation of the Michelson interferometer is shown[25] in Figure 4. The light beam from source S is divided by

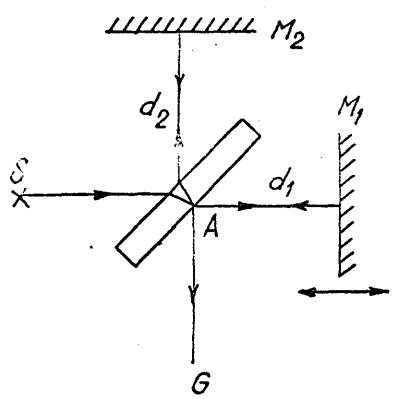

Figure 4

a beam splitter into two beams, the first falling on a plane moving

mirror M_1 and the second on a plane fixed mirror M_2. The 2 beams recombine at A and the emerging beam falls on a Golay detector G. The intensity of the recombined beam is a periodical function of the difference $\underline{x}$ of total path length of the two beams before recombination, which depends, in turn, of the position of M_1. For $x = 0$ and other $\underline{x}$ values for which the two beams arrive at A in phase all frequencies of the incident light interfere constructively; when the path difference $\underline{x}$ is such that the beams are 180^{o} out of phase, they interfere destructively. If the light is monochromatic (wavelength ω_o), the intensity of the light falling on the detector is[26]

$$I(x) = a_1^2 + a_2^2 + 2a_1a_2\cos 2\pi\omega_o x \qquad (32)$$

where a_1 and a_2 are the amplitudes of the two beams. If these amplitudes are equal, as in the case of unpolarized light,

$$I(x) = I(1 + \cos 2\pi\omega_o x) \qquad (33)$$

where $I = 2a^2 =$ constant. When the incident light is no longer monochromatic,

$$I(x) = \int_{-\infty}^{+\infty} I(\omega)d\omega + \int_{-\infty}^{+\infty} I(\omega)\cos 2\pi\omega x.d\omega . \qquad (34)$$

The value of the intensity at $x = 0$ is

$$I(0) \equiv I_o = 2\int_{-\infty}^{+\infty} I(\omega)d\omega . \qquad (35)$$

The difference

$$F(x) = I(x) - I_o/2 = \int_{-\infty}^{+\infty} I(\omega)\cos 2\pi\omega x.d\omega \qquad (36)$$

is called the <u>interfereogram function</u>. For monochromatic light, the interferogram is simply a single cosine wave, whose modulation frequency is generally in the audio range. A polychromatic source

will produce a number of overlapping cosine waves, which can be analysed by means of Fourier transform. The Fourier transform of the right hand side of eq. (36) is

$$I(\omega) = \int_{-\infty}^{+\infty} F(x)\cos 2\pi\omega x.dx. \qquad (37)$$

In practice only a finite interval of distances (-X,+X) can be scanned, so that

$$I(\omega) = \int_{-X}^{+X} F(x)\cos 2\pi\omega x.dx. \qquad (38)$$

F(x) is symmetrical about the zero path difference, so that

$$I(\omega) = 2\int_{0}^{+X} F(x)\cos 2\pi\omega x.dx. \qquad (39)$$

The greater the displacement X of the mirror M_1, the greater is the information contained in the interferogram. Equation (39) becomes useful if integration is replaced by summation over a finite number of $\underline{x}$ values:

$$I(\omega) = 2\sum_{0}^{X} F(x)\cos 2\pi\omega x.\Delta x. \qquad (40)$$

In this summation, points have to be sampled at intervals of

$$\Delta x \leqslant 1/(2\omega_{max}) \qquad (41)$$

in order to obtain from the interferogram all the available information in the frequency range $0 < \omega < \omega_{max}$. E.g., if $\omega_{max} = 400$ cm^{-1}, $\Delta x = 12.5\mu$ and the detector signal must be sampled at least every 12.5μ of path length difference. The resolution depends on the total displacement X of the moving mirror and on the number of points sampled. Since the resolution $\Delta\omega = 1/X$, the number of points which are to be taken from the interferogram is

$$N = \frac{X}{\Delta x} = \frac{2\omega_{max}}{\Delta\omega}. \qquad (42)$$

For $\omega_{max} = 400\ cm^{-1}$ and a required resolution of $0.5\ cm^{-1}$, N = 1600 points are needed.

The interfereogram thus obtained is not a spectrum, but contains virtually all the energy-frequency information within it. The spectrum can be obtained by carrying out the Fourier transformation of the interferogram. This involves complex calculations and modern instruments have a linked small computer to do this task[27]. Alternatively, the interferogram analog data may be digitized, punched on paper tape and the subsequent calculations may be carried out by a large digital computer. The number of the Golay signal measurements taken is a function of the wavenumber range and resolution sought. Since even the best synchronous motor cannot assure an even speed for the moving mirror, the control of its movement is governed by means of a Moiré grating, attached to the moving mirror. The intensity peaks of the Moiré fringes thus generated tell the computer when to take readings. This method assures that measurements are taken at regular intervals.

The Research and Industrial Instruments Company Ltd. (RIIC) FS 720 Fourier Transform Interferometer, which was used in the present work, is represented schematically in Figure 5. The source is a water cooled Hg lamp. The modulated light is sent over a polyethyleneterephtalate (Mylar) film beam splitter. The thickness of the beam splitter (6-100μ) is chosen according to the frequency range to be measured.

The solid samples are prepared as pressed disks (pellets) in polyethylene, which has good transmittance in the far infrared.

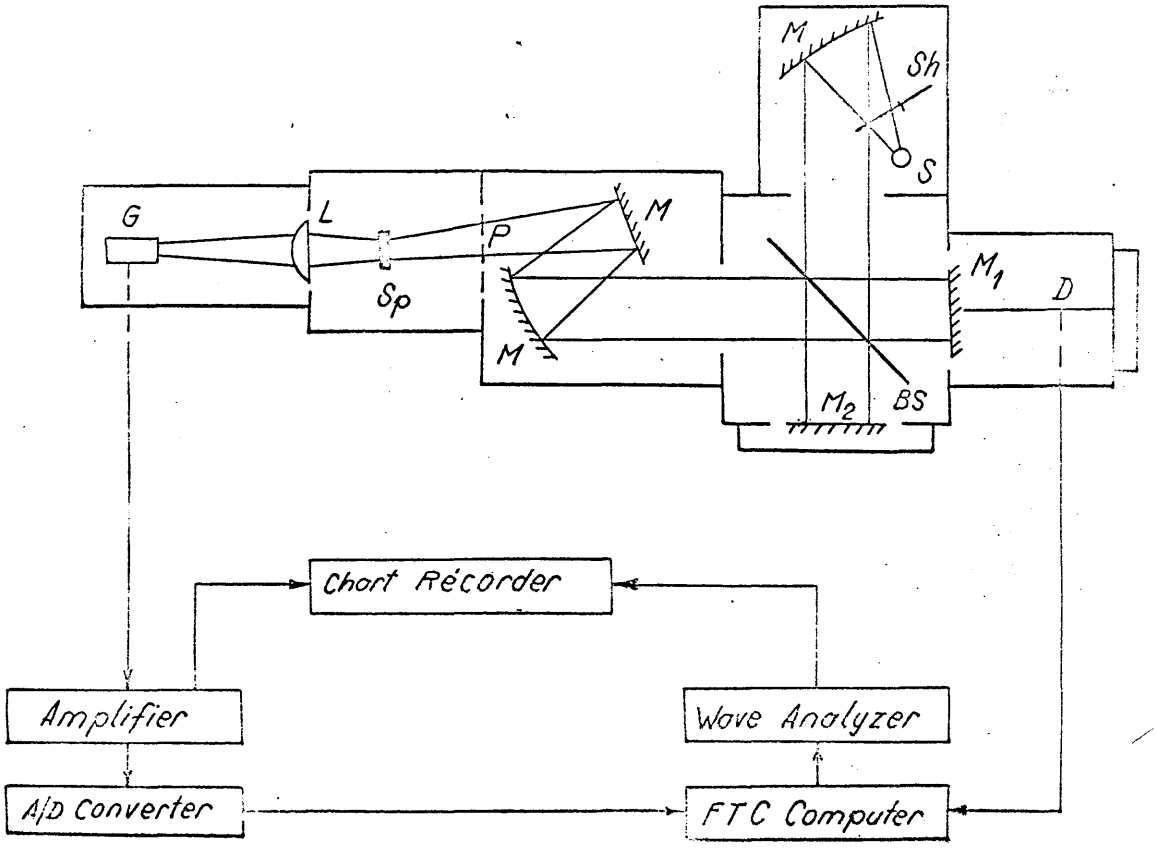

Figure 5

RIIC FS 720 Fourier Transform Interferometer and computing block

S-infrared source, M_1-plane moving mirror, M_2-plane fixed mirror, BS-beam splitter, Sp-sample, G-Golay pneumatic detector, D-drive of the moving mirror and gear box, C-chopper, M-condensing mirrors, P-polyethylene window, L-lens

The absorption of the polyethylene itself can be eliminated by running first its spectrum, then the spectrum of the sample embedded in polyethylene, and by rationing the two spectra. In

Figure 6 the interferogram and the corresponding spectrum of solid GeO_2 (rutile structure) is shown.

For recording reflectance spectra, only the sample chamber of the spectrometer has to be modified. The sample - a certain face of a single crystal - is placed in an appropiate holder, sometimes provided with a goniometer in order to ascertain the crystal orientation. The light beam may be sent, by an appropiate arrangement of mirrors, upon a plane face of the sample and collected from it after reflection. By using wire grid polarisers, the electric vector of the light may be oriented as desired with respect to the crystallographic axes. This technique enables measurement of the polarization properties of the active modes.

Reflectance spectroscopy is particularly helpful in studying samples which have large absorption coefficients. In such cases it is usually very difficult to prepare samples which are sufficiently thin to allow measurements of the stronger bands. A reflectance spectrum may be used to compute the dielectric parameters, including the absorption index, of the sample[28], on the basis of the classical electromagnetic theory. Practical computations are carried out by using the Kramers-Kronig relations[29]:

$$n = \frac{1 - R}{1 + R - 2\sqrt{R}\cos\theta(\omega)} \qquad (43)$$

and

$$k = \frac{-2R\sin\theta(\omega)}{1 + R - 2\sqrt{R}\cos\theta(\omega)} \qquad (44)$$

where $\underline{n}$ and $\underline{k}$ are the refractive and absorption indices, respec-

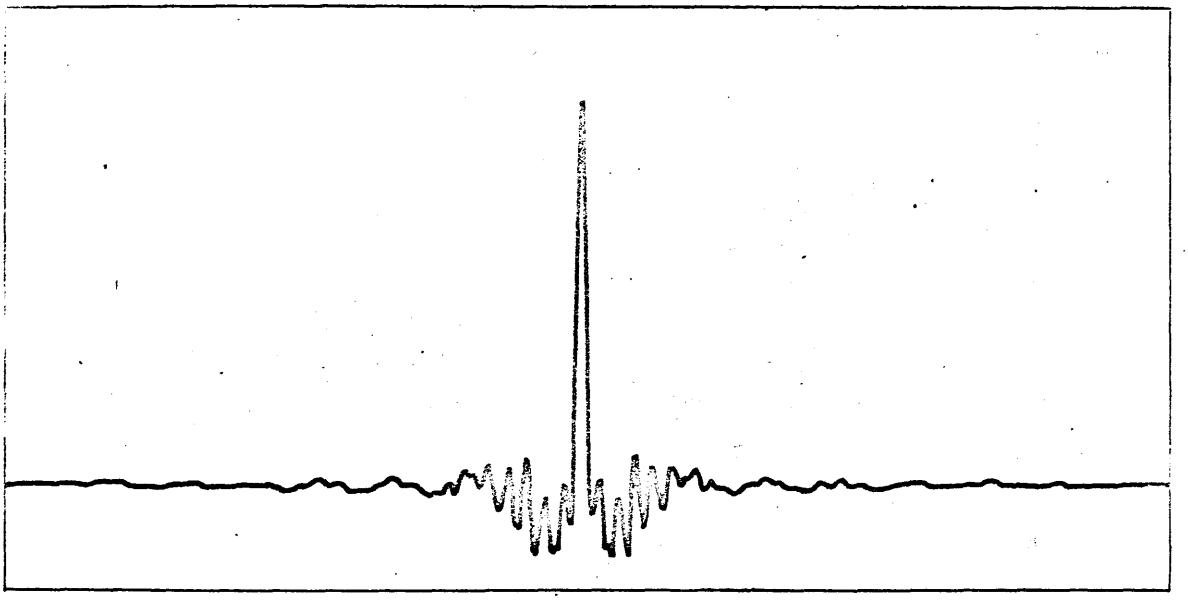

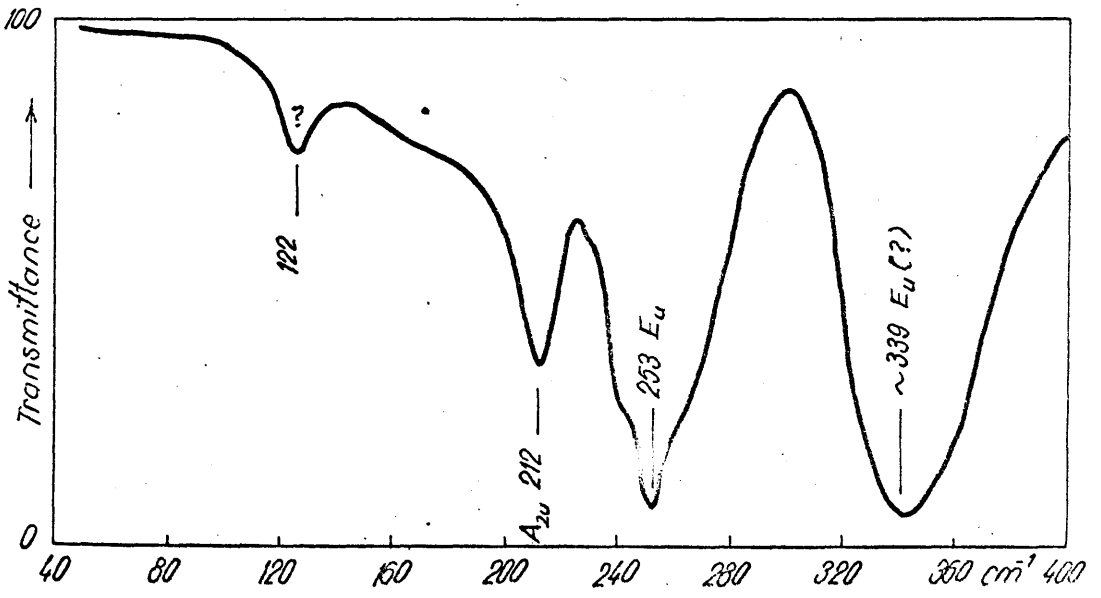
100
Transmittance
0
?
122
A_{2u} 212
253 E_u
~339 E_u (?)
40
80
120
160
200
240
280
320
360 cm^{-1}
400

Figure 6

tively, R is the reflectivity and $\theta(\omega)$ is the phase. The value of $\theta(\omega)$ may be found from the equation

$$\theta_m = \frac{2\omega_m}{\pi} \int \frac{\log\sqrt{R}}{\omega^2 - \omega_m^2} \, d\omega. \qquad (45)$$

where ω_m is a given frequency at which the value of θ, i.e. θ_m, is required. In practice, the limits of integration in eq. (45) are chosen within the known reflectance spectrum. Computer programs are now available[30] for routinely performing Kramers-Kronig transformations.

Sometimes, even an absorption spectrum has to be corrected for errors which are usually neglected and which are due to the influence of the changes in the reflectivity of the sample at the absorption maxima[31]. In these cases, Kramers-Kronig relations may also be used to find the correct location of the absorption bands.

(ii) Raman spectroscopy is essentially an inelastic scattering process of the photons when they interact with the molecules of the sample. The energy lost by the photon is used to excite certain vibrational modes of the molecule, which become, under certain circumstances depending of the molecular symmetry, active (Stokes lines); sometimes, deactivation of excited vibrational states of the molecule results in a gain of energy (anti-Stokes lines). For crystals, the vibrations of the lattice participate and the scattering process may be visualised as an inelastic collision between photons and phonons. The first order Raman spectrum reflects the scattering processes in which a single phonon is created (or destroyed) in the lattice at the expense of

photon energy loss (or gain).

The main physical parameter of the molecule (or crystal) which governs the occurence of a Raman effect is the electronic polarizability symmetric tensor α. The magnitude of various components α_{ij} of this tensor may be estimated approximately by different procedures, based either on classical electromagnetic theory[32], or on the expansion of α in a series with respect to small displacements of the normal coordinates from the equilibrium configuration[32]. However, the main problem is in fact to determine whether the various components α_{ij} are or are not equal to zero. This problem may be easily solved using group theory, as indicated in Chapter 1 (eq. 28). Experimentally, the various α_{ij} components may be determined using polarized exciting radiation. This way, the symmetries of the vibrational modes corresponding to different Raman bands can be identified.

A Raman spectrum is generated when a high-intensity beam of monochromatic light is passed into and scattered by a sample. Alongside the exciting (Rayleigh) line ω_o, the spectrum will contain additional weak (Raman) lines ω_i on both sides of the exciting line. In order to obtain a good Raman spectrum, the exciting line used must have very good monochromaticity; in classical light sources, like the Hg (Toronto) lamp, this is realised through appropriate filters which allow a single exciting line to be passed into the sample. Such sources have considerable drawbacks, mainly arising from the difficulty of concentrating the diffuse output of the lamp upon the sample, the difficulty of eliminating parasitic

light, and the high luminosity required to the monochromator. These difficulties have retarded advances in Raman spectroscopy as compared to infrared absorption spectroscopy. The main obstacle in the development of Raman spectroscopy was the exciting source, a problem which was solved with the discovery of the laser. The laser meets all the requirements for a very good Raman source - narrowness, perfect monochromaticity and linear polarization of the exciting line, continuous output power, low power requirements, small beam divergence, etc. By using the laser in connection with old dispersing instruments, a tenfold increase in the signal-to-background ratio may be obtained. The sample preparation may be also greatly simplified and much smaller quantities of compounds are necessary.

The first type of laser used[33] was a ruby pulsed laser, which emits at 6943 Å. The first commercial laser Raman spectrometer appeared in 1964, based on a continuous He-Ne source and photoelectric detection[34].

The advantages of using the laser as exciting source in Raman spectroscopy may be summed up as follows:

a. High monochromaticity. The width of the line emitted by a He-Ne laser reaches 0.05 cm^{-1} (as compared to 0.25 cm^{-1} for the Hg lamp). This allows observation of bands which are situated in the immediate vicinity of the exciting line.

b. Stability of laser beam. This refers to both spatial and temporal stability. It brings about the almost complete disappearence of the continuous background in the spectrum.

c. Easy measurement of the depolarization ratios. The light emitted by the laser being perfectly polarized linearly, it is easy to set up a simple optical arrangement for the measurement of the depolarization ratios without energy loss. However, when the laser beam suffers too many reflections on the walls of the cell, the determination are not very accurate.

d. High power density. This enables one to use relatively low power output lasers (e.g. a He-Ne laser of about 100 mW gives better results than a 0.5-2 kW Toronto lamp). A further consequence is the possibility of running spectra of powdered solid samples. The detectors used may be of a lower sensitivity compared with those used in conventional Raman spectroscopy. The time required to record a spectrum is much shorter. Small amounts of compound and low volume cells are needed.

e. Large choice of exciting line wavelengths. Various mixtures of gases may be chosen, each of which giving a laser beam with different wavelength:

Gas	Wavelength (Å)
He-Cd	4416
Ar	4880 or 5145
Kr	5682 or 6471
He-Ne	6328

Moreover, construction of the tunable laser is now under way. This choice of the wavelength makes possible to obtain spectra from variously coloured samples. It is, however, preferable in some cases to use red lasers, like He-Ne, to avoid photodecom-

position of the studied compounds and, still more important, to enhance the signal-to-noise (S/N) ratio. The S/N ratio is approximately proportional[35] to the square root of the photon flux at the photomultiplier. Since the photon energy is proportional to the frequency, the 'fourth power law'[32] (the intensity of the scattered radiation is proportional to ω^4)

$$I_s \sim \omega^4 \qquad (46)$$

becomes

$$I_s \sim \omega^3$$

and

$$S/N \sim \omega^{3/2} \qquad (47)$$

Larger S/N ratios may be obtained[34] through other improvements in the optics, e.g. $S/N \sim \omega^{1/2}$. This fact suggests the use of long wavelength lasers for excitation. Their radiation has the advantage of being less absorbed by coloured samples. Alternatively, when the photostability of the compounds permits, short wavelength lasers (He-Cd) may be used, because detectors are generally more sensitive in this region.

f. Spectra of opaque samples can be obtained easily through reflection of the laser beam on the sample.

The laser source is very well suited to the examination of single crystals because the narrow beam of monochromatic, linearly polarized radiation can be easily and accurately directed onto small oriented crystalline faces. Single crystal spectra offer an unambiguous assignment of the molecular and lattice modes. Intensity measurements are easy to make. They allow determination

of the various $\partial\alpha/\partial Q$ values which are important in the study of the nature of bonds.

For single crystal studies, Damen, Porto and Tell[36] have introduced a convenient and useful notation for various situations occuring in Raman spectroscopy which takes account of the observation parameters. It is assumed that the Cartesian axes of the laboratory and the crystallographic axes are identical, with the z-axis of the crystal parallel to the principal or optic axis. Thus x(zx)y has the following meaning: incident beam arrives along x-axis, with its electric vector oriented in the z direction; scattered light is observed along y-axis and has the electric vector in the x direction. In this notation, the paranthesis contains the label of the derivative of the α_{zx} component of the polarizability tensor for each mode. Loudon[37] has given tables listing the symmetries of Raman active modes and the corresponding polarizability derivatives for the most important factor groups. Since we are not concerned with single crystals, we will not pursue further this matter here.

The optical excitation arrangement of the Spectra-Physics Model 125 (60 mW) laser in the Cary Instruments Corp. Model 81 Spectrometer, which was used in the present work, is shown in Figure 7. The geometry used in this instrument - laser and Raman beams coaxial (180°) - takes the most advantage of the energy of the laser. Other geometries, in which the angle between the two beams varies from 0 to 90°, are also possible. Illumination under 90° is preferred in case of single crystals because it allows ea-

sier interpretation of the results. Alignment of the cell and laser beam is critical and reliable spectra can only be obtained if the exciting beam enters the cell such that total reflection occurs on the walls. Polarizations are measured by using a Polaroid film in the Raman beam, and by rotating the plane of polarization of the exciting line from parallel to perpendicular by turning the half-wave plate through 45° about the beam axis. In order to run crystalline samples, the desired face of the crystal is held directly against the flat face of the hemispheric collector

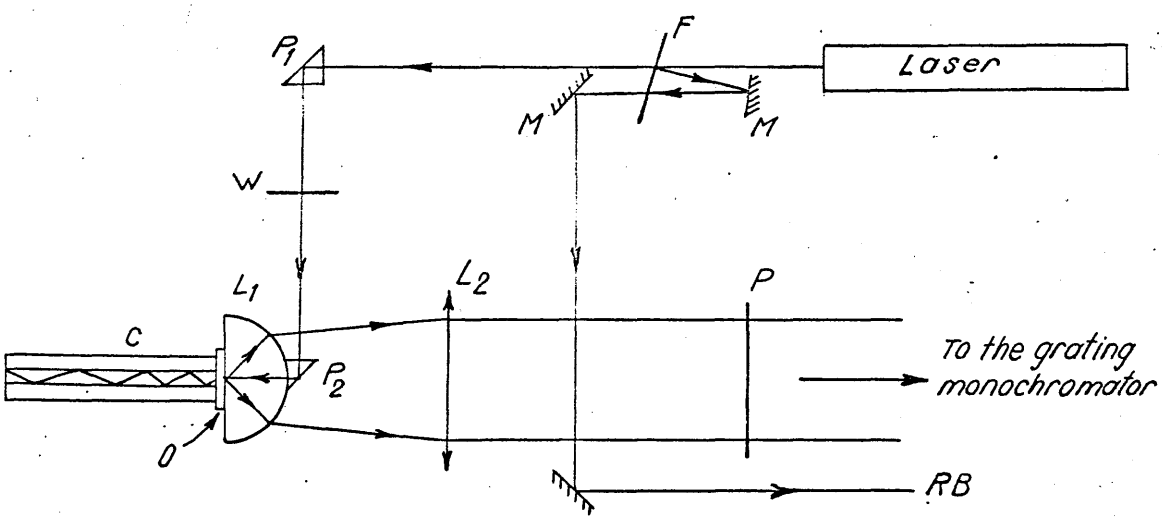

Figure 7

Cary 81 Laser Raman Spectrometer

F-filter for 6328 Å radiation, M-mirrors, P_1,P_2-45° prisms (P_2 has 1 mm square faces, so that it only causes a 3% intensity loss), W-half-wave plate, L_1-hemispherical collector lens, L_2-condensing lens (about 8 mmØ), P-Polaroid filter, RB-refernce beam, C-sample cell, O-glycerol between cell's end and hemispherical lens, to allow optical contact.

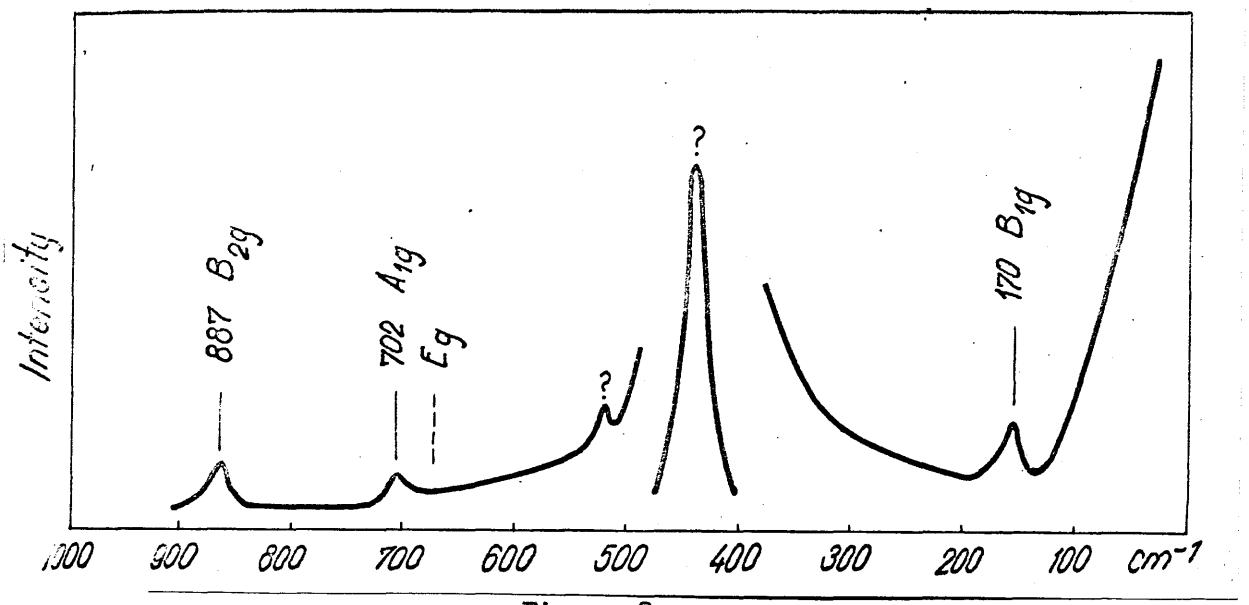

Figure 8

Raman spectrum of solid GeO_2

(The unassigned bands might be due to some unidentified impurities present in the sample)

lens. Solid powder samples are placed in glass tubes, whose flat end is held in the same manner as for liquid samples (Fig. 7). The monochromator is a double grating Littrow, with double slits incorporated. Detection is by a photomultiplier, the recorder being coupled to measure the difference $\Delta\omega$ between exciting and Raman scattered frequencies.

The laser Raman spectrum of solid GeO_2 (rutile structure) is shown in Figure 8. Assignment of the bands is made following the work of Porto et al.[38] for TiO_2.

For a more detailed discussion of laser Raman spectroscopy, two excellent and up-to-dated reviews of the topics are available[39].

Chapter 3 FACTOR GROUP ANALYSIS OF CRYSTALLINE A_2MF_6 COMPOUNDS

The crystalline lattices of the A_2MF_6 compounds studied in this work contain isolated MF_6^{2-} anions and A^+ cations[40]. In the cubic (O_h^5) structures, the MF_6^{2-} anions, which generally have a perfect octahedral O_h point symmetry, are placed in an octahedral site symmetry; in other structures, the site occupied by the MF_6^{2-} anions may be of a lower symmetry, but the anions continue to be isolated from each other and from the surrounding cations, unlike the case of other fluorocomplexes, in which the MF_6^{n-} octahedra share[41] edges (Na_2CuF_4), faces (K_2MnF_4) or corners [$(NH_4)_2MnF_5$, $RbFeF_4$]. The interaction between the A^+ and MF_6^{2-} ions is relatively weak as compared to the intramolecular forces within the MF_6^{2-} groups themselves[41]. Therefore, it is to be expected that the fundamental infrared absorption and Raman scattering bands of the anion itself, e.g. as they appear in the solution spectra, should appear in the solid state spectra almost unchanged for a given compound - save for a small shift due to lattice interaction (which varies with the nature of A^+ and with A^+-MF_6^{2-} distances) and a possible splitting of the MF_6^{2-} characteristic bands when the symmetry of the surrounding lattice is lower than that of a perfect cubic.

The most significant change in the spectra of the solid state compounds as compared to the solution spectra is, however, the

appearence of new absorption and scattering bands in the low energy range. These are entirely characteristic of the solid state and are the lattice active optical modes (see Chapter 1).

All these results can be predicted by means of the factor group analysis (FGA) method (Chapter 1), i.e. by considering a single unit cell and assuming that the vibrations of all unit cells of the crystal take place in phase. The translation and factor group selection rules are applied, as previously described. At the center of the first Brillouin zone, all three acoustic branches have zero frequency, and all the observed fundamental modes may be assigned, in principle, to the active optical branches which result from FGA.

This approach is rigorous for the assignment of fundamental modes. For combination bands, which arise from combinations of fundamental modes of appropriate symmetry, no definite predictions can be made on the basis of a simple model which neglects the effects of non-central regions of the zone[18,19], even if the species of the resulting mode is clearly allowed or forbidden by the factor group selection rules.

Therefore, in this discussion, only the fundamental modes of the four A_2MF_6 structures considered will be classified at the center of the Brillouin zone, according to the FGA method in its latest standard form[10,20,22].

A detailed description of these structures will be given later in this chapter, but we emphasize here that the O_h^5, D_{3d}^3 and C_{6v}^4 structures are closely related to each other. Indeed, by choosing

for the cubic structure a cell with the c-axis along the hexagonal C_3 symmetry axis, the ratio of the 3 c-axes of the D_{3d}^3, C_{6v}^4 and O_h^5 structures is, for almost all compounds which crystallize in these forms[41], very close to 1:2:3. This suggests that the differences in c are due to a periodical repetition of certain identical basic layers, which are present in all 3 mentioned structures. These are close-packed layers, whose composition is AF_3.

The stabilisation energies of the three widespread A_2MF_6 structures, as estimated through Madelung constants[42], are found to be almost identical. This supports the idea that these structures are in fact polymorphic. The alkali ions A^+ are coordinated by F atoms, the coordination number being always 12, i.e. that characteristic of close-packing, in all three mentioned structures, although the A-F distances are not always equal. The coordination of A^+ (A = K, Rb, Cs) by F is very different from that encountered in Na_2SiF_6 (D_3^2 space group), where c.n. = 8, and the 8 Na-F distances range between very different values (see later).

All these facts, irrespective of the particular nature of the bonding[41] or incidental distortions of the octahedra due to Jahn-Teller[43] or other effects, enable one to establish analogies between the results of the vibrational analysis in each case and to see more clearly the effect of the lattice environment upon the behaviour of the vibrational modes of MF_6^{2-} anions.

(i) A_2MF_6 compounds of O_h^5 ($Fm3m$) space group
('K_2PtCl_6' or 'K_2SiF_6' structure)

The crystallographic unit cell contains 4 formula-units and the

atoms have the following positions[44]:

M: (4a) 000; f.c.

A: (8c) $\pm(\frac{1}{4}\frac{1}{4}\frac{1}{4})$; f.c.

F: (2e) $\pm$(u00; 0u0; 00u); f.c.

the parameter u varying from compound to compound ($u \sim 0.19$-0.24). Each M atom is surrounded by 6 F atoms which form a regular octahedron. A atoms are equally distant from 12 F atoms. The lattice may be considered as a sequence of AF_3 layers along the C_3 axis of the unit cell. The nature of M-F bond in these compounds involves a certain amount of covalent character (see Chapter 7), which is certainly different in such compounds as Cs_2SiF_6 and Cs_2MnF_6. A common feature is nevertheless that the bond is strong enough to prevent the MF_6^{2-} anion from dissociating in solution in most cases.

The Bravais unit cell necessary to carry out the FGA may be chosen as in Figure 9; it contains one formula-unit and exhibits

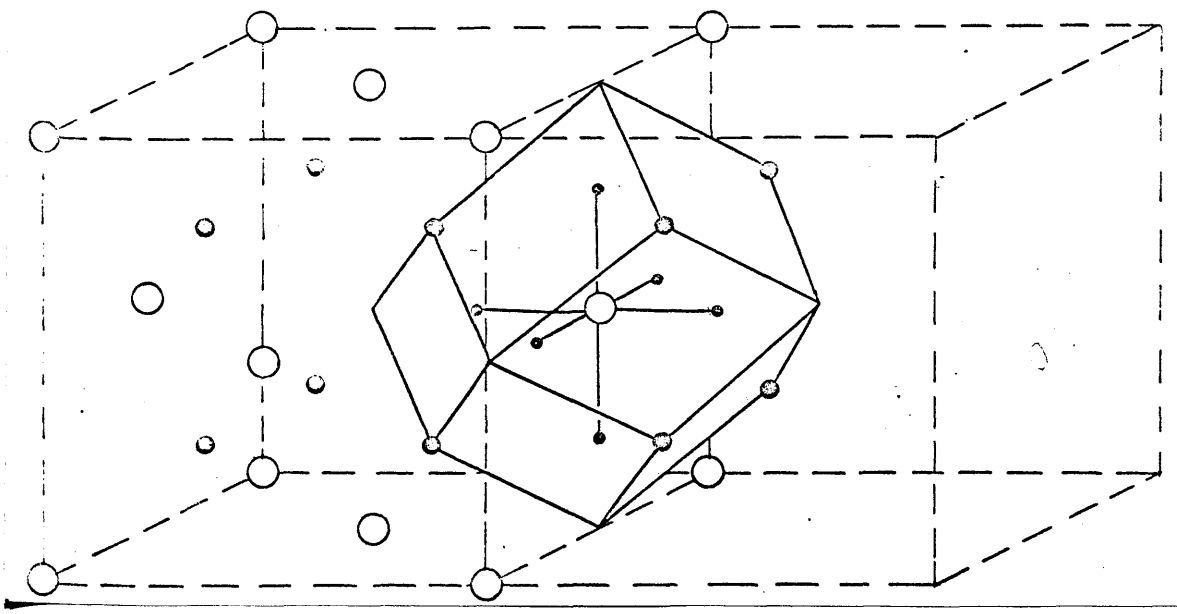

Figure 9

the full symmetry of O_h factor group. This cell is different from that used by Shimanouchi and co-workers[45] (Fig. 10) for the factor group analysis of some hexaclorometallates(IV); this seems to stoi-

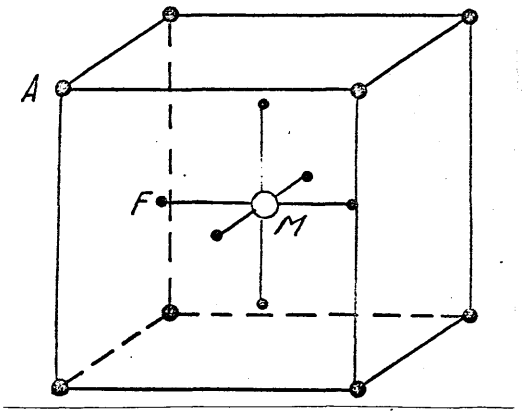

Figure 10

chiometrically incorrect because contains a single A atom, but the final results are the same as ours. The number of total (n_i), acoustic (T), translatory-lattice (T'), rotatory-lattice (R'), and internal (n_i') modes are given in Table 2 for each irreducible representation of the O_h group, as well as the reduction of the α tensor.

The infrared-active modes are:

$$\underset{(\nu_3,\ \nu_4)}{2F_{1u}(\text{internal})} + \underset{(\nu_7)}{F_{1u}(\text{translatory-lattice})}$$

Raman-active modes:

$$\underset{(\nu_1)}{A_{1g}} + \underset{(\nu_2)}{E_g} + \underset{(\nu_5)}{F_{2g}(\text{internal})} + \underset{(\nu_8)}{F_{2g}(\text{translatory-lattice})}$$

Inactive modes:

$$\underset{(\nu_6)}{F_{2u}(\text{internal})} + \underset{(\nu_9)}{F_{1g}(\text{rotatory-lattice})}$$

The acoustic mode F_{1u} (ν_{10}) is supposed to have zero frequency

Table 2

Classification of normal vibration modes of cubic (O_h^5) A_2MF_6 compounds

O_h^5	n_i	T	α	T'	R*	n_i'
A_{1g}	1	0	1	0	0	1
A_{2g}	0	0	0	0	0	0
E_g	1	0	1	0	0	1
F_{1g}	1	0	0	0	1	0
F_{2g}	2	0	1	1	0	1
A_{1u}	0	0	0	0	0	0
A_{2u}	0	0	0	0	0	0
E_u	0	0	0	0	0	0
F_{1u}	4	1	0	1	0	2
F_{2u}	1	0	0	0	0	1
Number of degrees of freedom	27	3	//	6	3	15

(see Chapter 1 and also reference 46 for a more detailed discussion).

This vibrational pattern can be easily correlated with the vibrational spectra of the compounds in solution. The infrared spectrum of a solution containing MF_6^{2-} ions exhibits two bands - ν_3 and ν_4 - which represent the M-F stretching and F-M-F angle bending infrared-active modes, respectively. These bands appear in the solid state spectrum too, and due to the perfect symmetric environment of the regular MF_6^{2-} octahedra they remain triply degenerate (F_{1u}). In the infrared spectrum of the solid state a third F_{1u} band will appear (ν_7), which is an infrared-active lattice mode. The Raman spectra of MF_6^{2-}-containing solutions consist of 3 bands - ν_1, ν_2 and ν_5, and they remain as such (A_{1g}, E_g and F_{2g}, respectively) in the solid state spectrum, but a further F_{2g} (ν_8) band appears in the lattice region.

It should be noted that the same results (with the exception of the lattice modes prediction) might be alternatively derived by using a site group analysis: since the site occupied by the MF_6^{2-} anions has the same (O_h) symmetry as the molecular unit, the same active modes will be present in both the free molecule and the crystal.

(ii) A_2MF_6 compounds of D_{3d}^3 ($P\bar{3}m1$) space group ('K_2GeF_6' structure)

The crystalographic unit cell contains 1 formula-unit, the atoms having the positions[47]:

M: (1a) 000

A: (2d) $\pm(\frac{1}{3}\,\frac{2}{3}\,u)$ $(u \sim 0.69\text{-}0.75)$

F: (6i) $\pm(u\bar{u}v;2\bar{u}\ \bar{u}\ v;u\ 2u\ v)$ $(u \sim 0.14\text{-}0.18;\ v \sim 0.19\text{-}0.26)$

The MF_6^{2-} octahedra are not regular. In order to express the deviation of their configuration from regular octahedral, let us note d the M-F distance and d' the d projection on the horizontal plane containing the upper (or lower) 3 F atoms in the unit cell (Figure 11). The distance between 2 F atoms situated at the same height is

$$r_{F-F} = d'\sqrt{3}$$

and the distance between 2 neighbouring F atoms in different hori-

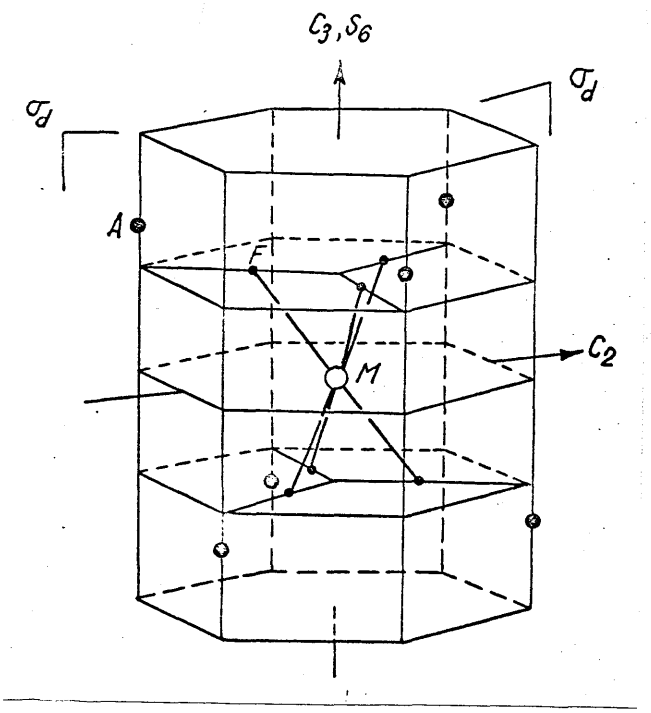

Figure 11

zontal planes is

$$r'_{F-F} = \sqrt{2d^2 - 2d^2\cos\gamma} = d\sqrt{2(1 - \cos\gamma)}$$

where γ is the angle between the bonds of these 2 atoms with the

central atom M. Distances d and d' may be found from the geometrical relations

$$d = \sqrt{3(ua_o)^2 + (vc_o)^2}$$

$$d' = \sqrt{3}(ua_o)$$

so that the distances between the F atoms in a horizontal plane and in different horizontal planes will be equal (and the octahedron will be regular) when

$$r_{F-F} = r'_{F-F}$$

which leads to the condition

$$\sqrt{2(1 - \cos\gamma)\left[1 + \frac{1}{3}\left(\frac{vc_o}{ua_o}\right)^2\right]} = \sqrt{3}.$$

For $\gamma = 90^o$, this condition reduces to

$$w \equiv \frac{ua_o}{vc_o} = \sqrt{\frac{2}{3}} = 0.816496.$$

The tolerance ratio w may be taken as a measure of the octahedron distortion. In Table 3 some geometrical parameters, including w, are listed for various molecules which crystallize in D^3_{3d} space group. For K_2GeF_6 w = 0.81306 and therefore the GeF_6^{2-} octahedra are almost regular. For other compounds, the distortion is larger if we use the unit cell parameters given by Wyckoff[47].

The 2 A atoms in the unit cell are situated on the C_3 axis of the (assumed) regular MF_6^{2-} octahedron. The 12 A-F distances are no longer equal, as in cubic compounds; they are divided[41] into three groups of 3, 6, and 3 equal distances. In the particular case of K_2GeF_6, which has a more regular structure, there are only two groups - 9 shorter and 3 longer A-F distances.

Table 3

Geometrical parameters of D_{3d}^3 A_2MF_6 molecules

Compound	a_o(Å)	c_o(Å)	u(F)	v(F)	w
K_2GeF_6	5.62	4.65	0.148	0.220	0.81306
Rb_2GeF_6	5.82	4.79	0.144	0.213	0.82143
γ-K_2TiF_6	5.715	4.656	...	...	...
K_2PtF_6	5.76	4.64	0.150	0.250	0.74483
Rb_2ZrF_6	6.16	4.82	0.167	0.206	1.03605
Cs_2ZrF_6	6.41	5.01	0.16	0.198	1.03398

The distortion of the MF_6^{2-} octahedra and the irregularities in the A-F distances should contribute to the appearence of extra bands additional to those predicted by FGA, i.e. from the consideration of the perfect MF_6^{2-} octahedron's surrounding. In fact, as we will see in Chapter 5, no such extra bands appear in the infrared or Raman spectra and, moreover, it is sometimes difficult even to observe the relatively small number of bands predicted by FGA[4]. The splitting of the ν_5 mode, for example, has been recorded only for the compounds in which the octahedron distortion is largest - Rb_2MF_6 and Cs_2MF_6, M = Zr, Hf. For these compounds the tolerance ratio $\underline{w}$ is much larger than $\sqrt{2/3}$ (see Table 3). This rather unimportant change of the spectrum in passing from the ideal cubic to the trigonal structure has to be explained by almost non-existing energetic differences between these modifications.

The Bravais cell utilized for the FGA is shown in Figure 11 and the FGA results[4] are listed in Table 4.

Infrared-active modes:

$$\underset{(\nu_3', \nu_4')}{2A_{2u}} + \underset{(\nu_3'', \nu_4'', \nu_6'')}{3E_u(\text{internal})} + \underset{(\nu_7')}{A_{2u}} + \underset{(\nu_7'')}{E_u(\text{translatory-lattice})}$$

Raman-active modes:

$$\underset{(\nu_1, \nu_5')}{2A_{1g}} + \underset{(\nu_2, \nu_5'')}{2E_g(\text{internal})} + \underset{(\nu_8'', \nu_9'')}{2E_g(\text{translatory+rotatory lattice})} + \underset{(\nu_8')}{A_{1g}(\text{translatory-lattice})}$$

Optically-inactive modes:

$$\underset{(\nu_6')}{A_{1u}(\text{internal})} + \underset{(\nu_9')}{A_{2g}(\text{rotatory-lattice})}$$

Table 4

Classification of normal vibration modes of trigonal (D^3_{3d}) A_2MF_6 compounds

D^3_{3d}	n_i	T	α	T'	R'	n'_i
A_{1g}	3	0	2	1	0	2
A_{2g}	1	0	0	0	1	0
E_g	4	0	2	1	1	2
A_{1u}	1	0	0	0	0	1
A_{2u}	4	1	0	1	0	2
E_u	5	1	0	1	0	3
Number of degrees of freedom	27	3	//	6	3	15

Table 5

Geometrical parameters of C^4_{6v} A_2MF_6 molecules

Compound	a_o(Å)	c_o(Å)	u(M)	$u(A_1)$	$u(A_2)$	$u(F_1)$	$v(F_1)$	$u(F_2)$	$v(F_2)$
β-K_2MnF_6	5.67	9.35	0.25	0.90	0.60	0.19	0.36	0.48	0.14
Rb_2MnF_6	5.855	9.503	0.25	0.895	0.605	0.195	0.355	0.472	0.145
Rb_2GeF_6	5.94	9.63	0.25	0.89	0.61	0.18	0.35	0.49	0.15

We could get the same results (with respect to internal modes) by using the site symmetry approach. Indeed, the site symmetry of the MF_6^{2-} octahedra in D_{3d}^3 class compounds containing a single formula-unit is[8] D_{3d}. By using the correlation tables[21] between the groups O_h and D_{3d}, we find the following reducible representation of the motions in the new symmetry:

$$D_{3d}: \quad 2A_{1g} + 2E_g + A_{1u} + 2A_{2u} + 3E_u$$

from which the $2A_{2u} + 3E_u$ modes are infrared-active and the $2A_{1g} + 2E_g$ are Raman-active.

The increased number of bands of the MF_6^{2-} octahedra both in infrared and Raman spectra, as compared with the relatively clean spectra of the cubic compounds, originate mainly in the removal of triple degeneracy in the new site symmetry of the anion.

(iii) A_2MF_6 compounds of C_{6v}^4 ($P6_3mc$) space group ('K_2MnF_6' structure)

The crystallographic unit cell contains 2 formula-units, the atoms being in the positions[48]:

M: (2b) $\frac{1}{3}\frac{2}{3}u; \frac{2}{3}, \frac{1}{3}, u+\frac{1}{2}$
A(1): (2b) $\frac{1}{3}\frac{2}{3}u; \frac{2}{3}, \frac{1}{3}, u+\frac{1}{2}$
A(2): (2a) $00u; 0,0,u+\frac{1}{2}$
F(1): (6c) $u\bar{u}v; u,2u,v; 2u,\bar{u},v; \bar{u},u,v+\frac{1}{2}; \bar{u},2\bar{u},v+\frac{1}{2}, 2u,u,v+\frac{1}{2}$
F(2): (6c) $u\bar{u}v; u,2u,v; 2u,\bar{u},v; \bar{u},u,v+\frac{1}{2}; \bar{u},2\bar{u},v+\frac{1}{2}; 2u,u,v+\frac{1}{2}$

The parameters $\underline{u}$ and $\underline{v}$ of various atoms and for various compounds which crystallize under this space group are given in Table 5[48]. In C_{6v}^4 A_2MF_6 structures, the A^+ cations continue to be 12-coordinated by F atoms, the A-F distances being split in three groups[41] of 6+3+3 equal distances, as in the trigonal form (the 6 equal

distances being the shorter).

In order to find the smallest Bravais cell necessary for factor group analysis, a method proposed by Winston and Halford[20] was used. The site symmetry of the MF_6^{2-} anions in this arrangement is C_{3v}. The representation O_h: $A_{1g}+E_g+F_{2g}+2F_{1u}+F_{2u}$ of the anion's motions in this new environment becomes C_{3v}: $4A_1+A_2+5E$, from which only A_2 is optically inactive. The site group being a subgroup of the factor group, one can easily find the correlation between their irreducible representations by using the relation

$$n_i^{(F)} = \sum_j a_{ij} n_j^{(S)} \qquad (48)$$

where $n_j^{(S)}$ is the number of times the j-th irreducible representation of the site group appears in the representation of the motions of the site occupant, $n_i^{(F)}$ is the number of times the i-th irreducible representation of the factor group appears in the reducible representation of the motions, and the coefficients a_{ij} are given by

$$a_{ij} = \frac{1}{h} \sum_{R \text{ in } S} \chi_j^{(S)}(R)^* \chi_i^{(F)}(R) \qquad (49)$$

(h-order of site group S).

This procedure gives in the present case $n_{A_1}^{(F)} = 4$, $n_{A_2}^{(F)} = 1$, $n_{B_1}^{(F)} = 4$, $n_{B_2}^{(F)} = 1$, $n_{E_1}^{(F)} = 5$, and $n_{E_2}^{(F)} = 5$, so that the structure of the representation will be

$$4A_1 + A_2 + 4B_1 + B_2 + 5E_1 + 5E_2$$

having 30 degrees of freedom; the smallest Bravais cell will contain 2 formula-units, and can be chosen as in Figure 12 (identical to the crystallographic unit cell).

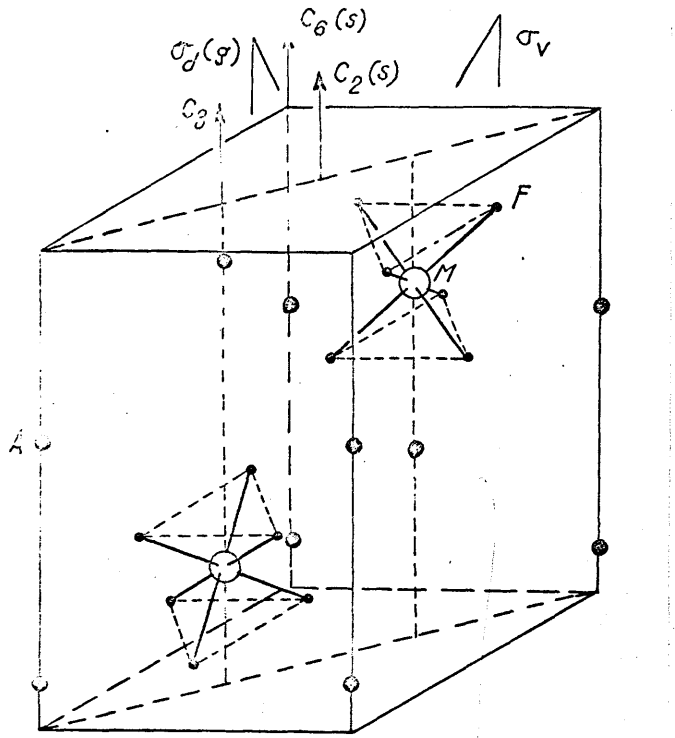

Figure 12

The results of the FGA carried out on this cell are given in Table 6. The lack of a center of symmetry allows a large number of bands to be both infrared and Raman-active.

Infrared-active modes:

$$4A_1 + 5E_1(\text{internal}) + 2A_1(\text{translatory-lattice}) + 3E_1(\text{translatory+rotatory-lattice})$$

Raman-active modes:

$$4A_1 + 5E_1 + 5E_2(\text{internal}) + 2A_1(\text{translatory-lattice}) + 3E_1(\text{translatory+rotoatory-lattice}) + 4E_2(\text{translatory-lattice})$$

Inactive modes:

$$A_2 + 4B_1 + B_2(\text{internal}) + A_2(\text{rotatory-lattice}) + 3B_1(\text{translatory+rotatory-lattice})$$

Table 6

Classification of normal vibration modes of hexagonal (C_{6v}^4) A_2MF_6 compounds

C_{6v}^4	n_i	T	α	T'	R'	n_i'
A_1	7	1	2	2	0	4
A_2	2	0	0	0	1	1
B_1	7	0	0	3	0	4
B_2	2	0	0	0	1	1
E_2	9	0	1	3	1	5
Number of degrees of freedom	54	3	//	15	6	30

In this case, the site group analysis gives, as already mentioned, the reducible representation $4A_1 + 5E$ for the motions of the atoms constituting the MF_6^{2-} group, so that both infrared and Raman spectra would consist of 9 (internal) bands. The extra bands indicated by FGA are due to existing interactions between the two molecules within the unit cell, which cannot be taken into account by SGA. As mentioned in Chapter 1, the SGA is related to a single molecule or molecular ion, which is ascribed the symmetry of the particular site in which it is placed in the unit cell. This way, SGA offers no possibility to take into account intermolecular vibrations, whether these are genuine lattice or other kinds of intermolecular vibrations. They can be only found by using FGA.

Owing to the large number of such intermolecular non-lattice interactions, it is difficult in this case to assign the internal modes which result from FGA to the previous six internal modes of the regular MF_6^{2-} anion. (In the case of D_{3d}^3 A_2MF_6, with only one formula-unit per unit cell, no such interactions occur and the operation is straightforward.) The interaction non-lattice modes can manifest themselves in the spectra in various ways[46]. Thus, the non-degenerate modes of MF_6^{2-} groups can duplicate themselves, appearing as two neighbouring bands in the spectra of crystalline compounds whose unit cell contains more than one formula-unit. As we shall see in Chapter 5, this is actually the case with the Raman-active ν_1 band of K_2MnF_6 (C_{6v}^4 space group) and of Na_2SiF_6 and Na_2GeF_6 (D_3^2 space group). The separation between the components reaches 10-15 cm^{-1} at the most. Such a small difference between

the respective transition energies shows that the site effects upon the vibrational behaviour of the molecule are much less important than the effects of the molecular symmetry itself. In some cases, a mode arising from interactions between two or more molecules in the same unit cell, even if active, may manifest with such a weak intensity as not to be observed at all. In a certain sense, these interaction internal modes could be treated as pseudo-lattice modes, although their frequencies may be generally higher than the frequencies of proper lattice modes. A justification of this point of view would be that the corresponding extra bands should only appear in solid state spectra.

Site group analysis shows that the triply degenerate F modes of the regular MF_6^{2-} groups are split in the crystal into A + E modes, but no definite assignment of the observed components can be made otherwise. The observed vibrational spectra of the C_{6v}^4 A_2MF_6 compounds have, in fact, much fewer bands than predicted by factor or even site group analyses. This might be qualitatively explained by assuming that some of the bands - those which represent motions in isolated octahedra - will have identical frequencies, and consequently the number of observed bands in the spectra will be lower than predicted. A small number of the new internal modes represent, as mentioned, interactions between the two molecules in the unit cell and it is to be expected that sometimes they will have low intensity and will be not easily observable.

(iv) A_2MF_6 compounds of D_3^2 (P321) space group

This structure is also trigonal, but the overall symmetry is

much lower than in D_{3d}^3 space group. There are 3 formula-units in the crystalographic unit cell, the atoms being arranged as follows:

M(1): (1a) 000
M(2): (2d) $\pm(\frac{1}{3}\ \frac{2}{3}\ v)$
A(1): (3e) uu0
A(2): (3f) uu$\frac{1}{2}$
F(1), F(2) and F(3): (6g) uvw

For Na_2SiF_6, the parameters u,v, and w are[41,49]:

$v(Si_2) = 0.506$; $u(Na_1) = 0.379$; $u(Na_2) = 0.714$; $u(F_1) = 0.087$;
$v(F_1) = -0.092$; $w(F_1) = 0.810$; $u(F_2) = 0.444$; $v(F_2) = -0.401$;
$w(F_2) = 0.701$; $u(F_3) = 0.230$; $v(F_3) = -0.260$; $w(F_3) = 0.310$.

For Na_2GeF_6, the parameters are not known so far.

The three MF_6^{2-} ions in the unit cell, although similar in shape (almost perfect octahedra), dimension and site, are of two independent kinds with respect to their position in the lattice (rotation around c-axis). Their site symmetry is C_2. Each Na atom is in an octahedral hole, with 6 F neighbours at distances which range from 2.18 to 2.45 Å in Na_2SiF_6[49].

In this very unsymmetrical arrangement, probably brought about by the small size of the cations, it is expected that the spectra will be very rich. The C_2 site being non-centrosymmetric, the Laporte rule is relaxed and many transitions should gain activity both in the infrared and Raman; all degeneracies should be removed, the representation of nuclear motions being reduced to 8A + 7B for each one of the MF_6^{2-} ions. On the other hand, the factor group splitting is not so drastic. If Winston and Halford's method[20] is applied in order to carry out the reduction from the site group C_2

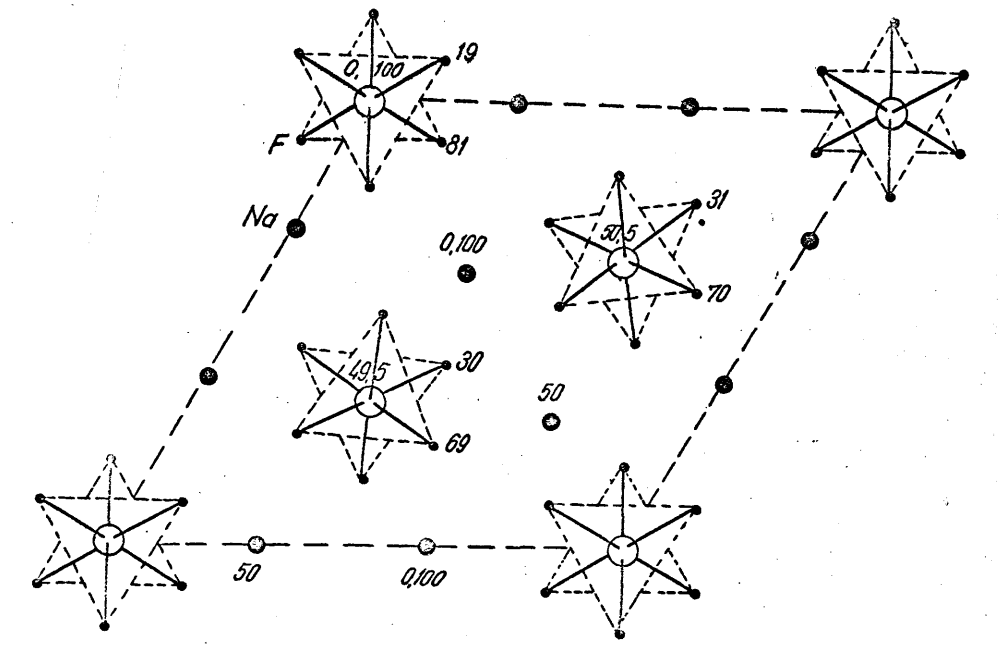

Figure 13

to factor group D_3, the reduced representation

$$8A_1 + 7A_2 + 15E$$

is obtained. This has 45 degrees of freedom and thus the smallest Bravais cell is formed from 3 formula-units. It may again be considered as identical with the crystalographic unit cell (Figure 13). The results of a factor group analysis carried out on this cell are listed in Table 7.

Infrared-active modes:

$7A_2 + 15E$(internal) $+ 7A_2$(translatory + rotatory-lattice)
$+ 11E$(translatory + rotatory-lattice)

Raman-active modes:

$8A_1 + 15E$(internal) $+ 4A_1$(translatory + rotatory-lattice)
$+ 11E$(translatory + rotatory-lattice)

Table 7

Classification of normal vibration modes of trigonal (D_3^2) A_2MF_6 compounds

D_3^2	n_i	T	α	T'	R'	n_i'
A_1	12	0	2	3	1	8
A_2	15	1	0	5	2	7
E	27	1	2	8	3	15
Number of degrees of freedom	81	3	//	24	9	45

There are no inactive modes.

The site group analysis is, as in the preceding case of hexagonal C_{6v}^4 A_2MF_6 compounds, unreliable, because intermolecular non-lattice modes, arising from interactions between the three molecules in the unit cell, cannot be found by this method.

The observed spectra of the compounds in this class contain fewer bands than predicted by FGA. Not all the bands predicted to appear by this method are bound to appear in the spectra at different frequencies. Many of them, those which represent identical motions in different MF_6^{2-} groups, will have identical or almost identical frequencies, thus diminishing the number of observed distinct bands. Pseudo-lattice and lattice bands will appear in the same way as for C_{6v}^4 A_2MF_6 compounds.

Chapter 4 EXPERIMENTAL

The various factors that may influence the structure of A_2MF_6 compounds, which will be reviewed in Chapter 7, prevent the preparation of a definite structure by deliberately tailoring the preparation conditions. In this situation, we chose to follow standard literature preparative techniques and to subsequently examine the compounds to identify their crystalline structure.

Preparation Details

The hexafluorosilicates A_2SiF_6 and -germanates A_2GeF_6 (A = Na, K, Rb, Cs) were prepared from aqueous solutions[50], from SiO_2/GeO_2 and ACl or AF. Platinum and Teflon vessels were used. Several recrystallizations from water were made before use. The compounds are white and very stable.

Potassium hexafluoromanganate(IV) K_2MnF_6 was obtained either by fluorination at 375-400 °C of a $MnCl_2$ + 2ACl mixture[51], or by electrolysis at 2.5 V, in HF, of Mn(III) and the corresponding alkali metal fluoride[52]. Rb_2MnF_6 and Cs_2MnF_6 were prepared by the former method only. The compounds obtained by either of these methods are yellow, but they are moisture-sensitive and become reddish in time. They were therefore handled in the controlled atmosphere of a dry box.

X-Ray Structure

The unit cell dimensions and the space groups of all compounds prepared were determined by X-ray powder photographs. The photo-

graphs were obtained by using Cu $K\alpha_1$ radiation and a 114.6 mmØ Debye-Scherrer camera, with a Straumanis film arrangement. The samples were sealed in 0.5 mm quartz capillaries.

The diffraction lines obtained for each compound were measured with an accuracy of 0.02 and the diffraction angle θ_{obs} and $\sin^2 \theta_{obs}$ calculated.

The values of $\sin^2 \theta_{calc}$ for various reflection planes hkl were calculated for cubic and hexagonal structures by using the relationships[53]:

- cubic structure:

$$d_{hkl} = \frac{a_o}{\sqrt{h^2+k^2+l^2}} \qquad (50)$$

where a_o is the assumed length of the unit cell;

- hexagonal (including trigonal) structure:

$$d_{hkl} = \frac{a_o}{\sqrt{\frac{4}{3}(h^2+hk+k^2) + \frac{l^2}{c_o^2}}} \qquad (51)$$

where a_o and c_o are the assumed lengths of the unit cell along a- and c-axis, respectively.

The interplanar distances d_{hkl} are related to the diffraction angle θ_{calc} by the Bragg relation,

$$n\lambda = 2d_{hkl}\sin\theta_{calc} \qquad (52)$$

where λ is the wavelength of the X radiation used and n is an integer. Therefore

- for cubic structures:

$$\sin^2 \theta_c = \frac{n^2\lambda^2}{4a_o^2}(h^2+k^2+l^2) \qquad (53)$$

- for hexagonal structures:

$$\sin^2\theta_c = \frac{n^2\lambda^2}{4a_o^2}\left[\frac{4}{3}(h^2+hk+k^2) + \frac{l^2}{c_o^2}\right] \qquad (54)$$

The unit cell dimensions a_o and c_o were corrected by means of a desk digital computer until the best fit between $\sin^2\theta_c$ and $\sin^2\theta_o$ (c and o symbolizing calculate and observed values, respectively) was reached, for a large number of reflection planes.

The crystallographic system to which the cell belongs may generally be identified by the missing reflection lines on the Debye-Scherrer X-ray photograph[54].

For a face-centered cubic structure, the lines which are extinct are those corresponding to the reflection planes whose Miller indices hkl give for

$$N = h^2 + k^2 + l^2$$

a value of 1, 2, 5, 6, 7, 9, 10, 13, 14, 15, 17, 18, 21, 22, 23, etc.

For a hexagonal structure, the extinct lines correspond to the planes whose Miller indices hk give for

$$N = h^2 + hk + k^2$$

a value of 2, 5, 6, 8, 9, 10, 11, 14, 15, 17, 18, 20, 22, 23, etc.

Table 8 lists the calculated (c) and observed (o) $\sin^2\theta$ values for all A_2MF_6 compounds whose spectra are reported in this work. The unit cell dimensions determined in the present work for these compounds, together with the literature data, are presented in Table 9.

Infrared and Raman Spectra

Near-infrared (above 400 cm^{-1}) spectra were run on a Perkin-Elmer

Table 8

X-Ray Powder Data for A_2MF_6 compounds

Cubic O_h^5 compounds

Intensity	Reflection plane (hkl)	K_2SiF_6		Rb_2SiF_6		Cs_2SiF_6	
		$\sin^2\theta_o$	$\sin^2\theta_c$	$\sin^2\theta_o$	$\sin^2\theta_c$	$\sin^2\theta_o$	$\sin^2\theta_c$
9	111	.0268	.0269	.0253	.0250	.0231	.0225
7	200	-	.0359	.0331	.0333	.0306	.0300
10	220	.0718	.0717	.0670	.0666	.0607	.0600
3	311	.0988	.0987	-	.0916	.0829	.0825
10	222	.1079	.1076	.1004	.0999	.0907	.0900
9	400	.1439	.1435	.1339	.1332	.1209	.1200
2	331	.1712	.1704	-	.1582	-	.1425
10	420	.1800	.1794	.1670	.1666	.1507	.1500
10	422	.2162	.2153	.2004	.1999	.1812	.1800
3	511,333	.2433	.2422	.2249	.2248	.2034	.2025
7	440	.2879	.2870	.2678	.2665	.2408	.2400
2	531	.3151	.3139	.2932	.2915	-	.2625
9	442,600	.3236	.3229	.3003	.2998	.2707	.2700
8	620	.3600	.3588	.3325	.3331	.3004	.3000
7	622	.3958	.3946	.3660	.3664	.3305	.3300
4	444	.4324	.4305	.3995	.3997	.3612	.3600
2	551,711	.4589	.4574	.4235	.4247	.3809	.3825
6	640	-		.4339	.4331	.3914	.3900
9	642	.5037	.5023	.4654	.4664	.4201	.4200
2	553,731	.5311	.5292	-	.4913	-	.4424
3	800	.5759	.5740	.5326	.5330	.4794	.4799
6	644,820	.6108	.6099	.5656	.5663	.5094	.5099
6	660,822	.6467	.6458	.5987	.5996	.5387	.5399
2	555,751	.6738	.6727	.6209	.6246	-	.5624
3	662	.6819	.6816	.6313	.6329	.5698	.5699
4	840	.7179	.7175	.6651	.6662	.5993	.5999
1	753,911	.7445	.7444	-	.6912	-	.6224
5	842	.7540	.7534	.6983	.6995	.6287	.6299

Cubic O_h^5 compounds (cont'd)

Intensity	Reflection plane (hkl)	Cs_2GeF_6		Rb_2MnF_6		Cs_2MnF_6	
		$\sin^2\theta_o$	$\sin^2\theta_c$	$\sin^2\theta_o$	$\sin^2\theta_c$	$\sin^2\theta_o$	$\sin^2\theta_c$
9	111	.0229	.0220	.0254	.0248	.0230	.0224
7	200	.0302	.0293	.0338	.0330	.0306	.0298
10	220	.0595	.0586	.0669	.0661	.0604	.0596
3	311	.0823	.0806	.0913	,0908	-	.0820
10	222	.0894	.0880	.0998	.0991	.0901	.0895
9	400	.1186	.1172	.1329	.1322	.1201	.1193
2	331	-	.1392	-	.1569	-	.1417
10	420	.1482	.1465	.1657	.1652	.1504	.1492
10	422	.1772	.1758	.1990	.1983	.1791	.1790
3	511,333	.1997	.1978	.2236	.2230	.2008	.2013
7	440	.2359	.2348	.2643	.2642	,2390	.2386
2	531	.2578	.2564	.2897	.2890	.2600	.2610
9	442,600	.2650	.2637	.2977	.2973	.2682	.2684
8	620	-	.2930	.3304	.3303	.2980	.2982
7	622	.3229	.3223	.3629	.3633	.3274	.3281
4	444	.3524	.3516	.3958	.3964	.3574	.3579
2	551,711	.3743	.3735	.4199	.4210	-	.3803
6	640	-	.3809	-	.4294	-	.3877
9	642	.4110	.4102	.4616	.4624	.4168	.4175
2	553,731	.4316	.4321	-	.4872	-	.4399
3	800	.4689	.4688	.5277	.5285	. -	.4772
6	644,820	.4978	.4980	.5601	.5615	.5063	.5070
6	660 ,822	.5272	.5273	.5935	.5946	.5353	.5362
2	555,751	.5481	.5493	-	.6193	-	.5592
3	662	.5559	.5566	-	.6276	-	.5667
4	840	.5853	.5859			.5958	.5965
1	753,911	-	.6079			.6202	.6182
5	842	.6139	.6152			-	.6263
4	664	.6430	.6445			.6550	.6561

Trigonal D_{3d}^3 compounds

Intensity	Reflection plane (hkl)	K_2GeF_6 $\sin^2\theta_o$	$\sin^2\theta_c$
7	100	.0250	.0250
7	001	.0281	.0274
10	101	.0531	.0525
9	110	.0749	.0751
3	111	.1031	.1026
5	002	.1104	.1097
10	201	.1285	.1276
8	102	.1356	.1348
2	210	.1773	.1753
2	112	.1857	.1849
7	211	.2030	.2027
8	202	.2104	.2099
4	300	.2262	.2254
3	003	.2470	.2469
3	301	.2538	.2528
1	103	.2735	.2720
9	212	.2860	.2850
8	220	.3011	.3005
9	113	.3224	.3221
6	203	.3467	.3471
7	311	.3533	.3530
3	401	.4287	.4281
2	312(004?)	.4359	.4353
3	104	.4629	.4640
3	303	.4716	.4723
3	321	.5030	.5032
4	402	.5105	.5104
3	410	.5253	.5259
3	322	.5837	.5855
7	214	.6132	.6143

Hexagonal C_{6v}^4 compounds

Intensity	Reflection plane (hkl)	K_2MnF_6 $\sin^2\theta_o$	K_2MnF_6 $\sin^2\theta_c$	Rb_2GeF_6 $\sin^2\theta_o$	Rb_2GeF_6 $\sin^2\theta_c$
1	100	-	.0243	.0224	.0224
6	002	.0283	.0278	.0258	.0256
9	101	.0321	.0312	.0288	.0288
10	102	.0526	.0521	.0479	.0479
10	110	.0737	.0730	.0676	.0673
7	103	.0870	.0868	.0795	.0800
2	200?	-	.0974	.0845	.0897
6	201	.1050	.1043	.0960	.0961
4	004	.1112	.1112	.1022	.1024
10	202	.1262	.1252	.1155	.1153
3	104+113	-	.1355 .1355	.1252	.1248 .1249
8	203	.1604	.1599	.1470	.1473
3	114	-	.1842	.1680	.1697
8	105+212	.1970	.1982 (212)	.1823	.1823 .1825
2	204	.2082	.2086	.1915	.1921
8	300	.2190	.2091	.2016	.2018
9	213	.2328	.2329	.2142	.2145
9	205	.2698	.2711	.2493	.2496
7	214+303	.2819	.2816 .2816	.2585	.2593 .2594
9	220	.2922	.2922	.2684	.2690
2	304	-	.3303	.3024	.3042
10	007	.3430	.3408	.3159	.3135
7	313	.3780	.3790	.3480	.3490
2	224	.4025	.4034	.3703	.3714
3	402	.4164	.4174	.3841	.3843
2	314	-	.4277	.3923	.3938
2	207	.4391	.4378	.4012	.4032
4	403	.4509	.4521	.4151	.4163
7	225	.4667	.4659	.4299	.4289
5	410	.5094	.5113	.4686	.4708
3	412	-	.5390	.4968	.4964

Hexagonal D_3^2 compounds (b - broad line)

Intensity	Reflection plane (hkl)	Na_2SiF_6		Na_2GeF_6	
		$\sin^2\theta_o$	$\sin^2\theta_c$	$\sin^2\theta_o$	$\sin^2\theta_c$
10	001	.0233	.0234	.0225	.0226
10	110	.0303	.0302	.0288	.0294
10	200+101	.0366b	.0403 .0335	.0328	.0324 (101)
10	111	.0539	.0536	.0522	.0520
10	201	.0638	.0637	.0613	.0617
6	210	.0709	.0705	-	-
9	002+211	.0945b	.0935 .0939	.0915	.0905 .0911
10	301	.1142	.1141	.1103	.1107
7	220	.1217	.1209	-	.1174
6	202	.1330b	.1338	-	.1296
7	221	.1448	.1443	.1392	.1400
6	311	.1548	.1544	.1490	.1498
8	212	.1644b	.1640	.1600	.1590
10	302+401	.1843b	.1842 .1847	.1787	.1786 .1792
3	320	.1923	.1915	-	.1860
9	222+321	.2155	.2144 .2149	.2076	.2079 .2086
6	312	.2254	.2245	.2187	.2177
8	411	.2359	.2351	.2266	.2281
3	113	.2427	.2406	.2355	.2331
6	402	.2547b	.2548	-	.2471
9	330+501	.2732	.2721 .2754	.2622	.2643 (330)
8	420	.2826	.2822	.2738	.2741
7	412+421	.3064	.3052 .3056	.2955	.2960 .2967
2	223	.3303	.3313	-	.3211
4	511	.3369	.3358	-	.3260
1	502	.3443	.3455	-	.3352
1	332	.3647	.3656	-	.3548
4	004+422	.3754	.3740 .3757	-	.3621 .3646
6	520	.3943	.3931	-	.3817
4	114+323	.4043	.4042 .4049	.3912	.3915 (114)

Table 9

Space groups and lattice constants of some A_2MF_6 compounds

Compound	Space group	z	Unit cell parameters				Refs.
			a_o (Å)		c_o (Å)		
			Present work	Other refernces	Present work	Other references	
Na_2SiF_6	D_3^2	3	8.86	8.859	5.04	5.038	49
K_2SiF_6	O_h^5	4	8.13	8.133	-	-	55,56
				8.17			57
Rb_2SiF_6	"	"	8.44	8.446	-	-	57
				8.452			56
Cs_2SiF_6	"	"	8.895	8.89	-	-	55
				8.919			56
				8.867			57
Na_2GeF_6	D_3^2	3	8.99	8.99	5.12	5.12	58
K_2GeF_6	D_{3d}^3	1	5.62	5.62	4.65	4.65	59
Rb_2GeF_6	C_{6v}^4	2	5.94	5.94	9.63	9.63	60
Cs_2GeF_6	O_h^5	4	9.00	8.99	-	-	61
				9.021			56
K_2MnF_6	C_{6v}^4	2	5.70	5.67	9.24	9.35	60,62
Rb_2MnF_6	O_h^5	4	8.476	8.430	-	-	60,62
Cs_2MnF_6	"	"	8.92	8.92	-	-	62

Model 225 Spectrophotometer. Samples were prepared as Nujol mulls between CsI plates, the hygroscopic compounds being handled in a dry box. For the far-infrared (400-40 cm^{-1}) range, a RIIC Fourier Transform Interfereometer was used, with Melinex beam splitter (8μ sampling interval, 5 cm^{-1} resolution - see Chapter 2). The compounds were embedded in polyethylene under 12 t/sq.in. pressure, the concentration per unit surface area varying from 5 to 20 mg/sq.in. The spectra were recorded both at room and liquid nitrogen temperatures. For the low temperature far-infrared spectra a special RIIC cell was used. The temperature was measured by means of a thermocouple and precision bridge with $\pm 10\text{-}15\ ^{o}C$ accuracy. After reaching the liquid nitrogen temperature thirty minutes were allowed before running the spectra.

Raman spectra were obtained on a Cary 81 Spectrometer*, provided with a He-Ne laser as excitation source. The monochromator slits were set at 5 cm^{-1}. Samples (as powders) were introduced in Pyrex tubes one end of which was closed and ground flat. For hygroscopic samples (the hexafluoromanganates), the tubes were filled and sealed in the dry box. The flat end of the cell was placed against the hemispherical lens, the scattered photons being therefore observed at 180^{o} (see the arrangement in Figure 7).

* The author wishes to thank Dr. R.H. Nuttall and Mrs. Ann McConnell for permission to use the Raman spectrometer of the University of Strathclyde.

Chapter 5 INTERPRETATION OF THE SPECTRA

The recorded infrared and Raman spectra of the investigated A_2MF_6 compounds are presented in Figures 14-19 (low temperature spectra being indicated by dotted lines). The positions of maxima of fundamental and some combination bands, as well as their assignment - when this could be reasonably made - is also indicated.

As a general feature, the observed spectra can be interpreted on the basis of factor group analysis results (Chapter 3), though not all the modes predicted by FGA to be active either in infrared or in Raman spectra could actually be observed.

Almost all fundamental internal modes which are predicted to be present in infrared or Raman spectra were observed. Some lattice fundamentals were obtained in the infrared spectrum, but none in the Raman spectrum (with the possible exception of Cs_2MnF_6).

The predicted factor group splitting of some internal bands in trigonal and hexagonal compounds can be qualitatively accounted for, although no definite assignments could be made without precise polarisation measurements. Their species remain to be determined unambiguously by examining the spectra of single crystal samples.

In all cases, the internal active fundamentals appear in the solid state infrared and Raman spectra at almost the same positions as those reported for the corresponding solutions[1,2,63,64]. In Table 10 the positions of the fundamental internal vibrational modes are shown for solid state and solution spectra. This small shift

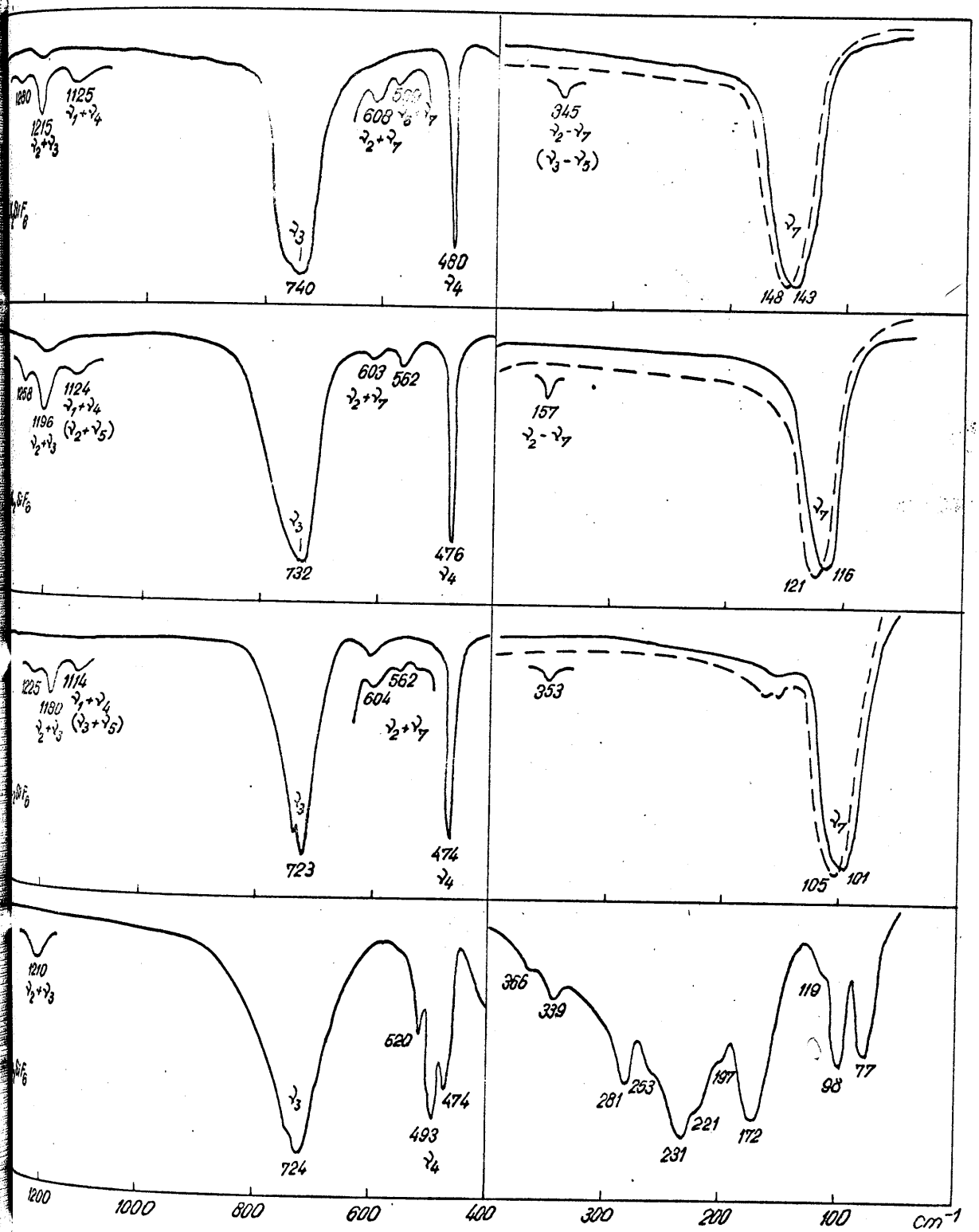

room temperature

liquid N_2 temperature

Figure 14

Infrared spectra of A_2SiF_6 compounds

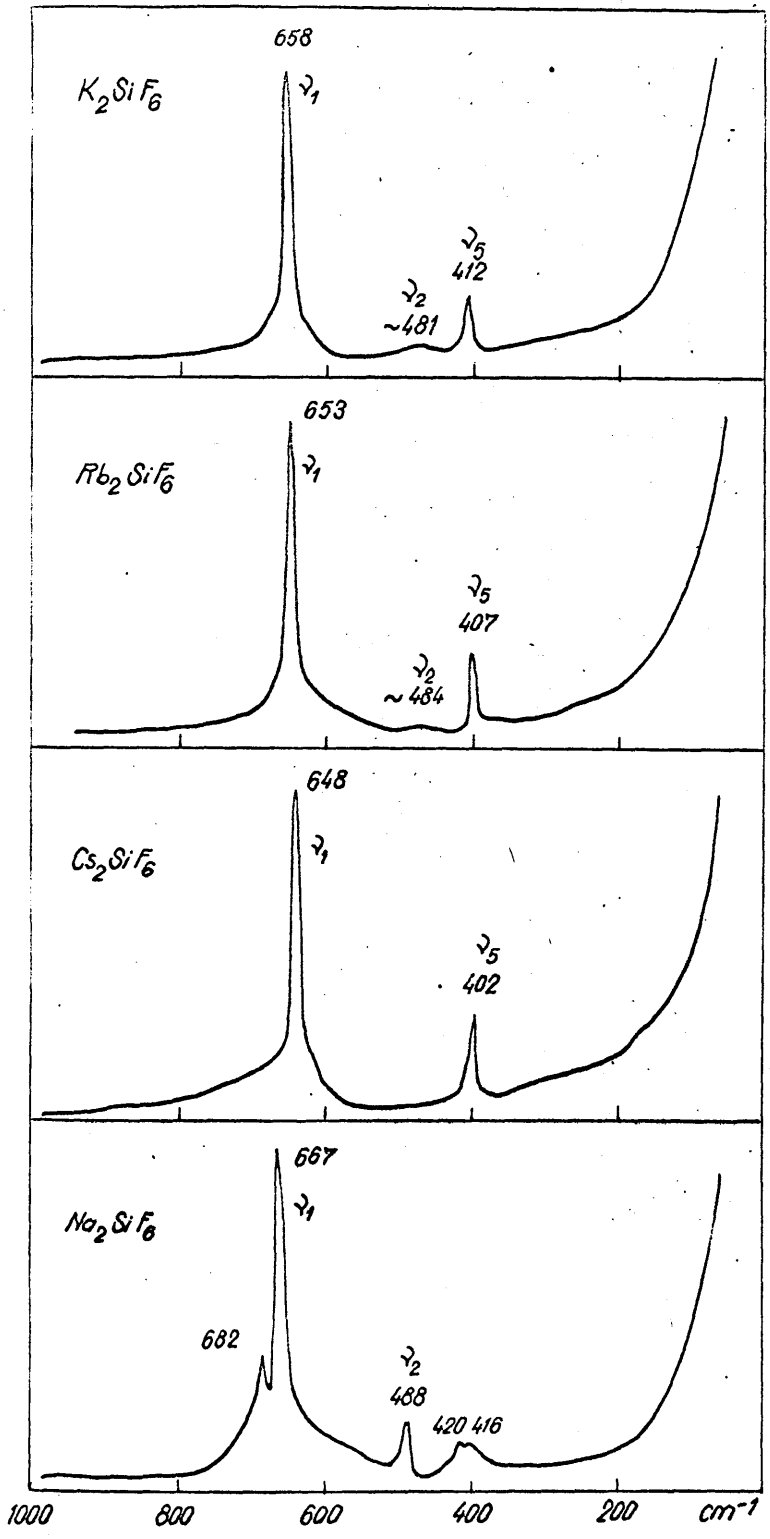

Figure 15

Raman spectra of A_2SiF_6 compounds

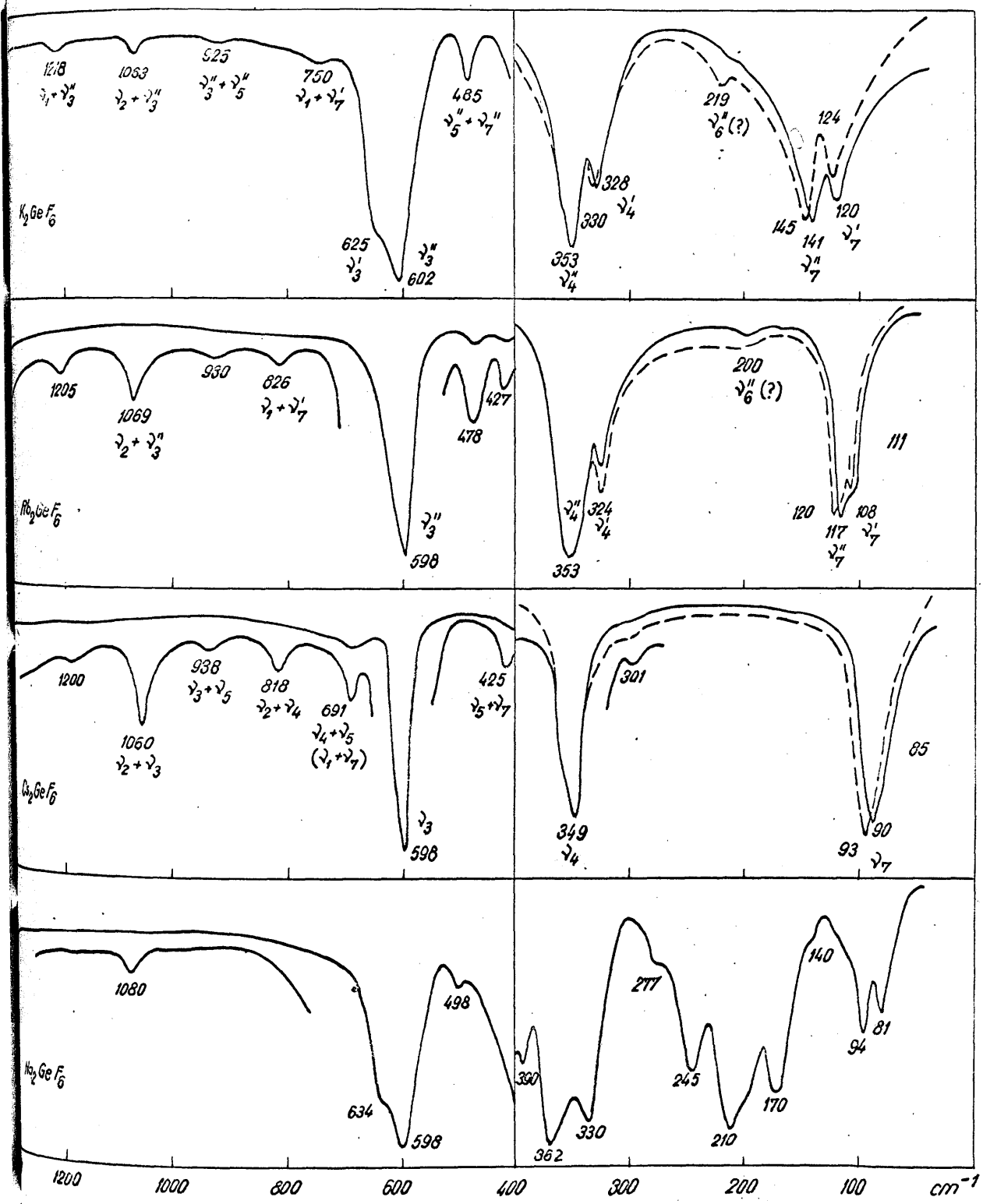

Figure 16

Infrared spectra of A_2GeF_6 compounds

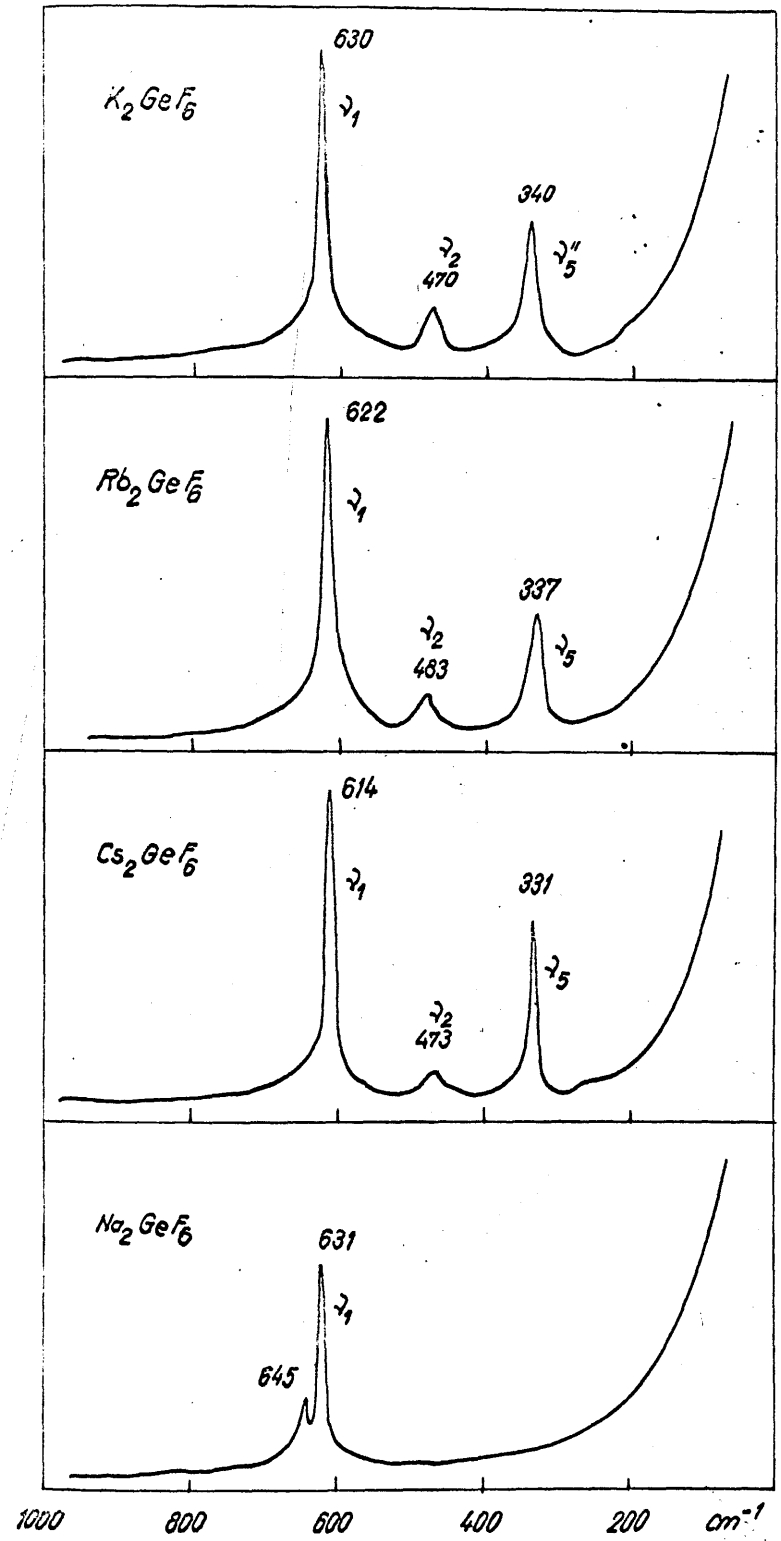

Figure 17

Raman spectra of A_2GeF_6 compounds

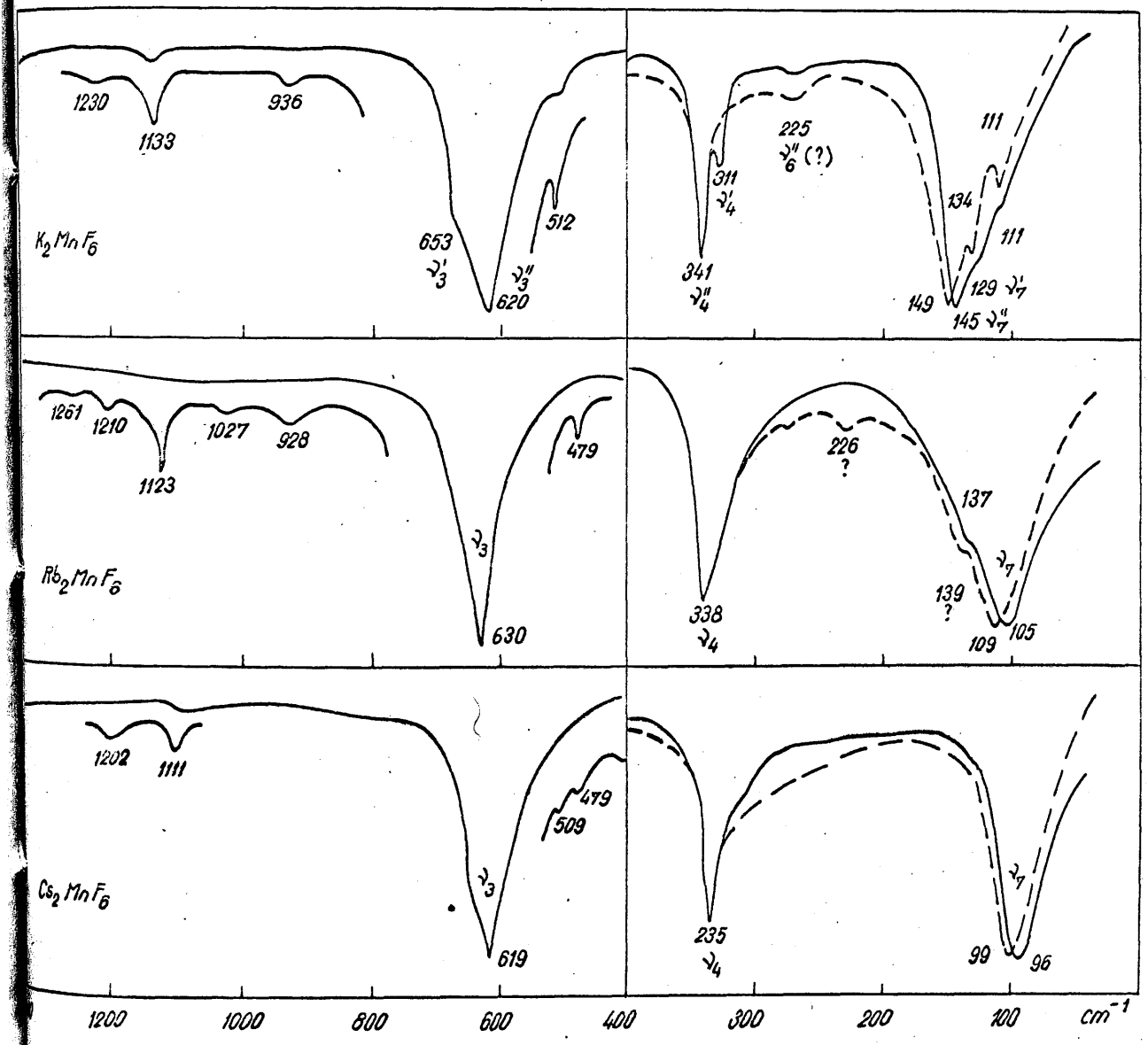

Figure 18

Infrared spectra of A_2MnF_6 compounds

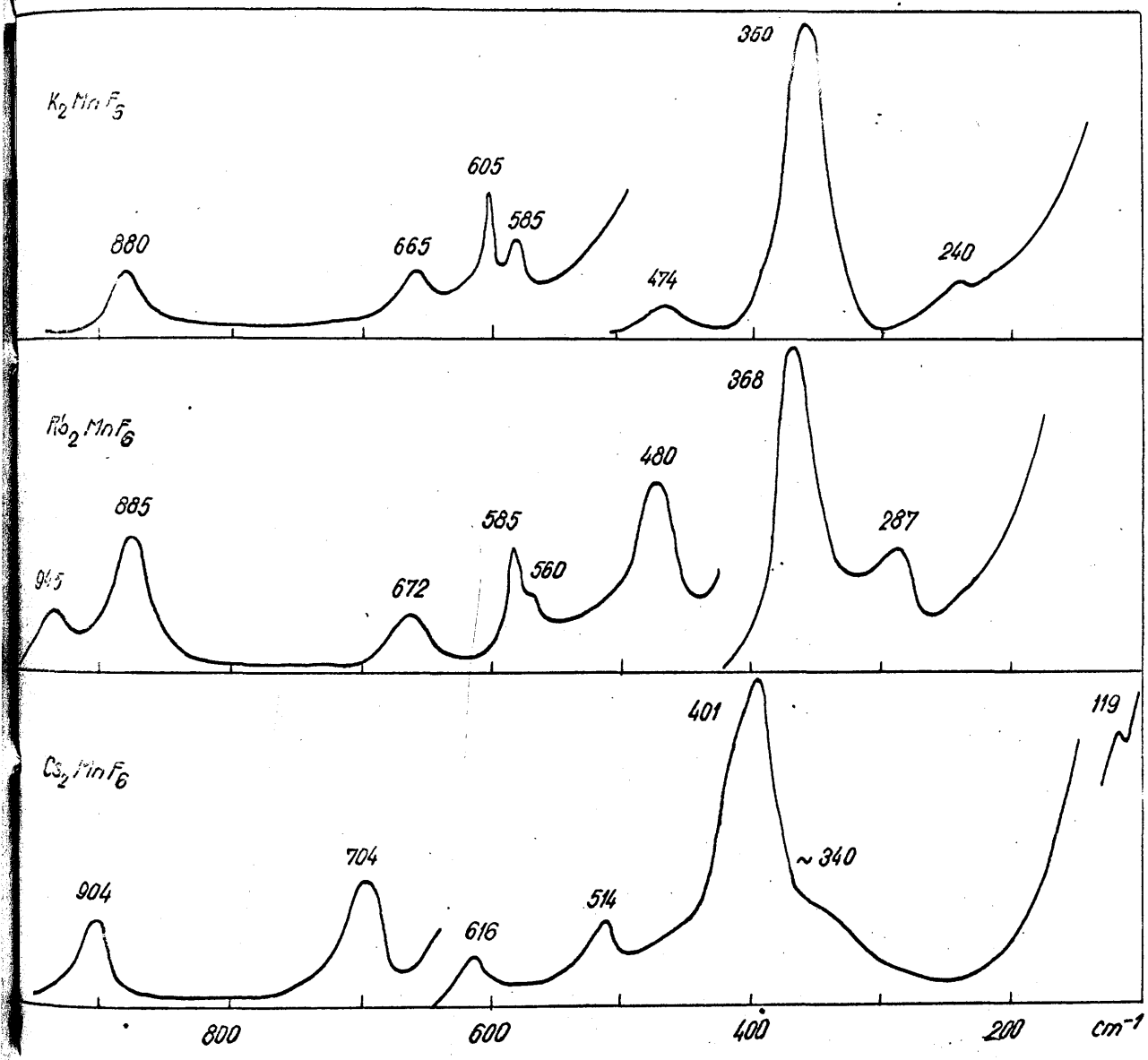

Figure 19

Raman spectra of A_2MnF_6 compounds

Table 10

Infrared and Raman internal mode fundamentals for some A_2MF_6 compounds (solid state and solution) (in cm^{-1})

Compound	Sample state	ν_1	ν_2	ν_3	ν_4	ν_5	Reference
A_2SiF_6	SiF_6^{2-}	656	465	740	485	400	66
	Na_2SiF_6	667	488	724* ...	493* 474	420 416	This work
	K_2SiF_6	658	481	740	480	412	"
	Rb_2SiF_6	653	484	732	476	407	"
	Cs_2SiF_6	648	...	723	474	402	"
A_2GeF_6	GeF_6^{2-}	627	454	600	350	318	63
	Na_2GeF_6	631	...	634 598*	362* 330	...	This work
	K_2GeF_6	630	470	625 602*	353* 328	340	"
	Rb_2GeF_6	622	483	598	353* 324	337	"
	Cs_2GeF_6	614	473	598	342	331	"
A_2MnF_6	MnF_6^{2-}	615	480	...	...	282	67
	K_2MnF_6	600@	510@	630@	338@	308@	68
	"	600	507	620	340	310	69
	"	605	422&	653 620*	341* 311	231&	This work
	Rb_2MnF_6	585	436&	630	338	244&	"
	Cs_2MnF_6	615	480&	...	...	282&	67
	"	616	478&	619	335	288&	This work

* Main peak if splitting occurs.

@ From reflectance and Raman spectra.

& Calculated from combination bands in Raman spectra, according to the assignments listed in Table 13. These assignments remain questionable.

on passing from solutions to solid state suggests a limited influence, besides factor group splitting, of the lattice environment upon the vibrations of the MF_6^{2-} anion. The small bandwidth of the combination bands which involve lattice modes also supports this conclusion[65]. For the A_2MF_6 compounds for whcih force constant calculations have been carried out, i.e. those crystallizing in the O_h^5 space group, a small amount of mixing between molecular and lattice modes has been found (see Chapter 7), and it is reasonable to believe that the same is likely to be true for the other structures. Of the two infrared-active molecular fundamentals ν_3 and ν_4, the former has a relatively higher degree of mixing with the lattice mode ν_7, in all structures. From the point of view of group theory mixing between ν_3 and ν_7 and between ν_4 and ν_7 are equally permitted. The mixing of ν_7 with ν_3 (rather than with ν_4) might be explained by the resemblance of the motions in these vibration modes, as can be seen from Table 18 and Figure 22 (Chapter 7). The mixing may account for the large half-width of the ν_3 band, observed in all compounds (except Cs_2GeF_6). Of the three Raman-active molecular modes, only ν_5 interacts with the lattice motions of similar symmetry and for this band too a certain broadening may be noticed as compared with the same band in the solution spectra.

The F_{2u} (ν_6) internal mode, which is inactive under perfect octahedral symmetry (in solution or in crystalline cubic O_h^5 compounds), become infrared-active in a trigonal or hexagonal surrounding. Although the corresponding band may appear in the spectrum,

its position cannot be located with certainty without the assistance of force constant evaluation. We have estimated the force constants for the cubic O_h^5 compounds listed in Table 9 (see Chapter 6). The resulting frequency of ν_6 mode is ca. 255 cm^{-1} for SiF_6^{2-}, ca. 194 cm^{-1} for GeF_6^{2-}, and ca. 203 cm^{-1} for MnF_6^{2-}. Weak bands near these frequencies were observed in the spectra of trigonal and hexagonal compounds (Figures 14, 16, 18). Therefore these bands can be reasonably taken as representing the ν_6 mode. No similar situation was encountered in the Raman spectra, where ν_6 should have an active component in the case of hexagonal compounds. Table 11 lists the calculated and observed ν_6 frequencies for various compounds.

In the trigonal (D_{3d}^3 and D_3^2) compounds, all three infrared-active modes are predicted to be split in the solid state; this splitting was actually observed in K_2GeF_6, Na_2GeF_6 and Na_2SiF_6. No definite assignemnts of the species of the observed components could be made. The splitting for the two molecular F_{1u} modes of K_2GeF_6 is ca. 20 cm^{-1}; for Na_2GeF_6, ca. 35 cm^{-1}; and for Na_2SiF_6, ca. 20 cm^{-1}. The F_{1u} lattice mode ν_7 is also split under trigonal symmetry, the magnitude of the splitting being 21, 13 and 21 cm^{-1} for K_2GeF_6, Na_2GeF_6 and Na_2SiF_6, respectively (cf. Table 12).

For the hexagonal (C_{6v}^4) compounds, a site splitting ($F_{1u} \longrightarrow A_1 + E_1$) is predicted for triply degenerate modes, both components being active in infrared and Raman spectra. Both ν_4 and ν_7 F_{1u} bands show 2 components in the infrared spectra of K_2MnF_6 and Rb_2GeF_6, but no trace of the corresponding components was observed

Table 11

Frequency of the ν_6 molecular mode (in cm^{-1})

Compound	Calculated*	Observed (infrared)
Na_2SiF_6	~255	253 231** 221
Na_2GeF_6	~194	245 210** 170
K_2GeF_6	~194	219 (ν_6'')
Rb_2GeF_6	~194	200
K_2MnF_6	~203	225

* From force constant estimation for the respective cubic (O_h^5) A_2MF_6 compounds.

** Main peak if splitting occurs.

Table 12

Observed infrared-active lattice modes of A_2MF_6 compounds (in cm^{-1})

Compound	Space group	Mode	Room temperature	Liq. nitrogen temperature
Na_2SiF_6	D_3^2	$A_2 + E$	77 + 98	...
K_2SiF_6	O_h^5	F_{1u}	143	148
Rb_2SiF_6	"	"	116	121
Cs_2SiF_6	"	"	101	105
Na_2GeF_6	D_3^2	$A_2 + E$	81 + 94	...
K_2GeF_6	D_{3d}^3	$A_{2u} + E_u$	120 + 141	124 + 145
Rb_2GeF_6	C_{6v}^4	$A_1 + E_1$	108 + 117	110 + 120
Cs_2GeF_6	O_h^5	F_{1u}	90	93
K_2MnF_6	C_{6v}^4	$A_1 + E_1$	129 + 145	134 + 149
Rb_2MnF_6	O_h^5	F_{1u}	105	109
Cs_2MnF_6	"	"	96	99

A low-energy band was observed at 119 cm^{-1} in the Raman spectrum of Cs_2MnF_6, but it cannot be taken as the Raman-active lattice mode $F_{2g}(\nu_8)$ for reasons which will be discussed later in this Chapter.

in the Raman spectra. Therefore, it might be inferred that the Raman activity gained as a consequence of the hexagonal environment in these compounds must be weak enough, and so must be the environmental perturbation upon the concerned vibrational modes. The ν_3 F_{1u} band is markedly asymmetric in the spectra of these compounds, an indication of unresolved splitting at room temperature.

The Raman spectra for all compounds (with the possible exception of Cs_2MnF_6) have as a common feature the fact that only the fundamental internal active modes could be recorded. The only crystalline effect which could be detected was the duplication of the ν_1 totally-symmetric band in the spectra of the compounds whose unit cell contains more than one formula-unit, i.e. K_2MnF_6, Na_2SiF_6 and Na_2GeF_6, as discussed in Chapter 3. No such duplication was noticed for Rb_2GeF_6. The ν_2 (E_g) mode was not observed in the case of Na_2GeF_6 and Cs_2SiF_6, and in all other cases its intensity is much lower than that of the ν_1 (A_{1g}) band. The ν_2 bands have a large half-width and their location is only approximate for all compounds.

The only spectra which do not show the usual intensity pattern met in the spectra of the A_2MF_6 compounds having isolated MF_6^{2-} octahedra are the Raman spectra of hexafluoromanganates(IV). Their spectra consist of a much larger number of bands than are present for other compounds in the same class, and the bands are much stronger. This anomaly has been observed also by other authors[67-69]. This complicated and unusual pattern (Fig. 19) might be explained

by considering that a resonance appears between the He-Ne laser exciting line (6328 Å) and either the $^4A_{2g} \longrightarrow {}^2E_g$ d-d absorption[67] or the $^2E_g \longrightarrow {}^4A_{2g}$ phosphorescence[68]. One of the 'hot bands' of the above spin-forbidden transition, located at 15,790 cm^{-1} overlaps with the laser excitation line (15,803 cm^{-1}). The resulting resonance emission is much more intensive than the Raman spectrum and obscures it[69]. This effect is particularly important for Cs_2MnF_6, but it is also present for K_2MnF_6 and Rb_2MnF_6. It has been found that almost all the bands occuring in the anomalous Raman spectra of hexafluoromanganates(IV) are in fact vibrational components of the mentioned electronic transition. Thus, all bands appearing in the Raman spectrum must be either fundamentals, or combinations of the vibration modes in the ground ($^4A_{2g}$) or excited (^2E_g) states of the molecule. Matwiyoff and Asprey have consequently derived[67] the frequency values of the normal Raman-active modes of Cs_2MnF_6 on the basis of measured frequencies of these anomalous bands. We applied this method to all alkali hexafluoromanganates(IV) whose Raman spectra had been available, the tentative assignments being given in Table 13. The resulting frequencies of ν_1, ν_2 and ν_5 modes are listed in Table 10. These values are not, however, very consistent with the trend observed in the A_2SiF_6 and A_2GeF_6 series for the same modes in passing from A = K to A = Rb and Cs (a general decrease in frequency). Neither do they agree with the values for ν_1, ν_2 and ν_5 which Pfeil[69] was able to determine as fundamentals in the Raman spectrum of K_2MnF_6 at low temperatures (i.e. 600, 507 and

310 cm^{-1}, respectively) or with the values found[67] for the free MnF_6^{2-} anion. (We should mention also that the frequency of the ν_2 (E_g) mode, as calculated from some combination bands appearing in the infrared spectra (Figs. 14, 16, 18) are different from those given in Table 10, i.e. 513, 493 and 492 cm^{-1} for K_2MnF_6, Rb_2MnF_6 and Cs_2MnF_6, respectively. These values agree, though, with those found by Pfeil[69] for the ν_2 band of K_2MnF_6 at 85 °K.)

As shown in Chapter 7, the frequencies of the ν_8 mode, as resulting from force constant estimation for Rb_2MnF_6 and Cs_2MnF_6 are very low - 71.3 and 21.6 cm^{-1}, respectively. These values differ appreciably from the corresponding frequencies found from combination bands in the Raman spectra - 118 and 113 cm^{-1}, respectively. (This is a reason for not having considered the 119 cm^{-1} band appearing in the Raman spectrum of Cs_2MnF_6 as the ν_8 lattice vibration mode of this compound.)

All these facts do not recommend the use of the combination absorption and emission bands in the Raman spectra for finding the frequencies of the fundamental modes. In carrying out force constant calculations for Rb_2MnF_6 and Cs_2MnF_6 (Chapters 6-7), we preferred to use for ν_1, ν_2 and ν_5 modes frequency values close to those found for the MnF_6^{2-} group instead of the values obtained from combination bands.

The resonance nature of the anomalous spectra of A_2MnF_6 compounds, discussed above, might be tested by recording the Raman spectra with an excitation source whose wavelength is different from 6328 Å.

Table 13

Raman spectra of A_2MnF_6 compounds
(solid state)

Compound	Frequencies of the observed bands (cm^{-1})	Tentative assignment	Calculated frequencies (cm^{-1})
K_2MnF_6	240	$2\nu_2 - \nu_1$	239
	360	$\nu_5 + \nu_8$	353
	474	$\nu_5 + 2\nu_8$	475
	585	?	
	605	ν_1	605
	665	$\nu_2 + 2\nu_8$	666
	880	$2\nu_2$	844
Rb_2MnF_6	287	$2\nu_2 - \nu_1$	287
	368	$\nu_5 + \nu_8$	362
	480	$\nu_5 + 2\nu_8$	480
	560	$\nu_2 + \nu_8$	554
	585	ν_1	585
	672	$\nu_2 + 2\nu_8$	672
	885	$2\nu_2$	885
	945	$\nu_1 + \nu_5 + \nu_8$	945
Cs_2MnF_6	119	ν_8 ?	113
	340	$2\nu_2 - \nu_1$	340
	401	$\nu_5 + \nu_8$	401
	514	$\nu_5 + 2\nu_8$	514
	616	ν_1	616
	704	$\nu_2 + 2\nu_8$	704
	904	$\nu_1 + \nu_5$	904

Apart from the factor group splitting of some infrared and Raman bands, the crystalline environment has no other major effects on the behaviour of the bands. The splitting is most dramatic in the compounds which have a very low symmetry, such as the sodium hexafluorometallates. The low symmetry of their structure, in which the anions occupy two different positions (cf. Chapter 3), must produce, according to FGA, a notable change in both infrared and Raman spectra as compared with the spectra of other hexafluorometallates. The internal modes have to be extensively split, and a larger number of lattice modes to appear. Nevertheless, not all active modes predicted by FGA could be observed. Of the 18 active lattice modes predicted to appear in the infrared spectra of Na_2MF_6 (M = Si, Ge), only 5 could be actually recorded; none of the 15 Raman-active lattice modes could be observed. Many of the lattice modes may have identical frequencies, so that the number of observable bands is diminished, or very low intensities, especially in the Raman spectra. The splitting predicted by FGA for the internal degenerate modes was generally observed (see Tables 10 and 12).

The spectra of Na_2SiF_6 and Na_2GeF_6 reported in this work disagree in many respects with those reprted by other workers[64,66]. The disagreement relates to both frequency values and site- or factor group splitting.

The effect of changing the cation upon the frequencies of the molecular modes of an A_2MF_6 series may be seen from Table 10 to be a slight decrease of the frequency for all modes and all com-

pounds (except the hexafluoromanganates, for which the frequency measurement is not very accurate) in the order K $\longrightarrow$ Rb $\longrightarrow$ Cs. This might be due to a decreasing cation-anion electrostatic interaction with increasing the ionic radius of the cation. If the frequencies of the molecular modes given in Table 10 for A_2MnF_6 compounds - which have been partly calculated from the combination bands appearing in the Raman spectra - are correct, then the reverse effect is observed for these compounds, i.e. a general, rather important increase of the Raman-active molecular modes frequencies with increasing the cation size. Since an intensification of the cation-anion interaction with increasing the cation size would be unexpected, owing to the essential ionic character of the $A^+ - MF_6^{2-}$ interaction, the effect seems inexplicable and casts some doubt upon the validity of deriving the fundamental frequencies from combination bands, especially when the lattice modes participate to these combinations (cf. Chapter 1 and Table 13).

Generally, the fact that the frequencies of the molecular modes are not changed drastically on passing from solutions to solid state proves that the lattice has little influence upon the vibrational behaviour of the MF_6^{2-} isolated groups. The fact that the lattice modes have much lower energies than any molecular mode also supports this conclusion.

The effect of temperature upon the frequencies of molecular modes is different from the effect upon the frequencies of lattice modes. While the molecular mode frequencies remain practically unchanged when passing from the room temperature to liquid

nitrogen temperature, the lattice modes shift towards higher frequencies (cf. Figs. 14, 16 and 18). The value of the shift is of about 3-5 cm^{-1}. This seems to be an effect of lattice shrinking, which leads to an increase in the energy of lattice vibrations. The molecular MF_6^{2-} groups remain again largely unaffected.

Chapter 6 FORCE CONSTANT CALCULATION

The interesting problem which arises when dealing with molecular vibrations is to get a correct and meaningful picture of the forces acting to keep the molecular or crystal equilibrium configuration and of the form of the intra- and intermolecular potential fields governing the nuclear motions. Vibrational spectroscopy is most helpful in this respect because it offers a set of observed frequencies which can be correlated with those calculated from a set of force constants. These force constants are then improved until the best fit between the calculated and the observed frequencies is obtained.

The force constants obtained in this manner are of great importance because they may be related to the electronic structure of the molecule in question. Indeed, the harmonic force constants can be obtained theoretically by calculating the second derivative of the electronic energy in terms of nuclear coordinates[70]. There are several ways to carry out such calculations[71,72], starting from the molecular wave functions previously estimated by an accurate method (self-consistent field molecular orbitals, configuration interaction molecular orbitals, etc.).

Calculation of force constants from vibrational spectroscopic data implies a definite form to be chosen for the interaction potential. This choice is made so that the frequencies calculated on its basis reproduce as well as possible the observed spectrum.

The potential of a crystal is usually expressed - following the same model used in the normal coordinate treatment of isolated molecules - as a function of the nuclear displacement coordinates, the force constants being involved as parameters (see relation (2), Chapter 1). A generalized valence force field (GVFF) may involve various kinds of stretching, bending, and torsion force constants, as well as interactions between them. However, this is not a practical form of potential, because generally the number of observed frequencies is lower than the number of force constants and these cannot all be estimated (see later for a mathematical reason). The difficulty may be avoided either by having available vibrational data for a number of isotopically-substituted molecules in the same class, or by measuring the Coriolis coupling constants[73].

Since both these methods are tedious and difficult, a simplified Urey-Bradley force field (UBFF) is usually taken[74]. It consists of stretching and bending force constants, and of repulsive force constants between non-directly bonded atoms. Sometimes, when the number of observed frequencies is large enough, some interaction force constants may be included.

Choosing a UBFF means to purposely limit the number of interactions to those which have a major physical significance. It has the drawback of underestimating the long-range interactions, which may play a very important role in crystals[17].

The UB potential function is usually written in the form[75]

$$V = \sum_i \left[\tfrac{1}{2}K_i(\Delta r_i)^2 + K'_i r_i(\Delta r_i)\right] + \sum_{i<j} \left[\tfrac{1}{2}H_{ij}r_o^2(\Delta\alpha_{ij})^2 + H'_{ij}r_o^2(\Delta\alpha_{ij})\right]$$
$$+ \sum_{i<j} \left[\tfrac{1}{2}F_{ij}(\Delta q_{ij})^2 + F'_{ij}q_{ij}(\Delta q_{ij})\right] \qquad (55)$$

where Δr_i, $\Delta \alpha_{ij}$, and Δq_{ij} are the changes in the bond lengths, bond angles and bond distances between non-bonded atoms, respectively. K_i and K_i' are stretching force constants, while H_{ij} and H_{ij}', and F_{ij} and F_{ij}' are bending and repulsive force constants, respectively. r_o, r_i and q_{ij} are the equilibrium distances. The redundant coordinates q_{ij} may be removed by using the relation

$$q_{ij}^2 = r_i^2 + r_j^2 - 2r_i r_j \cos \alpha_{ij} \tag{56}$$

and its derivative

$$\begin{aligned}\Delta q_{ij} = {} & s_{ij}(\Delta r_i) + s_{ji}(\Delta r_j) + (t_{ij}t_{ji})^{\frac{1}{2}}(r_j/r_i)^{\frac{1}{2}}(r_i \Delta \alpha_{ij}) \\ & + (1/2q_{ij})\Big[t_{ij}^2(\Delta r_i)^2 + t_{ji}^2(\Delta r_j)^2 - s_{ij}s_{ji}(r_j/r_i)(r_i \Delta \alpha_{ij})^2 \\ & - 2t_{ij}t_{ji}(\Delta r_i \Delta r_j) + 2t_{ij}s_{ji}(r_j/r_i)(\Delta r_i r_i \Delta \alpha_{ij}) \\ & + 2t_{ji}s_{ij}(\Delta r_i r_i \Delta \alpha_{ij})\Big]\end{aligned} \tag{57}$$

where

$$s_{ij} = \frac{r_i - r_j \cos \alpha_{ij}}{q_{ij}}, \quad t_{ij} = \frac{r_j \sin \alpha_{ij}}{q_{ij}} \tag{58}$$

Substitution of (56) and (57) into (55) and neglect of linear terms in Δr_i and $\Delta \alpha_{ij}$ leads to

$$\begin{aligned}V = {} & \tfrac{1}{2} \sum_i \Big[K_i + \sum_{j \neq i}(t_{ij}^2 F_{ij}' + s_{ij}^2 F_{ij})\Big](\Delta r_i)^2 \\ & + \tfrac{1}{2} \sum_{i<j} \Big[H_{ij} - s_{ij}s_{ji}F_{ij}' + t_{ij}t_{ji}F_{ij}\Big](r_{ij} \Delta \alpha_{ij})^2 \\ & + \sum_{i<j} \Big[-t_{ij}t_{ji}F_{ij}' + s_{ij}s_{ji}F_{ij}\Big](\Delta r_i)(\Delta r_j) \\ & + \sum_{i \neq j} \Big[t_{ij}s_{ji}F_{ij}' + t_{ji}s_{ij}F_{ij}\Big](r_j/r_i)^{\frac{1}{2}}(\Delta r_i)(r_{ij} \Delta \alpha_{ij})\end{aligned} \tag{59}$$

For octahedral MF_6^{n-} molecules, $r_i = r_j = r_o$, $\alpha_{ij} = 90^o$, $q_{ij} = q_o = r_o\sqrt{2}$, and

$$s_{ij} = s_{ji} = t_{ij} = t_{ji} = 1/\sqrt{2}$$

Therefore

$$V = \tfrac{1}{2}(K + 4\frac{F+F'}{2})\sum_{1}^{6}(\Delta r_i)^2 + \tfrac{1}{2}r_o^2(H + \frac{F-F'}{2})\sum_{i\neq j}^{12}(\Delta\alpha_{ij})^2$$
$$+ \tfrac{1}{2}(F - F')\sum_{\substack{i<j \\ i\neq i'+3}}^{10}(\Delta r_i)(\Delta r_j) + \tfrac{1}{2}r_o(F + F')\sum_{i\neq j}^{24}(\Delta r_i)(\Delta\alpha_{ij}) \qquad (60)$$

the potential energy being expressed parametrically in terms of four force constants. Since F' is usually taken as -(1/10)F, the number of independent force constants is reduced to three. The number of optically-active vibrational molecular (internal) modes for the MF_6^{2-} anion is 5, so that 2 additional force constants may be introduced in the calculation, as interaction force constants between two opposite M-F bonds (k) and between two non-coplanar adjacent F-M-F angles (h)[76,77]. Therefore, if we number the atoms as in Figure 20, the potential function will be

$$V_1 = V + k\sum_{\substack{\text{opposite} \\ \text{bonds}}}^{3}(\Delta r_i)(\Delta r_{i+3}) + hr_o^2\sum_{\substack{\text{adjacent} \\ \text{perpendicular} \\ \text{angles}}}^{24}(\Delta\alpha_{ij})(\Delta\alpha_{ik}) \qquad (61)$$

where V is given by equation (60), with F' = -0.1 F.

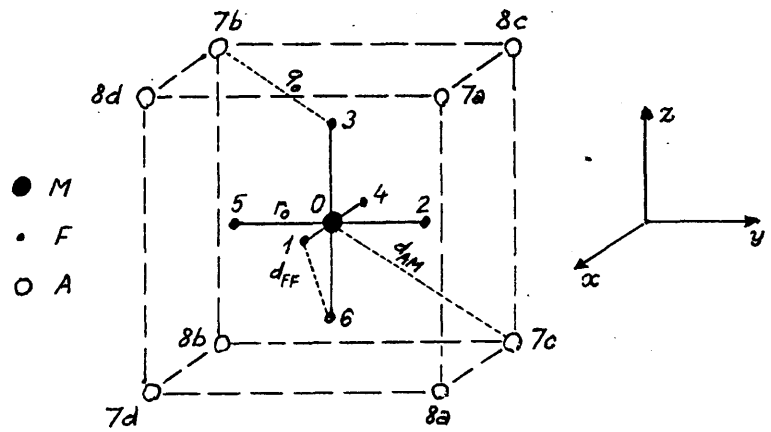

Figure 20

When one of the lattice modes ν_7 (F_{1u}, infrared-active) or ν_8 (F_{2g}, Raman-active) is also observed, as it is the case with our solid state spectra for A_2MF_6 (O_h^5) compounds, one more force constant can be introduced and its value calculated. We have chosen the $A^+ \ldots F^-$ interaction force constant, K_{AF}, as being representative of the forces acting in the crystal. The force constant K_{AA} of the repulsion between two neighbouring cations must be much smaller than K_{AF}, because the $A^+ \ldots A^+$ distance is longer than the $A^+ \ldots F^-$ distance. The potential energy will be

$$V_2 = V_1 + \tfrac{1}{2} K_{AF} \sum_{1}^{24} (\Delta q'_{ij})^2 \qquad (62)$$

where q'_{ij} represent the 24 shortest A...F distances (Fig. 20).

The 42 internal coordinates introduced by this potential function are:

$$\{\Delta r_1, \ldots, \Delta r_6\} = \{R_1, \ldots, R_6\} = \text{stretching of MF bonds}$$

$$\{\Delta\alpha_{12}, \Delta\alpha_{13}, \ldots, \Delta\alpha_{56}\} = \{R_7, \ldots, R_{18}\} = \text{bending of FMF angles}$$

$$\{\Delta q'_{1,7a}, \Delta q'_{1,8a}, \ldots, \Delta q'_{6,7d}, \Delta q'_{6,8d}\} = \{R_{19}, \ldots, R_{42}\}$$

$$= \text{variation of A...F distances} \qquad (63)$$

Since there are only 9 atoms in the unit cell, only 21 of these coordinates are independent. Some of the redundancy conditions, e.g. $\Delta\alpha_{12} + \Delta\alpha_{24} + \Delta\alpha_{45} + \Delta\alpha_{15} = 0$, etc., are obvious, but this is not true for all of them, so that we will use the whole set of internal coordinates (63), the redundant ones being eliminated automatically after calculation.

In what follows, we will use a method given by Shimanouchi and co-workers[78] in order to set up the secular equation which gives

the frequencies and the values of the force constants.

In this method, two sets of coordinates are used:

(i) A set of internal coordinates R_i, defined by

$$R = N \sum_{ijk} R_{ijk} \tag{64}$$

where N is a normalization factor, R_{ijk} is the internal coordinate vector of the Bravais cell of the lattice which is located by the indices i,j,k, and the summation is carried out over all the cells which surround the considered one. R are termed 'optically-active internal coordinates'. The potential energy and kinetic energy functions may be written, in these coordinates, as

$$2V = R' F^i R \qquad \text{and} \qquad 2T = \dot{R}' (G^i)^{-1} \dot{R} \tag{65}$$

where the prime indicates the transposed R column-matrix and the dot the differentiation in terms of time. F^i and G^i are the usual Wilson matrices[21], written in internal coordinates.

(ii) A set of Cartesian coordinates defined in the same way:

$$X = N \sum_{ijk} X_{ijk} \tag{66}$$

where X_{ijk} is the Cartesian coordinate vector associated with the Bravais cell ijk. The energy functions are

$$2V = X' F^c X \qquad \text{and} \qquad 2T = \dot{X}' (G^c)^{-1} \dot{X} \tag{67}$$

Moreover, weighed Cartesian coordinates X_m may be used instead of X, where

$$X_m = M^{\frac{1}{2}} X \tag{68}$$

M being the diagonal matrix of the masses of the atoms in the unit cell.

These two sets of coordinates are related to each other by the relation

$$R = BX \tag{69}$$

where B is the optically-active transformation matrix.

The advantage offered by the use of two sets of coordinates consists in the fact that the force constant matrix F may be more easily written in internal coordinates, while kinetic energy matrix G is straightforwardly obtained in Cartesian coordinates as the inverse diagonal matrix of the atomic masses:

$$G^c = M^{-1} \tag{70}$$

The symmetry of the unit cell can bring about a great simplification in calculations. Thus, symmetry coordinates are introduced by the relations

$$S^i = U^i R \tag{71}$$

and

$$S^c = U^c X \tag{72}$$

where U^i and U^c are the transformation matrices for the two sets of coordinates. The following relationshold:

$$F^{is} = U^i F^i U^{i'} \tag{73}$$

$$G^{cs} = U^c G^c U^{c'} \tag{74}$$

where F^{is} and G^{cs} are the F^i and G^c matrices written down in the corresponding symmetry coordinates.

The first step consists of writing the F matrix in Cartesian symmetry coordinates, in order to go on with the calculations in a single set of coordinates. The transformation may be carried out as follows:

$$F^{cs} = U^c F^c U^{c'} = U^c B' F^i B U^{c'} \tag{75}$$

Wilson's eigenvalues and eigenvectors equation may thus be written

$$G^{cs}F^{cs}L^{cs} = \Lambda L^{cs} \tag{76}$$

where Λ is the diagonal matrix of the eigenvalues and L^{cs} the matrix of the eigenvectors; L^{cs} represents also the transformation matrix from normal coordinates to Cartesian symmetry coordinates:

$$S^{c} = L^{cs}Q \tag{77}$$

This matrix must be normalized:

$$L^{cs\,\prime}L^{cs} = E \tag{78}$$

Alternatively, the weighed eigenvector matrix,

$$L_m^{cs} = M^{\frac{1}{2}}L^{cs} \tag{79}$$

with the normalization condition

$$L_m^{cs\,\prime}L_m^{cs} = M \tag{80}$$

may be used.

Equation (76) may be rewritten as

$$G^{cs\frac{1}{2}}G^{cs\frac{1}{2}}F^{cs}G^{cs\frac{1}{2}}(G^{cs})^{-\frac{1}{2}}L^{cs} = \Lambda L^{cs}$$

or

$$FL_m^{cs} = \Lambda L_m^{cs} \tag{81}$$

where use was made of eq. (79) and where

$$F = G^{cs\frac{1}{2}}F^{cs}G^{cs\frac{1}{2}} \tag{82}$$

is a symmetric matrix.

Equation (81) permits the evaluation of the eigenvalues (calculated frequencies) and of the eigenvectors, if the matrix F is known. By using the transformation relation

$$L_m^{c} = U^{c\,\prime}L_m^{cs} \tag{83}$$

we can find the weighed eigenvectors in the configuration Cartesian space, which have physical significance; they are related to the

amplitudes of vibration for each normal mode.

Solution of eq. (81) provides a number of eigenvalues $\lambda_i^{(c)}$ ($i = 1,\ldots,$number of active and inactive modes or number of symmetry Cartesian coordinates), which are related to the (calculated) frequencies by the relation

$$\nu_i^{(c)} = \frac{1}{2\pi c}\,(\lambda_i^{(c)})^{\frac{1}{2}} = 1302{,}83(\lambda_i^{(c)})^{\frac{1}{2}}\ \mathrm{cm}^{-1}$$

At the same time, a matrix L_m^{cs} will result, whose columns are the eigenvectors for every eigenvalue $\lambda_i^{(c)}$.

The procedure of force constant calculation consists in finding a matrix F such that the difference between the calculated and the observed frequencies will be minimum:

$$\nu_i^{(c)} - \nu_i^{(o)} = \text{minimum} \qquad (84)$$

for all frequencies which can be measured experimentally.

This can be best done by using the method of the Jacobian, proposed by Overend and Scherer[79] and now largely used[3,75,77,80,81]. The elements of the F matrix are written as linear combinations of a chosen set of force constants:

$$F_{ij} = \sum_k Z_{jk}^i \phi_k \qquad (85)$$

where the coefficients Z_{jk}^i are determined by the molecular geometry. If these coefficients are suitably arranged, the relation (84) may be written in matrix form,

$$F = Z\phi \qquad (86)$$

where ϕ is a vector of UB force constants. In this way, we separate the part of F which is determined by the molecular geometry and the atomic masses (Z) from the part which is determined by

the chosen set of force constants. Therefore, the problem of correcting F_{ij} elements until the best fit (84) is reached reduces to correcting a smaller number of components of the vector Φ.

Perturbation theory may now be used to find the corrections $\Delta\Phi$ which minimize the difference $\Delta\lambda_i = \lambda_i^{(c)} - \lambda_i^{(o)}$. For a small variation $\Delta\Phi$ of Φ, the F matrix will be

$$\Delta F = Z\Delta\Phi \tag{87}$$

and equation (81) becomes

$$(F+\Delta F)L_m^{cs} = (\Lambda^{(o)}+\Delta\Lambda)L_m^{cs} \tag{88}$$

where $\Delta\Lambda$ is the diagonal matrix of $\Delta\lambda_i$. Assuming that the zeroth order normal coordinates are good approximations for the true ones, i.e.

$$FL_m^{cs} = \Lambda^{(o)}L_m^{cs}$$

we have

$$FL_m^{cs} = \Delta\Lambda L_m^{cs} \tag{89}$$

where L_m^{cs} is the matrix of the non-perturbed eigenvectors. By multiplying (89) from left by $L_m^{cs'}$, we obtain

$$L_m^{cs'}(\Delta F)L_m^{cs} = M\Delta\Lambda$$

or

$$L^{cs'}(\Delta F)L^{cs} = \Delta\Lambda \tag{90}$$

where, for convenience, $\Delta\Lambda$ is now written as a column. The left hand side of this equation represents the Jacobian matrix of ΔF,

$$J(\Delta F) = L^{cs'}(\Delta F)L^{cs} \tag{91}$$

its elements being of the form

$$J_{kl} = (L^{cs'})_{km}(L^{cs})_{lm}(\Delta F)_{kl} \tag{92}$$

for a given eigenvalue λ_m and its corresponding eigenvector.

An element J_{kl} of the Jacobian matrix represents the variation of the eigenvalue λ_k when the force constant Φ_l is changed:

$$J_{kl} = \frac{\partial \lambda_k}{\partial \Phi_l} \tag{93}$$

Using (87), eq. (90) becomes

$$JZ\Delta\Phi = \Delta\Lambda \tag{94}$$

where a typical element of the (JZ) matrix has the form

$$(JZ)_{ij} = \sum_k \sum_\ell (L_m^{cs})_{ki} (L_m^{cs})_{li} z_{kl}^j \tag{95}$$

The matrix (JZ) has the size $\underline{n}$ X $\underline{m}$, where $\underline{n}$ is the order of the secular equation (81) and $\underline{m}$ is the number of UB force constants. The equation (94) cannot be solved unless $\underline{m} \leqslant \underline{n}$. The best way to solve (94) is by least squares. Both sides of eq. (94) are multiplyed from the left by a weight $\underline{n}$ X $\underline{n}$ matrix P and then by the transpose of (JZ):

$$(JZ)'P(JZ)\Delta\Phi = (JZ)'P\Delta\Lambda \tag{96}$$

where $P_{kk} = 1/\lambda_k^{(o)}$ and $P_{kl} = 0$ $(k \neq l)$.

This represents a system of $\underline{m}$ linear equations with $\underline{m}$ unknown values $\Delta\Phi_1, \ldots, \Delta\Phi_m$. The resulting $\Delta\Phi$ vector is added to the previous Φ vector of the original (guessed) force constants and use is made again of the relation (86) to rebuild a new F matrix. The new set of eigenvalues obtained by solving eq. (81) is compared with the set of observed frequencies and if the difference is still large, new corrections $\Delta\Phi$ are sought following the described procedure (and using a new Jacobian, built up from the corresponding eigenvectors). The calculation is discontinued when the desired degree of fit between the observed and the cal-

culated frequencies is reached, or when no further change in the force constants is observed.

This method is very suitable for computer operation and a program was devised for performing the calculation. For convenience, the difference $\Delta\nu_i = \nu_i^{(o)} - \nu_i^{(c)}$ was minimized instead of $\Delta\lambda_i = \lambda_i^{(c)} - \lambda_i^{(o)}$. In this case the force constant corrections are found from equation

$$(JZ)'P(JZ)\Delta\Phi = (JZ)'P\Delta\nu \qquad (96')$$

where

$$J_{kl} = \frac{\partial\nu_k}{\partial\Phi_l} \qquad (93')$$

$$(JZ)_{ij} = C\sum_k\sum_\ell (L_m^{cs})_{ki}(L_m^{cs})_{li}Z_{kl}^j/\nu_i^{(c)} \qquad (95')$$

$$P_{kk} = 1/\nu_k^{(o)} \text{ and } P_{kl} = 0 \ (k \neq l)$$

and C is a constant, whose value is determined from the choice of units (for ν's in cm^{-1}, force constants in mdyn/Å, masses in a.m.u. and distances in Å, $C = 0.848686.10^6$). Input data consist of the matrix Z, the vector of 6 assumed force constants, the set of observed frequencies $\nu_i^{(o)}$, and the masses of the 9 atoms in the unit cell. The coefficients Z_{kl}^j were calculated on a desk computer starting from the geometrical parameters quoted in Tables 9 and 15. Output data consist of the refined force constants, calculated frequencies, difference between calculated and observed frequencies, the eigenvectors L_m^{cs} for each normal mode, and the potential energy distribution among force constants. The eigenvectors L_m^c were obtained from L_m^{cs} on a desk computer.

The flowchart of the procedure is given in Figure 21.

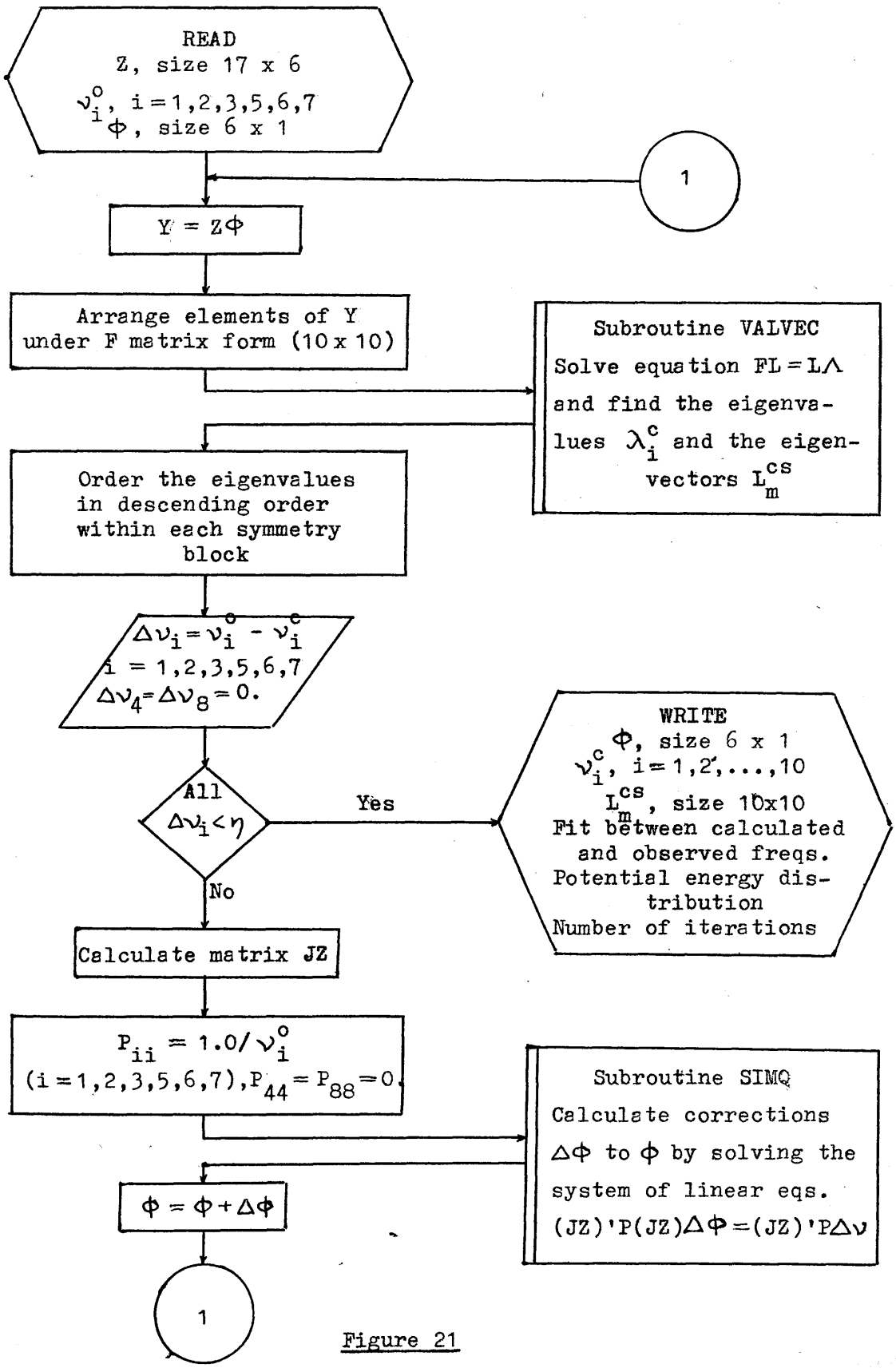
READ
Z, size 17 x 6
ν_i^o, i = 1,2,3,5,6,7
Φ, size 6 x 1
1
Y = ZΦ
Arrange elements of Y under F matrix form (10 x 10)
Subroutine VALVEC
Solve equation FL = LΛ and find the eigenvalues λ_i^c and the eigenvectors L_m^{cs}
Order the eigenvalues in descending order within each symmetry block
$\Delta\nu_i = \nu_i^o - \nu_i^c$
i = 1,2,3,5,6,7
$\Delta\nu_4 = \Delta\nu_8 = 0.$
All $\Delta\nu_i < \eta$
Yes
WRITE
Φ, size 6 x 1
ν_i^c, i = 1,2,...,10
L_m^{cs}, size 10x10
Fit between calculated and observed freqs.
Potential energy distribution
Number of iterations
No
Calculate matrix JZ
$P_{ii} = 1.0/\nu_i^o$
(i = 1,2,3,5,6,7), $P_{44} = P_{88} = 0.$
Subroutine SIMQ
Calculate corrections $\Delta\Phi$ to Φ by solving the system of linear eqs.
(JZ)'P(JZ)$\Delta\Phi$ = (JZ)'P$\Delta\nu$
$\Phi = \Phi + \Delta\Phi$
1

Figure 21

Preparatory work consists in choosing a suitable set of symmetrized Cartesian coordinates in order to split the F matrix into symmetry blocks. As shown in Chapter 3, the representation of the motions of the atoms in the unit cell, for A_2MF_6 compounds of O_h^5 space group reduces as follows:

$$\underbrace{A_{1g} + E_g + 2F_{1u} + F_{2g}}_{\nu_1 \quad \nu_2 \quad \nu_{3,4} \quad \nu_5 \quad \nu_6} + \underbrace{F_{2u} + F_{1u} + F_{2g}}_{\nu_7 \quad \nu_8 \quad \nu_9} + \underbrace{F_{1g} + F_{1u}}_{\nu_{10}}$$

molecular ('internal') modes of MF_6^{2-} ions — lattice modes — acoustic mode

The Raman spectrum consists of 4 bands (ν_1, ν_2, ν_5, ν_8) and the infrared spectrum of 3 bands (ν_3, ν_4, ν_7). Two modes (ν_6, ν_9) are inactive and one (ν_{10}) is acoustic and has zero frequency. A symmetry Cartesian coordinate was built for each of these 10 modes as follows (after renumbering the modes to group together the identical species):

$$\begin{aligned}
S_1^c(A_{1g}) &= (1/\sqrt{6})\,(x^1 + y^2 + z^3 - x^4 - y^5 - z^6)\\
S_2^c(E_g) &= (1/2\sqrt{3})(2x^1 - y^2 - z^3 - 2x^4 + y^5 + z^6)\\
S_3^c(F_{2g}) &= (1/2)(y^1 + x^2 - y^4 - x^5)\\
S_4^c(F_{2g}) &= (1/\sqrt{2})(z^7 - z^8)\\
S_5^c(F_{1u}) &= x^0\\
S_6^c(F_{1u}) &= (1/\sqrt{2})(x^1 + x^4)\\
S_7^c(F_{1u}) &= (1/2)(x^2 + x^3 + x^5 + x^6)\\
S_8^c(F1u) &= (1/\sqrt{2})(x^7 + x^8)\\
S_9^c(F_{1g}) &= (1/2)(y^1 - x^2 - y^4 + x^5)\\
S_{10}^c(F_{2u}) &= (1/2)(-x^2 + x^3 - x^5 + x^6)
\end{aligned} \qquad (97)$$

(x^i represents the x coordinate of the ith atom, etc., the numbering of the atoms and the axis orientation being taken as in Figure 20). The transpose matrix $U^{c'}$ of the corresponding U^c matrix is given on the following page as (98). In the set of symmetrized coordinates (97) only one is redundant and may be eliminated by using the redundancy condition

$$\sum_{\sigma}^{g} x^i = 0$$

which in our case becomes $S_5^c + 2S_6^c + 2S_7^c + 2S_8^c = 0$. We prefered, however, not to eliminate this redundant coordinate but work with the whole set (97).

The symmetrized G^{cs} matrix results from eq. (74) to be

$$G^{cs} = \begin{array}{c} \\ S_1^c \\ S_2^c \\ S_3^c \\ S_4^c \\ S_5^c \\ S_6^c \\ S_7^c \\ S_8^c \\ S_9^c \\ S_{10}^c \end{array} \begin{array}{c} \begin{array}{cccccccccc} S_1^c & S_2^c & S_3^c & S_4^c & S_5^c & S_6^c & S_7^c & S_8^c & S_9^c & S_{10}^c \end{array} \\ \begin{pmatrix} \mu_F & & & & & & & & & \\ & \mu_F & & & & & & & & \\ & & \mu_F & & & & & & & \\ & & & \mu_A & & & & & & \\ & & & & \mu_M & & & & & \\ & & & & & \mu_F & & & & \\ & & & & & & \mu_F & & & \\ & & & & & & & \mu_A & & \\ & & & & & & & & \mu_F & \\ & & & & & & & & & \mu_F \end{pmatrix} \end{array} \qquad (99)$$

where μ_M, μ_F and μ_A are the reciprocal masses of the M, F and A atoms, respectively.

Starting from the expression (62) for the potential energy function (where we denoted K, H, F, k, h, and K_{AF} force constants

$U^{c'} =$

	S_1	S_2	S_3	S_4	S_5	S_6	S_7	S_8	S_9	S_{10}
x^0					1					
y^0										
z^0										
x^1	$1/\sqrt{6}$	$1/\sqrt{3}$				$1/\sqrt{2}$				
y^1			1/2						1/2	
z^1										
x^2			1/2				1/2		-1/2	-1/2
y^2	$1/\sqrt{6}$	$-1/2\sqrt{3}$								
z^2										
x^3							1/2			1/2
y^3										
z^3	$1/\sqrt{6}$	$-1/2\sqrt{3}$								
x^4	$-1/\sqrt{6}$	$-1/\sqrt{3}$				$1/\sqrt{2}$				
y^4			-1/2						-1/2	
z^4										
x^5			-1/2				1/2		1/2	-1/2
y^5	$-1/\sqrt{6}$	$1/2\sqrt{3}$								
z^5										
x^6							1/2			1/2
y^6										
z^6	$-1/\sqrt{6}$	$1/2\sqrt{3}$								
x^7								$1/\sqrt{2}$		
y^7										
z^7				$1/\sqrt{2}$						
x^8								$1/\sqrt{2}$		
y^8										
z^8				$-1/\sqrt{2}$						

(98)

(Non-zero elements only)

by $k_1,\ldots,k_6$, respectively) we first write F^i and then find F^{cs} by a series of transformation given by equation (75). The necessary B matrix, giving the transformation from Cartesian to internal coordinates (eq. (69)) may be easily set up by using the rules given in the book of Wilson, Decius and Cross[82] (see also ref. 76). We give here the final symmetrized F matrix only, calculated from its definition (82):

$$F = \begin{pmatrix}
\mu_F A & & & & & & & & & & & \\
 & \mu_F B & & & & & & & & & & \\
 & & \mu_F D & \sqrt{\mu_F\mu_A}\,I & & & & & & & & \\
 & & \sqrt{\mu_F\mu_A}\,I & \mu_A E & & & & & & & & \\
 & & & & \mu_M J & \sqrt{\mu_M\mu_F}\,N & \sqrt{\mu_M\mu_F}\,P & 0 & & & & \\
 & & & & \sqrt{\mu_M\mu_F}\,N & \mu_F M & \mu_F R & \sqrt{\mu_A\mu_F}\,S & & & & \\
 & & & & \sqrt{\mu_M\mu_F}\,P & \mu_F R & \mu_F L & \sqrt{\mu_A\mu_F}\,I & & & & \\
 & & & & 0 & \sqrt{\mu_A\mu_F}\,S & \sqrt{\mu_A\mu_F}\,I & \mu_A E & & & & \\
 & & & & & & & & \mu_F C & & & \\
 & & & & & & & & & \mu_F T & &
\end{pmatrix} \qquad (100)$$

with $A = k_1 + 4k_3 + k_4 + 4a^2k_6$, $B = k_1 + 0.7k_3 + k_4 + 4a^2k_6$, $C = 4b^2k_6$, $D = 4k_2 + 2.2k_3 + 4b^2k_6$, $E = 4k_6$, $I = -4\ 2b^2k_6$, $J = 2(k_1 + 4k_2 + 0.4k_3 - k_4 + 8k_5)$, $M = k_1 + 1.8k_3 - k_4 + 4a^2k_6$, $L = 2k_2 + 1.1k_3 + 4k_5 + 4b^2k_6$, $N = 2(k_4 - k_1)$, $P = -(4k_2 + 0.4k_3 + 8k_5)$, $R = -\ 2X0.9k_3$, $S = -4a^2k_6$, $T = 2k_2 + 1.1k_3 - 4k_5 + 4b^2k_6$.

Thus, the Z matrix (size 17 X 6, elements Z^i_{jk}) may be written as in (101) (next page), where $\underline{a}$ and $\underline{b}$ are geometrical parameters, defined as[3]

$$a = \frac{d_{AA}/2 - d_{MF}}{d_{AF}}\ , \quad b = \frac{d_{AA}}{2d_{AF}}\ , \quad (a^2 + 2b^2 = 1) \qquad (102)$$

$$
Z = \begin{array}{c|c|cccccc}
 & i \backslash jk & 1 & 2 & 3 & 4 & 5 & 6 \\
(A_{1g}) & 11 & \mu_F & 0 & 4\mu_F & \mu_F & 0 & 4a^2\mu_F \\
(E_g) & 22 & \mu_F & 0 & 0.7\mu_F & \mu_F & 0 & 4a^2\mu_F \\
 & 33 & 0 & 4\mu_F & 2.2\mu_F & 0 & 0 & 4b^2\mu_F \\
(F_{2g}) & 44 & 0 & 0 & 0 & 0 & 0 & 4\mu_A \\
 & 34 & 0 & 0 & 0 & 0 & 0 & -4\sqrt{2\mu_F\mu_A}\,b^2 \\
 & 55 & 2\mu_M & 8\mu_M & 0.8\mu_M & -2\mu_M & 16\mu_M & 0 \\
 & 66 & \mu_F & 0 & 1.8\mu_F & -\mu_F & 0 & 4a^2\mu_F \\
 & 77 & 0 & 2\mu_F & 1.1\mu_F & 0 & 4\mu_F & 4b^2\mu_F \\
 & 88 & 0 & 0 & 0 & 0 & 0 & 4\mu_A \\
(F_{1u}) & 56 & -\sqrt{2\mu_M\mu_F} & 0 & 0 & \sqrt{2\mu_M\mu_F} & 0 & 0 \\
 & 57 & 0 & -4\sqrt{\mu_M\mu_F} & -0.4\sqrt{\mu_M\mu_F} & 0 & -8\sqrt{\mu_M\mu_F} & 0 \\
 & 58 & 0 & 0 & 0 & 0 & 0 & 0 \\
 & 67 & 0 & 0 & -0.9\sqrt{2}\mu_F & 0 & 0 & 0 \\
 & 68 & 0 & 0 & 0 & 0 & 0 & -4\sqrt{\mu_F\mu_A}\,a^2 \\
 & 78 & 0 & 0 & 0 & 0 & 0 & -4\sqrt{2\mu_F\mu_A}\,b^2 \\
(F_{1g}) & 99 & 0 & 0 & 0 & 0 & 0 & 4b^2\mu_F \\
(F_{2u}) & 1010 & 0 & 2\mu_F & 1.1\mu_F & 0 & -4\mu_F & 4b^2\mu_F
\end{array} \qquad (101)
$$

In evaluating the elements of F and Z, the atomic masses were taken in atomic units and the interatomic distances in Å. The interatomic distances were calculated according to the following geometrical relations

$$
d_{MF} = u_o a_o, \quad d_{MA} = (\sqrt{3}/4)a_o, \quad d_{AA} = (1/2)a_o,
$$
$$
d_{AF} = (u_o^2 - u_o/2 + 3/16)^{\frac{1}{2}}, \quad d_{FF} = 2d_{MF} \qquad (103)
$$

Table 14

Geometrical parameters of some cubic (O_h^5) A_2MF_6 compounds*

Compound	a_o	u_o	d_{AA} (ρ)	d_{AM}	d_{MF} (r_o)	d_{AF} (q_o)	d_{FF}	a	b	Ref.
K_2SiF_6	8.133	0.215	4.066	3.522	1.749	2.889	2.473	0.0985	0.7037	44
	8.13	0.215	4.065	3.520	1.748	2.888	2.473	0.0985	0.7038	**
Rb_2SiF_6	8.452	0.20	4.226	3.659	1.690	3.018		0.1400	0.7001	44
	8.44	0.20	4.220	3.655	1.688	3.014	2.387	0.1400	0.7000	**
Cs_2SiF_6	8.919	0.19	4.459	3.862	1.695	3.198		0.1673	0.6971	44
	8.87	0.19	4.435	3.841	1.685	3.181	2.383	0.1674	0.6971	**
Cs_2GeF_6	9.021	0.20	4.510	3.906	1.804	3.221		0.1400	0.7001	44
	8.97	0.20	4.485	3.884	1.794	3.203	2.537	0.1400	0.7001	**
Rb_2MnF_6	8.430	0.20	4.215	3.650	1.686	3.010	2.384	0.1400	0.7001	44
Cs_2MnF_6	8.92	0.195	4.460	3.862	1.739	3.191	2.460	0.1513	0.6988	44
K_2NiF_6	8.11	(0.20)	4.055	3.512	(1.622)(2.896)(2.294)			0.1400	0.7001	5

* Distances in Å.

** This work.

where $a_o/2$ is the length of the edge of the cell drawn in Figure 20 (a_o being the lentgh of the crystallographic unit cell), and u_o is a fraction of a_o which indicates the position of the atoms.

All geometrical parameters of the studied A_2MF_6 (O_h^5) molecules are listed in Table 14.

The program, written in FORTRAN IV on the basis of the flow-chart reported previously (Figure 21), is given in the Appendix. For solving the secular equation (81) the Jacobi diagonalization method was used (subroutine VALVEC, written by Shimanouchi and co-workers[81]), while for solving the system of linear equations (96') and finding the corrections $\Delta\phi$, the Gauss elimination method was used (subroutine SIMQ, courtesy of IBM, Scientific Subroutine Package).

All calculations were made on the IBM 360/30 computer of the University of Bucharest*. Satisfactory refinement of the force constants necessitated 3 to 6 recyclings of the intermediary data.

* The author is indebted to the Computing Centre of the University of Bucharest for permission to use the IBM Computer.

Chapter 7 FORCE CONSTANTS AND STRUCTURE OF A_2MF_6 MOLECULES

The force constants obtained for the cubic (O_h^5) A_2MF_6 compounds according to the procedure described in the preceding Chapter may assist in the interpretation of the observed vibration spectra of these compounds and of the compounds with related structures, as well as in drawing some conclusions about the nature of the bonding.

The problem consisted of finding a set of force constants which, following the usual FG-matrix formalism, reproduce as well as possible the observed vibrational spectrum of a compound. The number of vibrational frequencies observed being generally much smaller than the actual number of force constants involved in any molecular or crystal vibration, the procedure is by itself only approximate, assuming from the beginning the neglect of a large number of supposedly small force constants. Thus, even if the final refined set of force constants gives the best possible agreement between observed and calculated frequencies, any conclusion based on them must be treated with care. The calculated force constants must be considered as indices of a crude vibrational pattern, serving to simplify the picture of the complex molecular vibrational behaviour. Nevertheless, the force constants often help in understanding the nature of the nuclear motions and, to a lesser extent, of the nature of the chemical bonding between atoms in the molecule or crystal.

Since the three kinds of central M atoms - Si, Ge and Mn -

appearing in the A_2MF_6 compounds investigated in the preceding chapters have very close electronegativities (1.9, 1.8 and 1.5, respectively), the M-F bond is presumably nearly similar in all compounds. Apart from the electrostatic interaction between this central atom (M^{n+}) and fluorine (F^-), a certain amount of covalency must be involved. An estimation based on the electronegativity difference gives a 30 % covalent character for Si-F and Ge-F bonds, and a 20 % covalent character for Mn-F bonds. These metal-fluorine bonds are certainly the least covalent of all the metal-halogen bonds, a fact which is well supported by spectroscopic[3] and other data. The partial covalent character of the M-F bonds leads to M-F distances somewhat shorter than the sum of M and F ionic radii (Table 14). The ionic character, however, remains predominant and determines certain of the geometrical properties of the MF_6^{2-} groups - the structure similarity of the studied A_2MF_6 compounds, for example. Since most transition metal ions have ionic radii which do not exceed largely the size of the octahedral hole allowed by the 6 F^- ions (0.41 Å), a large number of fluorocomplexes will have a similar structure as far as the MF_6^{n-} group is concerned. For large M^{4+} radii and a relatively small cation (A = K), as it is the case e.g. for Zr or Hf (0.80 Å), the structure of the A_2MF_6 compounds is entirely different[4] (D_{2h}^{17} space group). For A = Rb, Cs, the structure is again regular (D_{3d}^{3} space group) and the ZrF_6^{2-} and HfF_6^{2-} groups are only slightly distorted.

Another important factor which influences the structure of a A_2MF_6 compound is the size of the alkali metal ion A^+. The hard-

sphere model of ions is sufficiently valid for the ternary fluorides to explain the various structures occuring in this class. Unlike the M^{4+} ions, whose ionic radii differ only slightly from one atom to another, the radii of the A^{+} cations increase rapidly from Na^{+} (0.95 Å) to Cs^{+} (1.69 Å). The Na^{+} ion is too small to build up a regular close-packed structure with the MF_6^{2-} groups, so that A-F distances will be irregular. From K^{+} (1.33 Å) on, close-packing is favored, and this is especially valid for Rb^{+} (1.48 Å) and Cs^{+} (1.69 Å). A coordination number of 12 is a rule for the A_2MF_6 compounds involving K, Rb or Cs. The ideal cubic structure is found for almost all Rb and all Cs hexafluorometallates(IV). However, distortions from this regular structure may occur, caused by the influence of unsymmetric polarization[41]. Examples are K_2MnF_6 and K_2GeF_6, in which the A-F distances are not equal, although the coordination number continues to be 12.

One of the force constants which is usually related to the covalent character of the M-F bond is K, the symmetric stretching M-F force constant. It is expected that K should decrease with the bond becoming less covalent. Thus, K should have lower values for hexafluoromanganates(IV) than for hexafluorosilicates and hexafluorogermanates. The values of K given in Table 15 do not agree with this conclusion. The value of K for hexafluoromanganates ($\sim$2.3 mdyn/Å) is somewhat larger than for hexafluorosilicates (1.8-1.9 mdyn/Å) and hexafluorogermanates (2.0 mdyn/Å), in spite of the mentioned differences in the amount of covalent bonding in these compounds. Therefore, K should not be straightforwardly

Table 15

Calculated force constants of cubic (O_h^5) A_2MF_6 compounds (in mdyn/Å)

Compound	K	H	F	k	h	K_{AF}
K_2SiF_6	1.937	0.054	0.688	0.167	0.075	0.078
Rb_2SiF_6	1.839	0.057	0.665	0.267	0.072	0.093
Cs_2SiF_6	1.743	0.056	0.678	0.236	0.071	0.070
Cs_2GeF_6	2.011	-0.015	0.520	0.124	0.064	0.070
Rb_2MnF_6	2.332	0.036	0.376	0.253	0.043	0.074
Cs_2MnF_6	2.309	0.011	0.422	0.243	0.042	0.075
K_2NiF_6*	2.563	0.681	0.154	0.391	0.012	-0.454

* Values obtained after only 3 iterations.

related to the covalent character of the metal-ligand bonds.

The way in which the values of K change in a series of A_2MF_6 compounds (M = fixed, A = K, Rb, Cs) is not regular nor very significant. There is a slight decrease in A_2SiF_6 compounds in passing from A = K to A = Cs, which indicates a weakening of the M-F bond strength in the compounds with heavier cations. The same appears to be true for Rb_2MnF_6 and Cs_2MnF_6. This weakening might be due to a redistribution of the electronic cloud of the anion under the influence of the cation electric charge, although the effect must be very weak. The A-F interaction, represented by the K_{AF} force constant, which is seen from Table 15 to have low values as compared to K, is very weak, thus permitting formation of stable, isolated MF_6 groups within the crystalline lattice.

F, the force constant of the non-directly bonded F...F atoms, has relatively large values for all compounds, especially the hexafluorosilicates, and it does not change appreciably with changing the cation A^+, but has different values for various central M atoms. Other authors[3] have pointed out that it does not vary appreciably with the F-F distance, but this is not obvious in our case since these distances are almost identical in the investigated compounds (cf. Table 14).

The bending (F-M-F) force constant H has low values, indicating an appreciable lack of oriented (directed) covalent bonds (a large ionic character of the M-F bonds). The interaction force constants k and h have also relatively low values, which do not depend significantly of the nature of the cation. They are however different

from zero and their contribution to the potential energy cannot be therefore neglected. The force constants obtained by us for K_2NiF_6 differ appreciably from the values of Reisfeld[5], which were obtained by neglecting the interaction force constants k and h, as well as the A...F lattice force constant K_{AF}.

The frequencies calculated using the sets of force constants listed in Table 15 are in very good agreement with the observed frequencies. An exception is the frequency of the ν_3 (F_{1u}) mode, for which the fit between the observed and calculated values is rather poor and could not be improved even after a large number of iterations. The calculated value of ν_3 oscillates with ±20-50 cm^{-1} around the observed value. This might be due to the large half-width and thus the inaccurate location of the band.

The procedure of calculation permitted an estimation of the frequencies of all 10 normal modes of cubic A_2MF_6 compounds in the solid state. These frequencies are given in Table 16. The calculated frequency of the molecular inactive mode ν_6 has been already reported in Table 11 and compared with those components of the mode which become infrared-active when the MF_6^{2-} anion is in an appropriate environment.

We have calculated also the percent potential energy distribution among the force constants to each vibration of cubic A_2MF_6 compounds, according to the relation[81]

$$(P.E.F.)_{ij} = \frac{(JZ)_{ij}\Phi_j}{\nu_i^c} \cdot 200\ \% \qquad (104)$$

Table 16

Calculated and observed frequencies of the normal modes of vibration of cubic (O_h^5) A_2MF_6 compounds in solid state (in cm^{-1})

Compound		Molecular modes						Lattice modes			Acoustic mode
		Raman			Infrared		In.	IR	R	In.	
		ν_1	ν_2	ν_5	ν_3^*	ν_4	ν_6	ν_7	ν_8	ν_9	ν_{10}
K_2SiF_6	obs	659.00	481.00	412.00	740.00	480.00	-	143.00	-	-	-
	calc	659.00	481.00	412.00	772.76	480.07	253.82	143.00	111.34	117.71	0.00
Rb_2SiF_6	obs	653.00	480.00	410.00	737.00	475.00	-	117.00	-	-	-
	calc	653.00	480.00	410.00	792.84	475.04	256.93	117.00	81.63	127.72	0.00
Cs_2SiF_6	obs	648.00	469.00[a]	407.00	723.00	474.00	-	100.00	-	-	-
	calc	648.00	469.00	407.00	775.85	474.03	252.02	100.00	57.52	110.14	0.00
Cs_2GeF_6	obs	614.00	473.00	331.00	598.00	349.00	-	90.00	-	-	-
	calc	614.00	473.00	331.00	619.84	349.85	194.13	90.01	56.16	110.40	0.00
Rb_2MnF_6	obs	605.00	505.00	317.00	630.00	338.00	-	105.00	-	-	-
	calc	605.00	505.00	317.00	652.19	338.10	201.95	105.00	71.28	113.74	0.00
Cs_2MnF_6	obs	616.00	505.00	317.00	619.00	335.00	-	96.00	-	-	-
	calc	616.00	505.00	317.00	629.96	335.16	203.41	96.00	21.58	114.42	0.00
K_2NiF_6	obs	562.00[b]	520.00[b]	310.00[b]	658.00[b]	345.00[b]	-	-	138.00[b]	-	-
	calc[c]	562.00	520.00	312.63	624.25	344.79	179.46	183.83	129.99	171.62	0.00

(IR - infrared, R - Raman, In. - inactive)

* The bad fit of ν_3 mode frequency is discussed in the text.

[a] Ref. 3.

[b] Ref. 5.

[c] 3 iterations only.

Table 17

Potential energy distribution among force constants for the normal modes of K_2SiF_6 (in %)

	K	H	F	k	h	K_{AF}
ν_1	44.8	0.0	56.6	-1.5	0.0	0.1
ν_2	84.2	0.0	18.6	-2.9	0.0	0.1
ν_3	78.2	2.8	10.4	0.0	7.6	0.0
ν_4	0.6	8.2	65.3	0.0	22.6	3.4
ν_5	0.0	11.4	79.1	0.0	0.0	9.6
ν_6	0.0	5.1	86.4	0.0	-4.2	12.5
ν_7	0.0	0.3	2.2	0.0	0.8	96.9
ν_8	0.0	1.2	8.3	0.0	0.0	90.7
ν_9	0.0	0.0	0.0	0.0	0.0	100.0
ν_{10}	...	...	...	...	...	...

$(P.E.F.)_{ij}$ indicates the significant force constants for the vibration ν_i. The results, listed as an example for K_2SiF_6 in Table 17, show that generally more than one force constant participates in each vibration and that no vibrational mode (except ν_9) is 'pure', i.e. arising from the contribution of a single force constant. The Raman-active ν_2 mode and the infrared-active ν_3 mode are due mainly (to the extent of 84 and 78 %, respectively) to the force constant K, thus being almost pure stretching vibrations. It is surprising to find that ν_1, which has been generally considered a pure stretching M-F vibration, is due largely (to the extent of 57 %) to the non-bonded F...F interaction force constant F. The ν_7 and ν_8 modes are preponderent lattice vibrations, as expected. The F-M-F bending force constant H contributes to a very small extent to all molecular and lattice vibrations.

The geometric representation of the normal vibration modes, as well as the amount of mixing between certain vibration which possess the symmetry required by group theory may be found from the Cartesian components of the normal coordinates, i.e. the eigenvectors $(L_m^c)_i$ resulting for every mode ν_i from equations (81) and (83). The results are given for K_2SiF_6 in Table 18 and Figure 22, where the displacements of the atoms in the unit cell are drawn approximately to scale. It may be seen that the ν_1, ν_2 and ν_6 modes almost pure molecular (internal) modes, while ν_3, ν_4 and ν_5 are molecular modes with various small amounts of lattice character. ν_7 and ν_8 are mainly lattice modes, but they are also mixed to a certain extent with the motions of the atoms within the MF_6^{2-} unit. The ν_{10}

Table 18

L_m^c matrix elements for K_2SiF_6

(All zero elements are omitted)

	ν_1	ν_2	ν_3	ν_4	ν_5	ν_6	ν_7	ν_8	ν_9	ν_{10}
x^0			0.78	0.42			-0.29			0.36
x^1	0.41	0.58	-0.44	0.40			-0.24			0.29
y^1					0.50			0.04	0.50	
x^2			-0.02	-0.35	0.50	-0.50	-0.20	0.04	-0.50	0.29
y^2	0.41	-0.29								
x^3			-0.02	-0.35		0.50	-0.20			0.29
z^3	0.41	-0.29								
x^4	-0.41	-0.58	-0.44	0.40			-0.24			0.29
y^4					-0.50	-0.04			-0.50	
x^5			-0.02	-0.35	-0.50	-0.50	-0.20	-0.04	0.50	0.29
y^5	-0.41	0.29								
x^6			-0.02	-0.35		0.50	-0.20			0.29
z^6	-0.41	0.29								
x^7			0.00	0.03			0.57			0.42
z^7					-0.06			0.70		
x^8			0.00	0.03			0.57			0.42
z^8					0.06			-0.70		

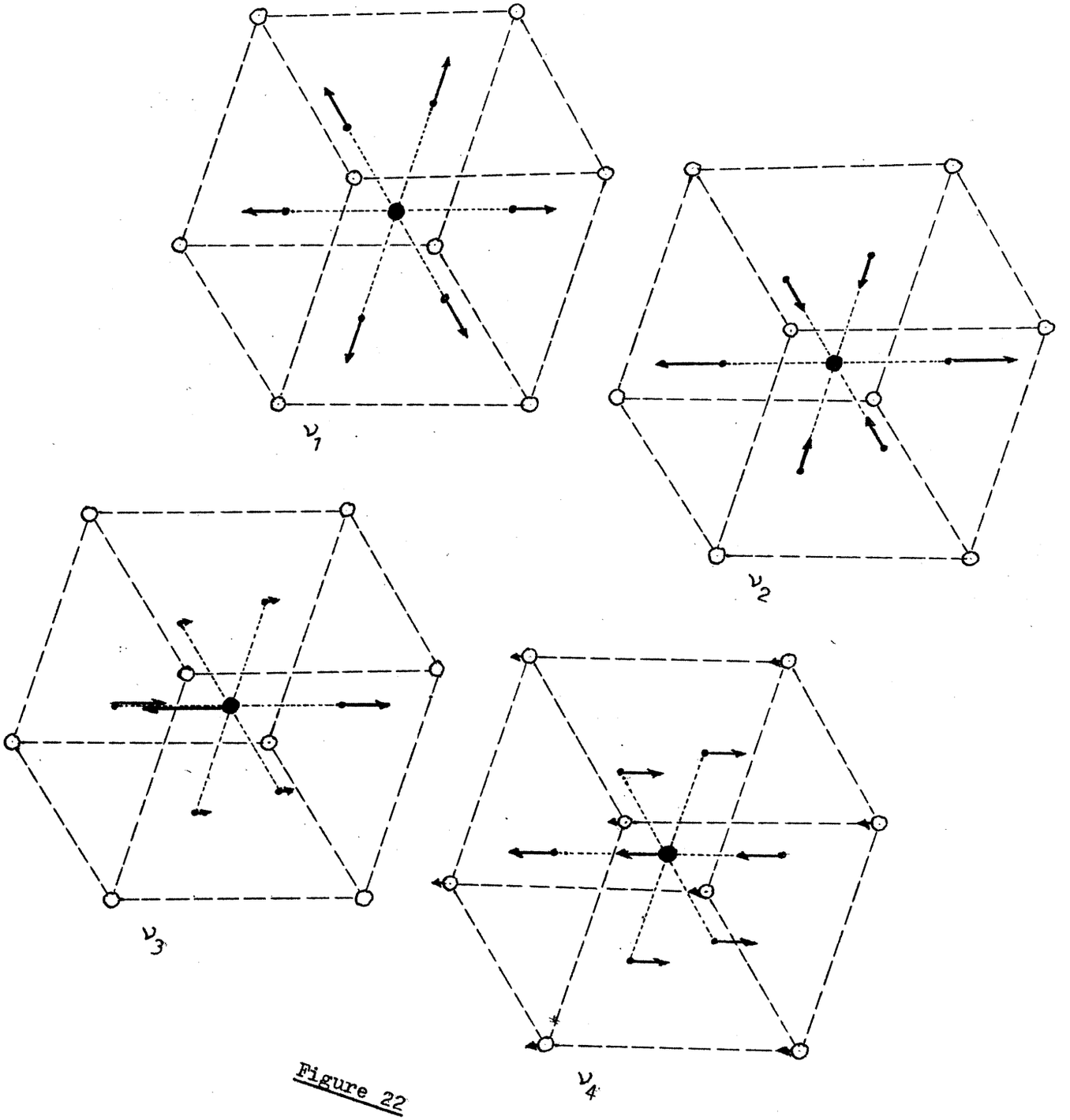

Figure 22

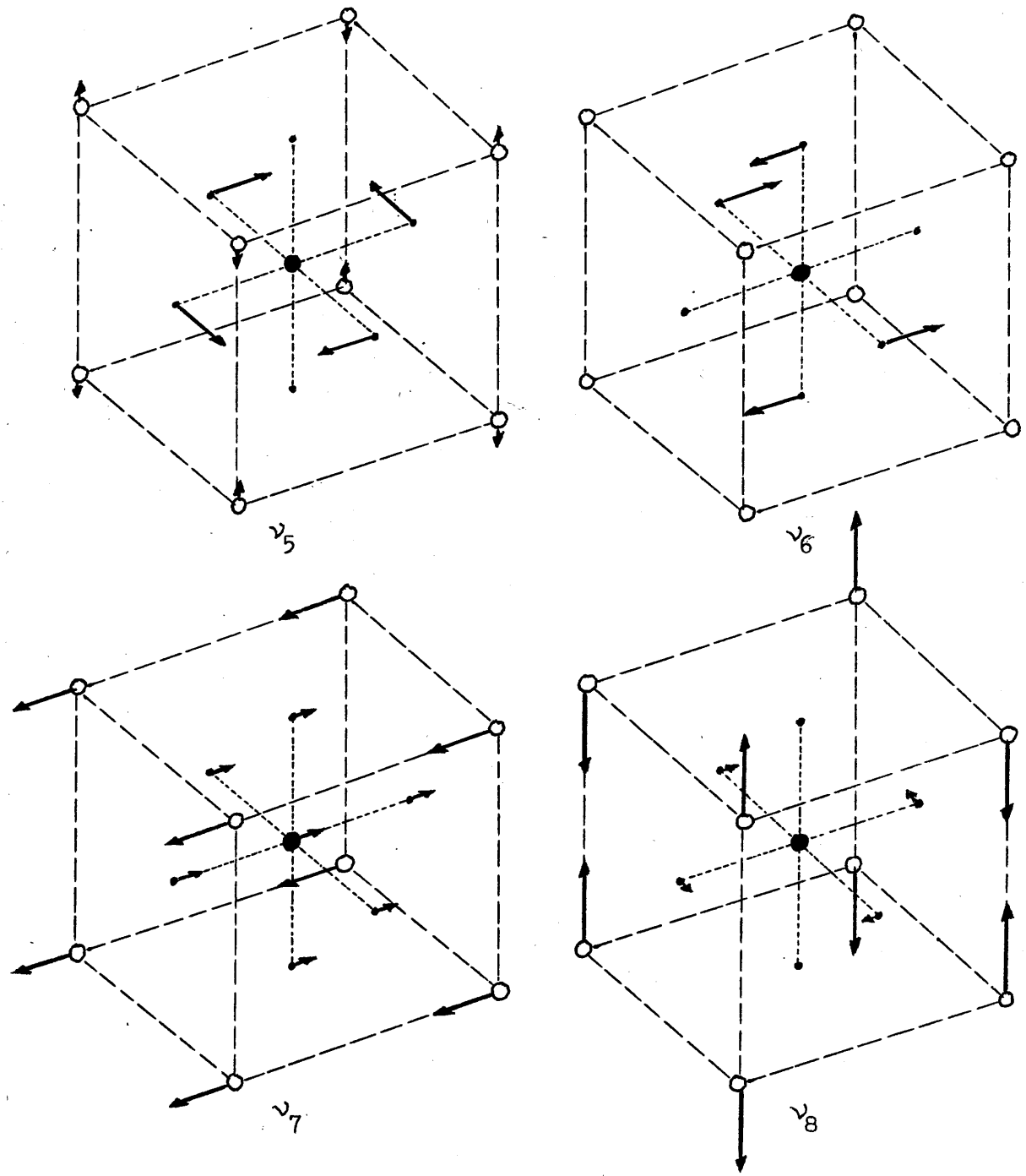

Figure 22 (cont'd)

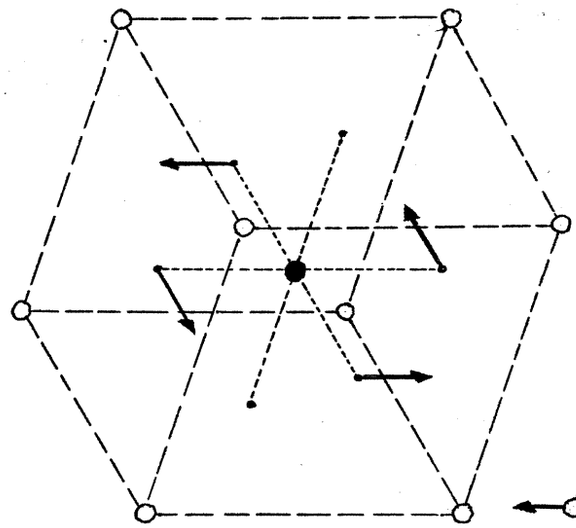

ν_9

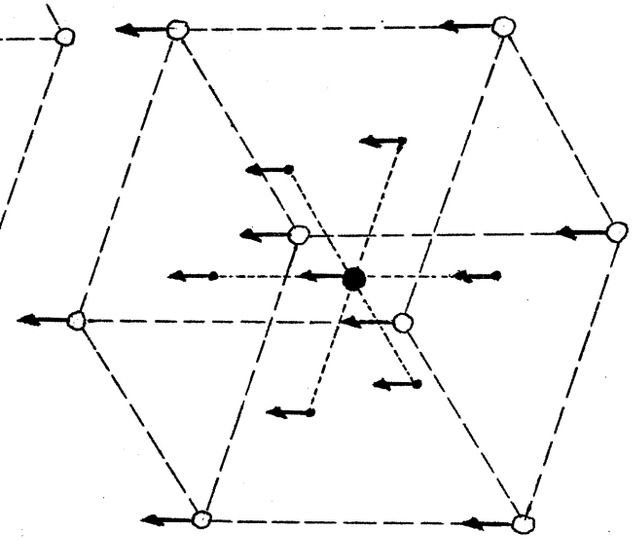

ν_{10}

Figure 22 (cont'd)

mode is an acoustic mode, as expected: the motions of all atoms in the unit cell constitute a translation of the unit cell as a whole. The rotational or translational character of the lattice modes may also be seen from the diagrams.

These data allow explanation on a reasonable basis of the already mentioned large half-width of certain bands in the infrared and Raman spectra, particularly that of the ν_3 and ν_5 bands. The band broadening is due to the interaction between molecular and lattice modes of appropriate symmetry. The results reported here for K_2SiF_6, as far as the nuclear motions and potential energy distribution are concerned, are quite general for all compounds with similar structure studied in this work, although the degree of mode mixing varies for each compound. The mixing of the lattice modes with the low-energy molecular modes may be interpreted as a modification of the respective molecular modes by action of interionic lattice forces. Strictly speaking, the vibrational energy levels of the MF_6^{2-} group are different in crystal and in solution, even if to a small extent. Hence the necessity of using only consistent solid state spectra when carrying out force constant calculations on such compounds.

Appendix FORTRAN PROGRAM FOR FORCE CONSTANT CALCULATION FOR CUBIC (O_h^5) A_2MF_6 COMPOUNDS

```
C     PROGRAM 'CONFORT' FOR FORCE CONSTANT REFINEMENT, CUBIC A2MF6
C     COMPOUNDS *** INPUT DATA - OBSERVED FREQUENCIES, Z MATRIX,
C     ASSUMED FORCE CONSTANTS *** OUTPUT DATA - CALCULATED
C     FREQUENCIES, IMPROVED FORCE CONSTANTS, CARTESIAN COMPONENTS
C     OF NORMAL VIBRATION MODES, POTENTIAL ENERGY DISTRIBUTION (PEF)
C     USED SUBROUTINES - 2 (VALVEC, SIMQ)
      (Job control statements)
       DIMENSION NB(6), Z(17,6), PHI(6), Y(17), F(10,10), EVAL(10),
     1           EVEC(10,10), FIT(8), V1(8,6), V2(8,6), V(8,6),
     2           VT(6,8), P(8,8), VTP(6,8), VV(6,6), VL(6), DELPHI(6),
     3           FREQC(10), PEF(10,6)
  110 FORMAT (6I2)
  120 FORMAT (8F10.7)
  130 FORMAT (6F7.3)
  140 FORMAT (6F10.7)
  150 FORMAT (' ', 27HOBSERVED FREQUENCIES (CM-1) // 5HNU 1 F8.2/
     1 5HNU 2 F8.2/5HNU 5 F8.2/5HNU 3 F8.2/5HNU 4 F8.2/5HNU 7 F8.2)
  155 FORMAT (' ', 29HCALCULATED FREQUENCIES (CM-1) // 10F8.2)
  170 FORMAT (' ', 22HEIGENVECTORS (COLUMNS) // 10(F10.7, 2X)/)
  180 FORMAT (' ', 24HFORCE CONSTANTS (MDYN/A) // 6(3X,F7.3))
  190 FORMAT (' ', 41HCONCORDANCE OF FREQUENCIES (OBS-CALC)     //
     1        8(2X,F10.7))
  195 FORMAT (' ', 20HNUMBER OF ITERATIONS  I3)
  900 FORMAT (' ', 10E13.5/)
  961 FORMAT (' ', 6HDELPHI /(3X,E15.7)
      READ (1,110) (NB(L), L=1,6)
      READ (1,120) ((Z(I,K), I=1,17), K=1,6)
      READ (1,130) (PHI(K), K=1,6)
      READ (1,140) FREQ01, FREQ02, FREQ03, FREQ05, FREQ06, FREQ07
      DO 295 I=1,8
      DO 295 J=1,8
  295 P(I,J) = 0.
      P(1,1) = 1./FREQ01
      P(2,2) = 1./FREQ02
      P(3,3) = 1./FREQ03
      P(4,4) = 0.
      P(5,5) = 1./FREQ05
      P(6,6) = 1./FREQ06
      P(7,7) = 1./FREQ07
      WRITE (3,150) FREQ01, FREQ02, FREQ03, FREQ05, FREQ06, FREQ07
```

```
      NIT = 1
   30 DO 50 I=1,17
      Y(I) = 0.
      DO 50 K=1,6
   50 Y(I) = Y(I) + Z(I,K)*PHI(K)
      DO 200 I=1,10
      DO 200 J=1,10
  200 F(I,J) = 0.
      DO 210 I=1,4
  210 F(I,I) = F(I,I) + Y(I)
      DO 215 I=5,8
  215 F(I,I) = F(I,I) + Y(I+1)
      F(3,4) = F(3,4) + Y(5)
      DO 220 I=6,8
  220 F(5,I) = F(5,I) + Y(I+4)
      F(6,7) = F(6,7) + Y(13)
      F(6,8) = F(6,8) + Y(14)
      F(7,8) = F(7,8) + Y(15)
      F(9,9) = F(9,9) + Y(16)
      F(10,10) = F(10,10) + Y(17)
      DO 230 I=1,10
      DO 230 J=1,10
  230 F(J,I) = F(I,J)
      WRITE (3,195) NIT
      CALL VALVEC (F,EVEC,10,1,1.0E-6)
      DO 240 I=1,10
      EVAL(I) = 0.
  240 IF (F(I,I) .GE. 1.0E-5) EVAL(I) = F(I,I)
      N = 0
      DO 248 L=1,6
      M = N + 1
      N = N + NB(L)
      IF (NB(L) .EQ. 1) GO TO 248
      N1 = N - 1
      DO 246 J = M, N1
      EVM = EVAL(J)
      JM = J
      J1 = J + 1
      DO 242 I = J1,N
      IF (EVM .GE. EVAL(I)) GO TO 242
      EVM = EVAL(I)
      JM = I
  242 CONTINUE
      EVAL(JM) = EVAL(J)
      EVAL(J) = EVM
      DO 244 K=M,N
      EVM = EVEC(K,J)
      EVEC(K,J) = EVEC(K,JM)
  244 EVEC(K,JM) = EVM
  246 CONTINUE
```

```
248 CONTINUE
    DO 336 I=1,10
336 FREQC(I) = 1302.84*SQRT(EVAL(I))
    WRITE (3,155) (FREQC(I), I=1,10)
    FIT(1) = FREQ01 - FREQC(1)
    FIT(2) = FREQ02 - FREQC(2)
    FIT(3) = FREQ03 - FREQC(3)
    FIT(4) = 0.
    FIT(5) = FREQ05 - FREQC(5)
    FIT(6) = FREQ06 - FREQC(6)
    FIT(7) = FREQ07 - FREQC(7)
    WRITE (3,190) (FIT(I), I=1,7)
    FITMAX = ABS(FIT(1))
    DO 250 K=1,7
    IF(FITMAX - ABS(FIT(K))) 249,250,250
249 FITMAX = ABS(FIT(K))
    I = K
250 CONTINUE
    IF (FITMAX .LE. 2.) GO TO 334
    DO 280 K=1,6
    DO 260 L=1,2
260 V(L,K) = Z(L,K)
    DO 270 L=3,4
270 V(L,K) = EVEC(3,L)**2*Z(3,K)+2*EVEC(3,L)*EVEC(4,L)*Z(5,K)
   1          + EVEC(4,L)**2*Z(4,K)
    DO 275 L=5,7
    V1(L,K) = 0.
    DO 272 I=5,8
    M = I + 1
272 V1(L,K) = V1(L,K) + EVEC(I,L)**2*Z(M,K)
    V2(L,K) = 2*(EVEC(5,L)*(EVEC(6,L)*Z(10,K)+EVEC(7,L)*Z(11,K)
   1           + EVEC(8,L)*Z(12,K)+EVEC(6,L)*(EVEC(7,L)*Z(13,K)
   2           + EVEC(8,L)*Z(14,K)+EVEC(7,L)*EVEC(8,L)*Z(15,K))
275 V(L,K) = V1(L,K) + V2(L,K)
    DO 280 L=1,7
    IF(FREQC(L) .EQ. 0.) FREQC(L) = 1.0E-30
    V(L,K) = V(L,K)*848686.0/FREQC(L)
    IF(V(L,K) .LT. 1.0E-30) V(L,K) = 0.
280 CONTINUE
    DO 285 K=1,6
    DO 285 L=1,7
285 VT(K,L) = V(L,K)
    DO 300 K=1,6
    DO 300 L=1,7
    VTP(K,L) = 0.
    DO 331 M=1,7
331 VTP(K,L) = VTP(K,L) + VT(K,M)*P(M,L)
300 CONTINUE
    DO 310 K=1,6
    DO 310 L=1,6
    VV(K,L) = 0.
```

```
      DO 310 M=1,7
  310 VV(K,L) = VV(K,L) + VTP(K,M)*V(M,L)
      DO 320 I=1,6
      VL(I) = 0.
      DO 320 J=1,7
  320 VL(I) = VTP(I,J)*FIT(J)
      CALL SIMQ(VV,VL,6,KS)
      DO 333 I=1,6
  333 DELPHI(I) = VL(I)
      DO 330 I=1,6
  330 PHI(I) = PHI(I) + DELPHI(I)
  334 WRITE (3,180) (PHI(I), I=1,6)
      DO 410 K=1,6
      DO 400 L=1,7
  400 PEF(L,K) = V(L,K)*PHI(K)/FREQC(L)*200.
      PEF(8,K) = 0.
      DO 410 L=9,10
      M = L + 7
      V(L,K) = Z(M,K)*848686.0/FREQC(L)
      PEF(L,K) = V(L,K)*PHI(K)/FREQC(L)*200.
  410 CONTINUE
      NIT = NIT + 1
      IF(NIT - 10) 332,332,335
  332 GO TO 30
  335 CONTINUE
      WRITE (3,170) ((EVEC(I,J), J=1,10), I=1,10)
      WRITE (3,405) ((PEF(L,K), K=1,6), L=1,10)
      END
```

Subroutine VALVEC may be any program for the diagonalisation of a matrix, giving the eigenvalues and eigenvectors. Its parameters are: F - matrix to be diagonalised; EVEC - unitary matrix of the eigenvectors; N = 10 - order of the matrix; IFU = 1 - index showing that both eigenvalues and eigenvectors must be calculated; FIN = 10^{-6} - indicator for shut-off, the final largest off-diagonal element. Subroutine SIMQ may be any program for solving a system of linear equations. VV - matrix of the coefficients of the unknown DELPHI; VL - vector of the free terms on right hand side; N = 6 - order of the system; KS - indicator for shut-off.

For K_2NiF_6, where the frequency of ν_8 lattice mode is known instead of ν_7, appropriate modifications in the program are necessary.

LITERATURE

1. K.R. Dixon, PhD Dissertation, Strathclyde University, Glasgow, 1966
2. D.H. Brown, K.R. Dixon, C.M. Livingston, R.H. Nuttall, and D.W.A. Sharp, J. Chem. Soc., 1967, 100
3. H. Poulet and M. Debeau, Spectrochim. Acta, 25A, 1553 (1969)
4. A.P. Lane and D.W.A. Sharp, J. Chem. Soc.(A), 1969, 2942
5. M. Reisfeld, J. Mol. Spectroscopy, 29, 109 (1969)
6. See, for example, J. Slater, 'Quantum Theory of Molecules and Solids', vol. 2, McGraw Hill, 1965, p. 1
7. A. Schoenflies, 'Krystallsysteme und Krystallstruktur', Teubner, Leipzig, 1891
8. R.S. Halford, J. Chem. Phys., 14, 8 (1946)
9. G. Herzberg, 'Infrared and Raman Spectra of Polyatomic Molecules', Van Nostrand, Princeton, 1945
10. S. Bhagavantam and T. Venkatarayudu, Proc. Indian Acad. Sci., 9A, 224 (1939); 13A, 543 (1941)
11. A. Butucelea, Stud. Cerc. Chim., 17, 199 (1969)
12. M.K. Grover and R. Silbey, J. Chem. Phys., 52, 2099 (1970)
13. V. Sergiescu, 'Introducere in fizica solidului', Ed. Tehnica, Bucuresti, 1956
14. M. Born and K. Huang, 'Dynamical Theory of Crystal Lattices', Clarendon (Oxford University Press), 1954
15. Thor A. Bak, Ed., 'Phonons and Phonon Interactions', Aarhus Summer School Lectures, 1963, publ. 1964, W.A. Benjamin Inc., New York-Amsterdam, p. 9
16. L.I. Schiff, 'Quantum Mechanics', McGraw Hill, New York, 1954

17. G. Taddei and S. Califano, Rivista del Nuovo Cimento, Ser. I, 1, 547 (1969)

18. S.S. Mitra, J. Chem. Phys., 39, 3031 (1963)

19. J.E. Cahill, K.L. Treuil, R.E. Miller, and G.E. Leroi, J. Chem. Phys., 49, 3320 (1968)

20. H. Winston and R.S. Halford, J. Chem. Phys., 17, 607 (1949)

21. E.B.R. Wilson, J.C. Decius, and P.C. Cross, 'Molecular Vibrations', John Wiley & Sons, New York, 1955

22. S.S. Mitra, Z. Krist., 116, 149 (1961); S.S. Mitra and P.J. Gielisse, Progress in Infrared Spectroscopy, 2, 47 (1964)

23. I.R. Beattie and T.R. Gilson, Proc. Roy. Soc. A, 307, 407 (1968); P.S. Narayanan, Proc. Indian Acad. Sci., 32A, 279 (1950); D. Krishnamurti, Proc. Indian Acad. Sci., 55A, 290 (1962)

24. Anonymous, The Spex Speaker, 14, 2 (1969)

25. W.J. Hurley, J. Chem. Educ., 43, 236 (1966)

26. A.A. Michelson, 'Studies in Optics', University of Chicago Press, Chicago, 1927, p. 35

27. H.A. Gebbie and G.A. Vanasse, Nature, 432, 178 (1956); Phys. Rev., 107, 1194 (1957)

28. For example, G.R. Wilkinson, in 'Infrared Spectroscopy and Molecular Structure', M. Davies, Ed., Elsevier, 1963

29. W.C. Price and T.S. Robinson, Proc. Phys. Soc., B66, 969 (1953)

30. Quantum Cemistry Program Exchange (QCPE), Program No. 107, available from QCPE.

31. D.W. James and M.J. Nolan, Progr. Inorg. Chem., 9, 195 (1968)

32. G. Placzek, in 'Handbuch der Radiologie', E. Marx, Ed., vol. 6, part 2, Akademischer Verlag, Berlin, 1934, p. 204

33. S.P.S. Porto and D.L. Wood, J. Opt. Soc. Amer., 52, 251 (1962)

34. R.C.C. Leite and S.P.S. Porto, J. Opt. Soc. Amer., 54, 981 (1964)

35. R.C. Hawes, K.P. George, D.C. Nelson, and R. Beckwith, Anal. Chem., 38, 1842 (1966)

36. T.C. Damen, S.P.S. Porto, and B. Tell, Phys. Rev., 142, 570 (1966)

37. R. Loudon, Advan. Phys., 13, 423 (1964); Proc. Phys. Soc., 82, 393 (1963)

38. S.P.S. Porto, P.A. Fleury, and T.C. Damen, Phys.Rev.,154,522 (1967)

39. A. Bertrand, Rev. Inst. Français Pétrole, 24, 893 (1969); P.J. Hendra and P.M. Stratton, Chem. Revs., 69, 325 (1969)

40. R.W.G. Wyckoff, 'Crystal Structures', Intersci. Publ., New York-Sidney-London, 1965, vol. 3

41. D. Babel, Structure and Bonding, 3, 1 (1967)

42. R. Hoppe, Angew. Chem.(Intern. Ed.), 5, 95 (1966)

43. A. Butucelea, Stud. Cerc. Chim., 18, 803 (1970)

44. Ref. 40, p. 339

45. J. Hiraishi, and T. Shimanouchi, Spectrochim. Acta, 22, 1483 (1966)

46. H. Poulet et J.-P. Mathieu, 'Spectres de vibration et symétrie des cristaux', Gordon and Breach, Paris-London-New York, 1970

47. Ref. 40, p. 349

48. Ref. 40, p. 354

49. A. Zalkin, J.D. Forrester, and D.H. Templeton, Acta Cryst., 17, 1408 (1964)

50. G. Brauer, 'Handbook of Preparative Inorganic Chemistry', Academic Press, New York-London, 1965, vol. 2, p. 216

51. E. Huss and W. Klemm, Z. anorg. Chem., 262, 25 (1950)

52. B. Cox and A.G. Sharpe, J. Chem. Soc., 1954, 1798

53. G.L. Clark, 'Applied X-Rays', McGraw-Hill, New York-London, 1940, p. 281

54. M.J. Buerger, 'X-Ray Crystallography', John Wiley & Sons, New York, 1949, p. 60

55. B. Cox and A.G. Sharpe, J. Chem. Soc., 1953, 1783

56. Ref. 40, pp. 341-3

57. J.A. Ketelaar, Z. Krist., 92, 155 (1935)

58. Ref. 40, p. 353

59. J.L. Hoard and W.B. Vincent, J. Amer. Chem. Soc., 61, 2849 (1939)

60. H. Bode and R. Brockermann, Z. anorg. Chem., 269, 173 (1952)

61. R.W.G. Wyckoff and J.H. Muller, Amer. J. Sci., 13, 347 (1927)

62. H. Bode and W. Wendt, Z. anorg. Chem., 269, 165 (1952)

63. J.E. Griffiths and D.E. Irish, Inorg. Chem., 3, 1134 (1964)

64. G.M. Begun and A.C. Rutenberg, Inorg. Chem., 6, 2212 (1967)

65. T.H. Walnut, J. Chem. Phys., 20, 58 (1952)

66. R.B. Badachhappe, G. Hunter, L.D. McCory, and J.L. Margrave, Inorg. Chem., 5, 929 (1966)

67. N.A. Matwiyoff and L.B. Asprey, Chem. Commun., 1970, 75

68. C.D. Flint, Chem. Commun., 1970, 482

69. A. Pfeil, Theoret. chim. Acta, 20, 159 (1971)

70. S. Bratoz, O. Chalvet, R. Daudel, R. Lefebvre, C. Moser, and L. Goodman, Pure Appl. Chem., 11, 261 (1965)

71. C.A. Coulson, Trans. Faraday Soc., 33, 1979 (1937)

72. S. Bratoz, 'Calcul des fonctions d'onde moléculaires', CNRS, Paris, 1958, p. 287

73. Ref. 9, p. 372

74. T. Shimanouchi, J. Chem. Phys., 17, 245, 734, 848 (1949)

75. K. Nakamoto, 'Infrared Spectra of Inorganic and Coordination Compounds, J. Wiley & Sons, New York-London, 1963, p. 57

76. C. Belgodere, 'Mémoire pour l'obtention du diplôme d'études supérieures de physique', Université de Paris, 1968. The author wishes to thank Prof. J.-P. Mathieu for having signalled him this work.

77. J. Hiraishi, I. Nakagawa, and T. Shimanouchi, Spectrochim. Acta, 20, 819 (1964)

78. T. Shimanouchi, M. Tsuboi, and T. Miyazawa, J. Chem. Phys., 35, 1597 (1961)

79. J. Overend and J.R. Scherer, J. Chem. Phys., 32, 1289 (1960)

80. J.H. Schachtschneider and R.G. Snyder, Spectrochim. Acta, 19, 117 (1963)

81. T. Shimanouchi, Ed., 'Normal Coordinate Treatment of Polyatomic Molecules', The University of Tokyo, Tokyo, 1968

82. Ref. 21, p. 54